Aus der Klinik für Anästhesiologie mit Schwerpunkt operative Intensivmedizin
der Medizinischen Fakultät Charité – Universitätsmedizin Berlin

DISSERTATION

Strukturelle Determinanten kognitiver Funktionen im MRT

zur Erlangung des akademischen Grades
Doctor medicinae (Dr. med.)

vorgelegt der Medizinischen Fakultät
Charité – Universitätsmedizin Berlin

von

Florian Lammers

aus Haselünne

Datum der Promotion: 5. März 2021

Inhaltsverzeichnis

1 Zusammenfassung

1.1 Übersicht

HINTERGRUND: Spezifische kognitive Prozesse können einzelnen Hirnregionen, aber auch weit aufgespannten Netzwerken aus einzelnen zerebralen Strukturen zugeordnet werden. Obwohl diese funktionelle Segregation aus fMRT- und Läsionsstudien gut belegt ist, wird gleichzeitig eine allgemeine Assoziation aus Hirngröße und kognitiver Leistungsfähigkeit angenommen. Es ist jedoch nicht zulänglich erforscht, ob die Relation von Volumen und kognitiver Funktion auch für einzelne kortikale und subkortikale Subregionen, z.B. cholinerge Zellgruppen im basalen Vorderhirn, gilt, oder ob dies ein Epiphänomen des übergeordneten Zusammenhangs zwischen Hirnvolumen und globaler Kognition ist. Des weiteren ist nicht bekannt, inwiefern dieser Zusammenhang durch Atrophie im Alter moduliert wird.

METHODIK: In dieser Arbeit wurden eine junge, kognitiv gesunde Stichprobe aus Rauchern und Nichtrauchern sowie eine ältere, kognitiv gesunde Population, die sich zu einer elektiven Operation in der Universitätsklinik vorstellte, untersucht. Neben neuropsychologischen Daten wurden strukturelle MRT-Daten erhoben und hinsichtlich der Volumina von Gehirn, kortikaler Areale und cholinerger Kerngebiete ausgewertet. Zusätzlich wurde die Brain Parenchyma Fraction (BPF) als ein Maß der Hirnatrophie bestimmt. Assoziationen zwischen MRT-basierten volumetrischen und neuropsychologischen Daten, insbesondere der globale Kognition und exekutiven Funktion, wurden in Regressionsanalysen unter Berücksichtigung demographischer Variablen bestimmt.

ERGEBNIS: Bei jungen gesunden Probanden ist das Volumen des linken Nucleus basalis Meynert mit dem Ergebnis im Trail-Making-Test assoziiert. Dieser Zusammenhang ist parabelförmig, sodass Probanden mit relativ kleinen sowie sehr großen Volumina schlechter abschließen. Bei älteren Patienten besteht ein linearer Zusammenhang zwischen Gesamtvolumen aller cholinergen Kerne im basalen Vorderhirn (BFCS) und globaler Kognition sowie Einzeltest einer umfangreichen neuropsychologischen Testbatterie. Dieser Effekt wird durch einen Zusammenhang von Hirnvolumen und globaler Kognition vermittelt. In derselben älteren Stichprobe ist das Volumen der gesamten grauen Substanz stärker mit dem Trail-Making-Test B assoziiert als das Volumen einzelner Lobi. Erst nach Bereinigung von Einflüssen durch Motorik und visuelle Fähigkeiten besteht eine spezifische Assoziation mit dem Volumen des Temporallappens. Die BPF als Maß für Hirnatrophie ist unabhängig von Lobus- oder BFCS-Volumen mit globaler und exekutiver Funktion assoziiert.

SCHLUSSFOLGERUNG: Die Volumina cholinerger Kerngebiete sind mit der kognitiven Funktion assoziiert. Während diese in einer jungen Population spezifisch mit visueller Aufmerksamkeit assoziiert sind, wird dieser Zusammenhang im Alter durch eine allgemeine Assoziation des Gesamthirnvolumens mit globaler Kognition vermittelt. Dieses Ergebnis lässt sich ebenso für das gesamte kortikale Volumen im Vergleich zu lobären Volumina reproduzieren. Im Alter scheinen eine Vielzahl zerebraler Strukturen in die Ausführung komplexer kognitiver Funktion involviert zu sein, sodass Volumina einzelner Regionen nur schwach mit der kognitiven Leistungsfähigkeit

korrelieren. Unabhängig vom Volumen scheint die Hirnatrophie die globalen kognitiven wie auch im Speziellen exekutiven Funktionen zu beeinflussen.

1.2 ABSTRACT

BACKGROUND: Specific cognitive processes can be assigned to individual brain regions as well as functionally distinct wide-range cerebral networks. Although this segregation is well known from functional MRI and lesion studies, a general association between brain size and cognitive performance has to be assumed. Nevertheless it is not well known whether the relation of volume and cognitive function is also valid for individual cortical and subcortical subregions, e.g. the basal forebrain cholinergic system (BFCS), or if this is an epiphenomenon relating to the global relationship of brain volume and global cognition. Furthermore, it is not known if this association is modulated by cerebral atrophy in ageing.

METHODOLOGY: In this study, a young, cognitively healthy sample of smokers and never-smokers as well as an elderly, cognitively healthy population who presented for elective surgery at a university clinic were examined. In addition to neuropsychological data, structural MRI data were collected and the volumes of brain, cortical areas and the basal forebrain cholinergic system have been assessed. Furthermore the brain parenchyma fraction (BPF), which is a measure of brain atrophy, has been assessed. Associations between MRI-based volumetric and neuropsychological data, in particular global cognition and executive functions, were determined in regression analyses adjusting for confounding demographic variables.

RESULTS: In young healthy participants, the volume of the left Nucleus basalis of Meynert is associated with Trail-Making-Test performance. This relationship is u-shaped and subjects with relatively small and very large volumes show poorer performance. Elderly patients show a linear correlation between total volume of the BFCS and global cognition as well as sub-tests of a comprehensive neuropsychological testing, which is mediated by a relationship between brain volume and global cognition. In the same elderly sample, the volume of total grey matter is found to have a stronger association with Trail-Making-Test B than individual lobe volume. After correction for motor function and visual abilities, a specific association with temporal lobe volume is found. BPF as a measure of brain atrophy is associated with global and executive function, independent of lobular grey matter or BFCS volume.

CONCLUSION: The volumes of cholinergic nuclei are associated with cognitive function. While these are specifically associated with visual attention in young populations, this association is mediated by a general association of total brain volume and global cognition in the elderly. This result can also be found for the total cortical volume compared to lobular volume. Multiple cerebral structures seem to be involved in complex cognitive functions during ageing and individual region volumes correlate weakly with cognitive performance. Regardless of volume, cerebral atrophy affects global cognitive as well as executive functions in particular.

1.3 EINFÜHRUNG

Es ist weithin akzeptiert, dass kognitive und mentale Prozesse an neuroanatomische Begebenheiten gekoppelt sind. So analysierte McDaniel (2005) 37 Studien, die über eine Korrelation von in-vivo

gemessenem Hirnvolumen und Intelligenz berichteten, und zeigte eine moderate Assoziation zwischen beiden Größen. Im Gegensatz zu diesem globalen Zusammenhang steht jedoch die Annahme, dass das Gehirn in segregierten Strukturen organisiert ist, die zahlreiche funktionell und anatomisch getrennte Netzwerke umfasst (Toga and Mazziotta 2000, Damoiseaux et al. 2006). Diese Theorien basieren jedoch auf funktionellen Bildgebungsstudien und es steht zur Diskussion, ob die Volumina einzelner Hirnregionen die Leistungsfähigkeit in einer spezifischen kognitiven Domäne beeinflussen (McLullich et al. 2002, Staff et al. 2002).

1.3.1 Anatomie des zentralen cholinergen Systems

Cholinerge Zellgruppen wurden erstmals von Mesulam in einer eigenen, sechs Kompartimente Ch1-Ch6 umfassenden Nomenklatur systematisiert (Mesulam et al. 1983).

Ch1 bis Ch4 liegen im basalen Vorderhirn (basal forebrain cholinergic system, BFCS). Ch1 umfasst Neuronen im medialen Septum und Ch2 liegt im vertikalen Kern des diagonalen Band von Broca. Beide projizieren in den Hippocampus. Ch3 korrespondiert mit Neuronen im horizontalen Kern im Band von Broca, die zum Bulbus olfactorius ziehen. Ch4 ist der Ursprungsort cholinerger Axone zum Neokortex und liegt im Nucleus basalis Meynert (magnocellularis, NBM). Daneben projiziert Ch4 in die Amygdala. Anteriore Abschnitte von Ch4 projizieren zu medialen, frontalen wie auch parietalen Regionen, wohingegen der posteriore Sektor von Ch4 die Temporallappen innerviert (Mesulam et al. 1983). Zusätzlich beschreiben manche Autoren bei Primaten den zusätzlichen Nucleus subputaminalis Ayala, dessen Axone zum Frontalkortex ziehen (Simić et al. 1999). Regionen Ch5 und Ch6 liegen in der pontomesenzephalen retikulären Formation und sind daher kein Teil des BFCS. Ch5 entspricht dem Nucleus tegmentalis pedunculopontinus und Ch6 dem Nucleus tegmentalis posterolateralis. Beide projizieren zum Thalamus (Mesulam et al. 1983). Weitere cholinerge Interneurone finden sich im Striatum (Difiglia 1987).

1.3.2 Relevanz des BFCS für Kognition

Die Relevanz cholinerger Neuronen für kognitive Prozesse ergibt sich aus verschieden tier- und humanexperimentellen wie auch Observations- und klinischen Studien. Tierstudien zeigten, dass selektive Läsionen im BFCS zu Aufmerksamkeits- und Gedächtnisdefiziten führen (Harati et al. 2008, Cai et al. 2012). Im Weiteren korreliert die Freisetzung von Acetylcholin (ACh) im frontalen Kortex mit dem korrekten Erkennen von Hinweisstimuli (Parikh et al. 2007). Eine ähnliche Relevanz für den Menschen wurde aus post-mortem Studien an Patienten mit Alzheimer Demenz (AD) abgeleitet, bei denen ein kognitives Defizit mit selektivem Verlust cholinerger Neuronen assoziiert wurde (White et al. 1977). Zudem können die kognitiven Symptome der AD durch Inhibitoren der Acetylcholinesterase (AChE) abgemildert werden. Diese steigern die Menge des ACh im synaptischen Spalts durch Inhibition der AChE, die ACh unter physiologischen Bedingungen abbaut (Birks und Grimley Evans 2015, Birks und Harvey 2018, Anand und Singh 2013). Umgekehrt können Antagonisten an cholinergen Rezeptoren ein kognitives Defizit induzieren (Bentley et al. 2011).

1.3.3 MRT des BFCS und Kognition

1.3.3.1 In-vivo Bildgebung des BFCS bei Alzheimer Demenz und Mild Cognitive Impairment (MCI)

Teipel (et al. 2005) verwendete als Erster eine automatisierte Segmentierung des BFCS in einer Studie mit AD Patienten und beschrieb zunehmende BFCS-Atrophie im Vergleich zur gesunden Kontrollgruppe. Grothe (et al. 2010) replizierte dieses Ergebnis in einer großen Querschnittsstudie. Longitudinale Folgestudien berichteten über Atrophie des BFCS bei Teilnehmern mit klinischem Progress zur Demenz (Grothe et al. 2013, Kilimann et al. 2014).

Grothe (et al. 2010) untersuchte Patienten mit amnestischem MCI und ältere Kontrollprobanden. MCI Patienten haben ein erhöhtes Risiko, eine AD zu entwickeln und weisen bereits kognitive Defizite auf, die ihr Alltagsleben jedoch nicht beeinträchtigen. Bei MCI-Patienten berichtete diese Studie über einen Verlust an grauer Substanz in Sektor Ch4. Ebenfalls korrelierte das Volumen einiger BFCS-Subregionen mit neuropsychologischen Testergebnissen in dieser Gruppe, nicht aber bei den Kontrollprobanden. Folgestudien bestätigten diese Befunde (Kiliman et al. 2014, 2017, Cantero et al. 2017). Nur eine Studie berichtete über eine Vergrößerung des anterioren BFCS bei MCI-Patienten, die später eine manifeste AD entwickelten (Butler et al. 2018).

1.3.3.2 In-vivo Bildgebung des BFCS und Kognition bei gesunden Populationen

Nur wenige Studien haben explizit die Zusammenhänge von BFCS-Volumen und Kognition bei gesunden Populationen untersucht. Die bereits beschriebene Studie von Grothe (et al. 2010) konnte keine signifikanten Assoziationen in einer gesunden älteren Kontrollpopulation nachweisen, obgleich diese bei MCI-Patienten vorlagen. Jedoch war die neurokognitive Testung in dieser Studie auf die Mini-Mental Status Examination (MMSE) und einen Test des verbalen Gedächtnisses beschränkt. Es ist möglich, dass die Effektstärke einer solchen Assoziation zu klein ist, um in einer kleinen Stichprobe (N=28) nachgewiesen werden zu können, oder dass die ausgewählten Tests nicht sensitiv genug waren. Ähnliche Einschränkungen gelten für die Arbeit von Choi (et al. 2012), obwohl in dieser Studie umfangreiche kognitive Testungen durchgeführt wurden.

Wolf (et al. 2014) untersuchte diese Fragestellung in einem Sample, das 43 gesunde ältere Probanden umfasste. Der Autor berichtet über eine signifikante Assoziation des posterioren BFCS mit globaler kognitiver Leistung, aber nicht mit Einzeltests. Die größten Vorbehalte zu dieser Studie gelten der untersuchten Population, die keine Generalisierung der Ergebnisse erlaubt. Die Probanden wurden an akademischen Einrichtungen via Anzeige rekrutiert und hatten einen sehr hohen IQ (im Mittel 138±16). Deshalb könnten weitere Assoziation von einem Deckeneffekt maskiert worden sein.

Eine spätere Studie von Grothe (et al. 2016) beschreibt eine große Stichprobe aus 132 MCI-Patienten und 177 gesunden Kontrollprobanden und untersucht die Assoziation von Kognition und BFCS-Volumen. Sie beschrieben signifikante Assoziationen des BFCS-Volumens mit Gedächtnis- und Aufmerksamkeitstest in der MCI-Gruppe, die in der gesunden Kontrollgruppe nicht reproduziert werden konnte. Die Autoren berichten jedoch über schwache Korrelationen mit Testergebnissen in der gesunden Kontrollgruppe, die erst nach Korrektur des Testens multipler

unabhängiger Hypothesen ihre Signifikanz verlieren. Die dort angewandte Bonferroni-Korrektur der p-Werte ist vermutlich unangemessen konservativ und könnte schwache Assoziationen maskiert haben, da die Leistungen in verschiedenen kognitiven Tests nicht vollständig unabhängig voneinander sind (Johnson et al. 2004, 2008). Ein weiterer Kritikpunkt betrifft die Verwendung einer BFCS-Segmentierung, die auf histologischen Daten eines einzelnen Individuums beruht.

Es existiert nur eine Studie, die eine Assoziation von BFCS-Volumen und Kognition in einem jungen, gesunden Kollektiv untersucht hat: Butler (et al. 2012) berichtet über eine Assoziation des Volumens von Ch1/2 mit Gedächtnistests bei gesunden jungen Probanden. Weder wurden hier posteriore BFCS-Sektoren noch andere kognitive Fähigkeiten untersucht.

1.3.4 Volumen kortikaler grauer Substanz und exekutive Funktionen

Yuan und Raz (2014) analysierten Studien, die über eine Korrelation von präfrontaler grauer Substanz und exekutiver Funktion berichteten und fanden einen moderaten Zusammenhang, jedoch ohne Berücksichtigung von Alter, Geschlecht oder Hirnvolumen. Neben frontalen Regionen scheint jedoch ein weitgespanntes kortikales Netzwerk einschließlich parietaler und temporaler Areale sowie des Motorkortex involviert zu sein, wenn exekutive Funktion im Trail-Making-Test (TMT) gemessen wird (Varjacic et al. 2018). Somit können Tests für Veränderungen sensitiv, aber kaum spezifisch für Veränderungen in einem kortikalen Areal sein. Weiterführende Studien haben daher eine spezifische Assoziation von lokaler kortikaler Dicke mit isolierten kognitiven (z.B. exekutiven) Funktionen infrage gestellt (Bettcher et al. 2017, Staff et al. 2006). Umgekehrt muss jedoch angemerkt werden, dass gerade der TMT eine Vielzahl kognitiver Fähigkeiten wie einfache visuelle und motorische, aber auch höhere exekutive Funktionen misst, sodass noch immer die Frage unbeantwortet bleibt, inwiefern regionale und globale kortikale Volumina die exekutive Komponente sowie das Gesamtergebnis im TMT beeinflussen (Crowe 1998).

Kortikale Atrophie bei Demenz ist belegt und korreliert mit der Atrophie des BFCS bei MCI und AD (Risacher et al. 2011, Grothe et al. 2010, Cantero et al. 2016, Kilimann et al. 2014, 2017). Es wird angenommen, dass ein gestörter retrograder Transport von nerve growth factor (NGF) vom Kortex zum BFCS den Zelltod cholinerger Neuronen begünstigt (Seiler und Schwab 1984). Es ist bisher jedoch unklar, inwiefern kortikale und cholinerge Atrophie spezifisch zur kognitiven Leistungsfähigkeit im Alter beitragen.

1.3.5 Hirnparenchymfraktion (BPF) und Kognition

Die Hirnparenchymfraktion (brain parenchyma fraction, BPF) ist das Verhältnis von Hirnvolumen zum intrakraniellen Volumen. Da das intrakranielle Volumen in der Kindheit vom Wachstum des Gehirns bestimmt wird und kaum altersabhängig schrumpft, kann es als Maß für das maximale Hirnvolumen gelten, wohingegen die BPF die Atrophie unabhängig von der ehemaligen Größe reflektiert (Davis und Wright 1977, Pfefferbaum et al. 1994, Matsumae et al. 1996). Die BPF ist im Alter sowie bei verschiedenen neurodegenerativen Erkrankungen vermindert, z.B. Multipler Sklerose (MS) und Demenz und korreliert hier mit der kognitiven Leistungsfähigkeit (Vågberg et al. 2017 , Rudick et al. 1999, Callahan et al. 2015, Hohol et al. 1997). Auch bei MS scheint die BPF nur nach langjährigem Verlauf mit einem kognitiven Defizit zu korrelieren (Cruz-Gómez et al.

2014, Deloire et al. 2005). Weitere Studien berichteten über Assoziationen von BPF und Kognitionen bei Patienten mit obstruktivem Schlafapnoe-Syndrom und myotoner Dystrophie (Torelli et al. 2011, Baldanzi et al. 2016). Janssen (et al. 2015) berichtete über Korrelationen mit kognitiven Tests bei Patienten mit HIV-Infektion, aber nicht bei gesunden Kontrollprobanden.

Nur eine Studie hat die Zusammenhänge von BPF und Kognition bei gesunden, älteren Probanden untersucht. Shenkin (et al. 2009) untersuchte Hirnvolumen, BPF und Kognition bei 115 Probanden im Alter von 75-81 Jahren. Diese Studie berichtete über Assoziationen von Kognition und Hirnvolumen, nicht jedoch mit der BPF. Obgleich diese Studie insgesamt eine hohe Qualität aufweist, gibt es einige Vorbehalte: Zum Einen wurde das intrakranielle Volumen nicht direkt gemessen, sondern auf Basis der intrakraniellen Fläche extrapoliert. Zweitens war die Stichprobe nicht homogen, da ein Teil der Probanden über lokale Anzeigen rekrutiert wurde, die übrigen jedoch Teilnehmer einer bereits abgeschlossenen Studie waren. Drittens umfasst das Sample nur eine sehr geringe Altersspanne, was die Auswertung altersabhängigen kognitiven Verfalls einschränkt. Damit ist bisher unklar, ob die BPF auch bei gesunden älteren Probanden mit einem altersbedingten kognitiven Defizit assoziiert ist.

1.3.6 Fragestellung

In dieser Arbeit werden strukturelle Determinanten kognitiver Funktionen im MRT untersucht. Hierzu zählen vor allem Volumina des BFCS bei jungen und älteren nicht-dementen Probanden. Des weiteren wird untersucht, ob spezifische Assoziationen zwischen lokaler grauer Substanz oder BFCS-Volumina und einzelnen kognitiven Teilkompetenzen bestehen, oder ob diese Assoziationen einer globalen Assoziation von Hirngröße und Kognition aufgelagert sind. Zusätzlich wird der Zusammenhang von BPF und Kognition bei älteren Probanden untersucht.

1.4 Methodik

In dieser Arbeit werden Daten aus zwei verschiedenen Studien analysiert.

1.4.1 Genetics of Nicotine Dependence and Neurobiological Phenotypes

Die Genetics of Nicotine Dependence and Neurobiological Phenotypes-Studie ist eine durch die Deutsche Forschungsgemeinschaft geförderte multizentrische, bevölkerungsbezogene Fall-Kontroll-Studie an Rauchern und Niemalsrauchern.

Zwischen 2007 und 2009 wurden 2396 Teilnehmer in den Studienzentren der psychiatrischen Universitätskliniken Aachen, Berlin, Bonn, Düsseldorf, Erlangen, Mainz und Mannheim (Deutschland) rekrutiert. Über lokale Melderegister wurden 55000 Teilnehmer schriftlich eingeladen. Interessierte waren für den Studieneinschluss geeignet, wenn sie zwischen 18 und 65 Jahren alt waren, zum Zeitpunkt des Studieneinschlusses rauchten oder Nichtraucher mit einem maximalen Lebenszeitkonsum von 20 Zigaretten waren, in Deutschland oder einem anliegendem Staat geboren wurden und Deutsch als Muttersprache sprachen. Ehemalige Raucher sowie Interessenten mit Substanzmissbrauch oder Achse-1-Diagnose nach DSM-IV innerhalb der letzten sechs Monate, Schwangerschaft, Erkrankung des zentralen Nervensystems oder zentral wirksamer

Medikation oder jedem weiteren Umstand, der mit dem Studienziel interferieren könnte, wurden von der Studie ausgeschlossen (Lindenberg et al. 2008). In einem Subprojekt wurden MRT-Daten einiger Probanden erhoben.

1.4.2 BioCog – Biomarker Development for Postoperative Cognitive Impairment in the Elderly

Die BioCog-Studie ist ein durch die Europäische Union gefördertes Projekt zur Entwicklung eines Biomarker-basierten Algorithmus zur Prädiktion post-operativen Deliriums (POD) und post-operativer kognitiver Dysfunktion (post-operative cognitive dysfunction, POCD). Die Studie wurde als prospektive multizentrische observatorische Kohortenstudie angelegt.

Patienten wurden an der Klinik für Anästhesiologie der Charité – Universitätsmedizin Berlin, Deutschland, und dem Universitair Medisch Centrum Utrecht, Niederlande, rekrutiert. Zwischen November 2014 und April 2017 wurden 1033 Patienten und 100 gesunde Kontrollprobanden eingeschlossen (Winterer et al. 2018).

Patienten ab 65 Jahren europäischer/kaukasischer Herkunft, die sich zu einem elektiven chirurgischen Eingriff mit erwarteter Dauer >60 Minuten vorstellten, wurden bei vorliegendem Einverständnis eingeschlossen. Ausschlusskriterien umfassten vorbestehende kognitive Einschränkung definiert als MMSE-Ergebnis unter 24 Punkten, relevante neuropsychiatrische Begleiterkrankungen, An- oder Hypakusis, die mit der kognitiven Testung interferieren könnte, zentral wirksame Medikation, Obdachlosigkeit oder mangelnde Möglichkeit, den Patienten für eine Folgeuntersuchung einzubestellen, die Teilnahme an einer klinischen Interventionsstudie und Unterbringung oder Einweisung aufgrund amtlicher oder richterlicher Anordnung.

Die hier ausgewerteten neurokognitiven und Bildgebungsdaten wurden innerhalb eines Zeitraums von 14 Tagen vor der OP erhoben.

1.4.3 Zerebrale Bildgebung mittels Magnetresonanztomographie (cMRT)

Die Hauptkomponenten eines Magnetresonanztomographen (MRT-Scanners) umfassen einen Magneten, Radiofrequenz- und Gradientenspulen. Der Magnet, bei modernen Geräten häufig ein Supraleiter, produziert ein statisches Magnetfeld B_0. Die Gradientenspulen erzeugen darin Magnetfeldgradienten, die eine Lokalisierung des MR-Signals ermöglichen. Radiofrequenzspulen dienen der Erzeugung eines oszillierenden magnetischen Feldes zur Exzitation von Spins und zum Empfang des MR-Signal aus der Spin-Relaxierung. Resonanz wird erzeugt, wenn sowohl Exzitationswelle wie auch Protonen (i.d.R. ^1H_2O-Wasserstoffprotonen) mit einer spezifischen Larmor-Frequenz schwingen. Der Kontrast wird durch die Modulation der Larmor-Frequenz der Protonen durch umliegendes Gewebe erreicht (Kuperman 2000).

Als rotierende Masse mit positiver Ladung haben Protonen ein magnetisches Moment, das ein kleines Magnetfeld erzeugt. Die Richtung der Rotationsachse kann anhand der Orientierung des Magnetfeldes bestimmt werden (Kuperman 2000).

Die MRT nutzt die Eigenschaft von Protonen, ihre Spins (Eigendrehimpuls) entlang eines äußeren Magnetfeldes B_0 auszurichten. Die Ausrichtung geschieht parallel oder antiparallel. Da die parallele Ausrichtung einen niedrigeren energetischen Zustand bedeutet, richten sich die meisten Spins parallel zu B_0 aus. Spins können sich summieren oder gegenseitig auslöschen, sodass viele Spins eine Netto- oder Massenmagnetisierung M_z entlang einer z-Achse erzeugen, die sogenannte longitudinale Magnetisierung. Zudem präzedieren die Protonen um die z-Achse, d.h. die Rotationsachse selbst ändert konstant ihre Orientierung entlang der Mantelfläche eines Kegels. Die Präzessionsfrequenz entspricht der Larmor-Frequenz. Die MRT nutzt diesen Effekt, um Resonanz zwischen Spins und einem oszillierenden magnetischen Feld senkrecht zu B_0 durch einen Wechselstrom in den Radiofrequenzspulen zu erzeugen (sog. Exzitation, Kuperman 2000).

Dabei wird der Magnetisierungsvektor M aus der z-Achse in die xy-Ebene des Magnetfeldes B_0 gekippt, entsprechend der Orientierung des zugeschalteten Magnetfeldes. Die Projektion des Magnetisierungsvektors M (M_{xy}) präzediert nun in der xy-Ebene und induziert einen Wechselstrom in der MR-Empfängerspule. Der Winkel zwischen M und der z-Achse wird flip-Winkel genannt. Nur im Falle eines flip-Winkels von 90° würde M vollständig in der xy-Ebene präzedieren und die longitudinale Magnetisierung betrüge $M_z=0$. Eine vermehrte antiparallele Ausrichtung von Spins, die mit einem höheren energetischen Zustand assoziiert ist, reduziert zusätzlich die longitudinale Magnetisierung, da sich Spins entlang z gegenseitig auslöschen (Toga und Mazziotta 2002). Zudem präzedieren die Spins phasenkohärent. Deshalb addieren sich jetzt die Magnetisierungsvektoren in der xy-Ebene, was eine transverse Magnetisierung erzeugt. Nach Exzitation fällt das MR-Signal ab und die longitudinale Magnetisierung M_z wird wiederhergestellt. Diese Zeit wird als T_1 bezeichnet. Die transverse Magnetisierung nimmt ab, weil die Spins ihre Phasenkohärenz verlieren. Die Zeit, die für diesen Vorgang benötigt wird, wird mit T_2 bezeichnet (Kuperman 2000).

Die Intensität S des MR-Signals hängt von einer Reihe gewebespezifischer Parameter wie auch der MR-Sequenz ab: $S = PD \cdot \left(1 - e^{-TR/T1}\right) \cdot e^{-TE/T2} \cdot e^{-b\,D}$. PD ist die Protonendichte und hängt vom Wassergehalt des Gewebes ab. D ist ein Maß der Wasserdiffusion, da erregte Spins dem Signal durch Brown'sche Molekularbewegung verlorengehen. TR, TE und b können innerhalb der MR-Sequenz manipuliert werden. TR ist die Repetitionszeit, also das Intervall zwischen zwei Spin-Exzitationen. Wenn die TR kurz ist (T_1-Wichtung), kann M_z nur in Geweben mit kurzer T_1 wiederhergestellt werden und trägt nur hier zum MR-Signal bei. TE ist die Echozeit. Dies ist die Zeitspanne zwischen Spin-Exzitation und Messung des MR-Signals. Um das MR-Signal zu erfassen, müssen die Spins erneut in Phase präzedieren. Dies kann z.B. durch einen 180°-Refokussierungspuls bei Spin-Echo-Sequenzen geschehen. Wird eine lange TE eingesetzt (T_2-Wichtung), haben Gewebe mit langer T_2 noch eine relevante transverse Magnetisierung, aber Gewebe mit kurzer T_2 produzieren nur ein schwaches Signal. Der Effekt von Protonendiffusion kann durch b gesteuert werden (Kuperman 2000, Mori und Zhang 2006).

1.4.4 MAGNETISATION-PREPARED RAPID ACQUISITION GRADIENT ECHO ZUR ANATOMISCHEN ZEREBRALEN BILDGEBUNG

Gradienten-Echo (GRE)-Sequenzen nutzen Phasen- und Frequenzkodierung entlang der xy-Ebene um die Herkunft des MR-Signals zu lokalisieren. Im Gegensatz zu Spin-Echo-Sequenzen wird hier der Schichtselektionsgradient zur Lokalisierung entlang der z-Achse unmittelbar nach der Spin-

Erregung umgekehrt, um die Spins zu refokussieren. Flip-Winkel betragen in GRE-Sequenzen in der Regel <90°, sodass M_z nicht von null regeneriert werden muss und T_1 kurz ist. So kann die TR kurz gewählt werden, was die Messzeit minimiert. Als Rapid acquisition gradient echo (RAGE) werden Sequenzen bezeichnet, deren TR weiter verkürzt wurde, um Bewegungsartefakte zu vermeiden (Kuperman 2000, Bernstein et al. 2004).

Bei magnetisation-prepared rapid gradient echo (MPRAGE)-Sequenzen geht der RAGE-Sequenz ein Magnetisierungsschritt (magnetisation preparation, MP) voraus, um den T_1-Kontrast zu steigern. Dieser wird von einer Phase gefolgt, in der die Magnetisierung wiederhergestellt wird. Die MP umfasst einen also Inversionspuls gefolgt von einem Verzögerungsintervall und optionaler Gradientenschaltung, um die transverse Magnetisierung zu neutralisieren. Ein optimaler MP-Inversionspuls schwenkt die longitudinale Magnetisierung um 180°, sodass der Magnetisierungsvektor M_z negativ wird, ohne dass eine transverse Magnetisierung entsteht. Die Wiederherstellungsperiode ist ein variables Intervall, in der sich die longitudinale Magnetisierung langsam wieder erholt. Aufgrund unterschiedlicher gewebespezifischer T_1, ist das Ausmaß, zu dem M_z dabei wieder seinen Ursprungszustand erreicht, je nach Gewebe unterschiedlich. Dies führt zu starken Unterschieden in der nachfolgenden transversen Magnetisierung. In der Regel folgen mehrere RAGE-Sequenzen einer MP, um die Bildakquise zu beschleunigen.

Der Einsatz von MP-Pulsen verbessert das Verhältnis von Kontrast zu Hintergrundrauschen in T_1-gewichteten Bildern, und verbessert so die Differenzierbarkeit von weißer und grauer Substanz (Mugler und Brookeman 1991).

1.4.5 Anatomische Segmentierung von MRT-Daten

Die manuelle Segmentierung stellt den Goldstandard bei volumetrischen Analysen von cMRT-Datensätzen dar (Fischl et al. 2004). Sie ist jedoch bei großen Datensätzen zeitaufwendig und die Reliabilität ist häufig gering, vor allem bei geringer Übung des Wissenschaftlers (Collins et al. 1995). Bezüglich des BFCS besteht das Problem, dass diese Struktur in üblichen MRT-Sequenzen kaum mit dem Nachbargewebe kontrastiert. Daher bieten hier automatisierte Algorithmen unter Anwendung probabilistischer Karten eine Alternative (Wolf et al. 2014).

1.4.5.1 SPM und DARTEL

Die SPM Software wird vom Functional Imaging Laboratory (FIL) des Wellcome Trust Centre for Neuroimaging am Institute of Neurology (UCL, London, UK) bereitgestellt (https://www.fil.ion.ucl.ac.uk/spm/). Teipel (et al. 2005) hat SPM erstmals zur Segmentierung des BFCS genutzt. In einer Folgestudie haben sie die Verwendung der DARTEL-Toolbox zusammen mit einer probabilistischen Karte zur Segmentierung des BFCS beschrieben (Grothe et al. 2010, Zaborszky et al. 2008).

In dieser Arbeit wurden die T_1-gewichteten MPRAGE-Daten mit den jeweils aktuellen SPM-Versionen 8 und 12 ausgewertet. SPM lässt zahlreiche Modifikationen der Algorithmen zu. Für diese Studien wurden die Standardeinstellungen beibehalten.

Vor Partitionierung der MRT-Datensätze in graue und weiße Substanz sowie weitere Gewebetypen wurden die Datensätze nach Standardvorgabe des Montreal Neurological Institute (MNI)

ausgerichtet (sog. Alignment, Ashburner und Friston 2005). Das ist notwendig, weil SPM voraussetzt, dass das Signal aus korrespondierenden Voxeln (Bildpunkten) aus ebenfalls korrespondierenden Hirnregionen stammt (Friston und Frackowiak 2004). Manuelles Alignment nach MNI-Standard kann durch Positionierung der anterioren Kommissur als Landmarke nah am Ursprung eines Referenzkoordinatensystems geschehen, sodass anteriore und posteriore Kommissur in eine transversale Ebene fallen. In dieser Studie wurde zusätzlich eine SPM-Erweiterung von Carlton Chu (FIL, UCL, London, UK) und Christophe Phillips (Cyclotron Research Centre, University of Lieges, Belgien) eingesetzt, die diesen Schritt automatisiert (https://github.com/CyclotronResearchCentre/spm_auto_reorient/).

Im Weiteren wurden die Datensätze in einzelne Gewebe segmentiert (graue und weiße Substanz, Liquorräume, übriges Gewebe und Hintergrund). Graue und weiße Substanz wurden anhand der Signalintensität identifiziert und die Voxel der entsprechenden Partition zugeordnet. Nach Alignment im MNI-Standard werden von der SPM-Software automatisch repräsentative Voxel ausgewählt, die mit hoher Wahrscheinlichkeit zum jeweiligen Gewebe gehören. Die Intensitäten dieser Voxel werden dann als Referenzwerte für die Segmentierung verwendet. SPM nutzt zusätzlich die Deformation eines segmentierten Musterdatensatzes, um die Gewebegrenzen zu definieren und erneut repräsentative Voxel für die Gewebeklassifizierung auszuwählen. Im SPM-Algorithmus werden Segmentierung, Bias-Korrektur und Gewebeklassifizierung iterativ durchgeführt (Ashburner and Friston 2005). Die SPM-Segmentierung ergibt eine Datei pro Gewebekategorie. Die Voxelintensität in jeder dieser Dateien repräsentiert die Wahrscheinlichkeit, dass der Voxel zum jeweiligen Gewebe gehört. Diese Dateien wurden in ein DARTEL-kompatibles Format konvertiert.

DARTEL steht für “Differential Anatomical Registration using Exponentiated Lie Algebra” und wurde als Software zur Bildregistrierung vorgestellt. Dieser Algorithmus generiert eine kontinuierliche Eins-zu-Eins Abbildung eines cMRT-Datensatzes auf einen anderen, wobei die Topologie erhalten bleibt. Diese Abbildungen werden als DARTEL flow fields bezeichnet und sind invertierbar sowie als Deformationen kombinierbar. Kombiniert man zum Beispiel eine vorwärts-gerichtete („forward“) Deformation und eine inverse („backward“) Deformation desselben flow fields, erhält man eine Identitätstransformation, bei der jeder Punkt im cMRT seine Ausgangskoordinaten beibehält – das Ergebnis ist also der Ursprungsdatensatz (Ashburner 2007). Kombinationen aus verschiedenen DARTEL flow fields bieten ein flexibles Gerüst für automatisierte Segmentierungen von cMRT-Datensätzen. Wurde eine Struktur in einem oder mehreren cMRT-Datensätzen identifiziert und markiert, können die Markierungen durch DARTEL-basierte Deformationen auf einen beliebigen anderen Datensatz übertragen werden. Verglichen mit anderen etablierten automatischen Bildregistrierungsprogrammen erreicht DARTEL eine hohe Konkordanz mit Ergebnissen manueller Registrierung. DARTEL hat keinen fest implementierten cMRT-Atlas, sodass es leicht für die Segmentierung einer beliebigen zu untersuchenden Hirnregion (region of interest, ROI) genutzt werden kann. Der Algorithmus ist wenig anfällig für Scanner-Effekte und vollständig automatisiert (Klein et al. 2009).

In dieser Arbeit wurde die DARTEL-Toolbox in SPM genutzt, um DARTEL-Templates basierend auf cMRT-Datensätzen der Studienpopulationen zu erstellen. DARTEL-Templates entstehen durch Mittlung der individuellen cMRTs, wobei mehrere Templates unterschiedlicher Bildschärfe erstellt

werden. Im nächsten Schritt müssen flow fields berechnet werden, die die Abbildung des individuellen cMRT-Datensatzes auf die Templates beschreiben. Zusätzlich wurde das flow field für die Abbildung eines MRT-Referenzdatensatzes (Colin27-Datensatz, http://www.bic.mni.mcgill.ca/ServicesAtlases/Colin27) auf das Template erstellt. Für Colin27 gibt es eine probabilistische Karte des BFCS (Holmes et al. 1998, Zaborszky et al. 2008).

Ein forward flow field beschreibt die Abbildung des DARTEL-Templates auf den individuellen cMRT-Datensatz, wohingegen ein backward flow field die Abbildung auf das DARTEL-Template beschreibt. Deshalb besteht eine Deformation, die Colin27 und die probabilistische Karte auf das individuelle cMRT abbildet aus einer „backward“ Deformation von Colin27 auf das Template und einer „forward“ Deformation vom Template zum cMRT des Probanden.

Methoden, welche die Deformation eines cMRT-Atlas oder einer probabilistischen Karte zur Segmentierung einzelner cMRTs nutzen, wurden von verschiedenen Autoren für volumen- wie auch oberflächenbasierte Segmentierungen kortikaler und subkortikaler Regionen beschrieben. Diese Herangehensweise erlaubt die flexible Kombination von Atlanten mit einzelnen Algorithmen (Collins et al. 1995). In dieser Arbeit wurde ein probabilistischer Atlas des basalen Vorderhirns von Zaborszky (et al. 2008) verwendet. Dieser Atlas basiert auf dem Colin27-Referenzdatensatz, in dem alle Voxel markiert wurden, die mit einer bestimmten Wahrscheinlichkeit cholinerge Neuronen beinhalten. Da die Abbildung von Colin27 auf das cMRT eines Probanden ebenfalls für die Abbildung des probabilistischen Atlanten gilt, können so BFCS-Volumina im cMRT bestimmt werden. Das Volumen wurde anhand der zugewiesenen Voxelzahl im deformierten Atlas ermittelt, wofür die Software 3D-Slicer (https://www.slicer.org/) und eine SPM-Erweiterung von Adrian Imfeld verwendet wurde (log_roi_batch, http://www.aimfeld.ch/neurotools/neurotools.html).

1.4.5.2 Probabilistische Karten des BFCS

Es gibt mehrere Atlanten des BFCS, die von Teipel (et al. 2005), Kiliman (et al. 2014) und Zaborszky (et al. 2008) beschrieben wurden. In dieser Arbeit wurde der probabilistische Atlas des BFCS von Zaborszky verwendet, da er im Gegensatz zu den anderen auf histologischen Schnitten mehrerer Individuen basiert und angesichts der hohen interindividuellen anatomischen Variabilität des BFCS repräsentativer ist. Für diesen Atlas wurden post-mortem cMRTs von zehn Körperspendern (37-85 Jahre) ohne dokumentierte neurologische oder psychiatrische Diagnose gesammelt. T1-gewichtete Sequenzen bei 1,5 Tesla Feldstärke wurden verwendet. Die Gehirne wurden fixiert und in Paraffin eingebettet. In koronaren Schnitten wurden Zellkörper mit einer modifizierten Silberfärbung nach Gallya angefärbt. Regionen mit gehäuften, magnozellulären Zytosomata wurden den cholinergen Sektoren entsprechend einer Modifikation von Mesulams Nomenklatur zugeordnet. Gallyas Methode ist keine für cholinerge Neuronen spezifische Färbung, dennoch ermöglicht die spezifische Morphologie eine Identifizierung der Zellen anhand ihrer Somata. Da ca. 90% der magnozellulären Neuronen im Sektor Ch4 cholinerg sind, kann mit dieser Methode das BFCS gut abgegrenzt werden (Zaborszky et al. 2008).

Die segmentierten Areale der histologischen Schnitte wurde auf die post-mortem cMRTs übertragen, wobei fixierungsbedingte Verzerrungen korrigiert werden mussten. Die dreidimensionalen Rekonstruktionen des BFCS der Körperspender wurden dann auf den T1-

gewichteten MRT-Rerefenzdatensatz Colin27 abgebildet. Probabilistische Karten wurden für vier Kompartimente des BFCS erstellt (Zaborszky et al. 2008).

1.4.5.3 Freesurfer

Freesurfer ist eine Segmentierungssoftware für Kortex und subkortikale Strukturen, die vom Laboratory for Computational Neuroimaging am Athinoula A. Martinos Center for Biomedical Imaging bereitgestellt wird.

Ähnlich wie SPM beginnt Freesurfer mit einer Bildregistrierung, orientiert sich hierbei jedoch nicht am MNI, sondern Talairach-Standard (Talairach 1993). Automatisch korrigiert Freesurfer Bildartefakte durch Feldinhomogenität und erstellt einen segmentierten Datensatz, der nur noch Hirngewebe ohne umliegende Strukturen enthält. Freesurfer identifiziert dann die weiße Substanz, entfernt übrige subkortikale Strukturen und erstellt zwei separate Datensätze für beide Hemisphären. Die Grenzfläche zwischen grauer und weißer Substanz kann aus diesen Datensätzen konstruiert werden und genutzt werden, um anschließend die Pia-Kontaktfläche zu konstruieren, welche die äußere Grenzfläche des Kortex beschreibt (Dale et al. 1999, Fischl und Dale 2000). Dieses Verfahren wurde gewählt, weil die Pia-Oberfläche einerseits zur Segmentierung des Kortex notwendig, ihre Konstruktion jedoch technisch schwierig ist, da Pia Mater und Kortex nur geringfügig kontrastieren und Segmentierungsfehler durch Kontakte benachbarter Gyri häufig auftreten. Die Grenzfläche von grauer und weißer Substanz kann wegen des höheren Kontrastes leichter bestimmt werden und die Konstruktion der Pia-Oberfläche leiten. Dabei werden Form und metrische Eigenschaften der subkortikalen Grenzfläche beibehalten, während diese der Pia-Kontaktfläche angenähert wird (Destrieux et al. 2010, Fischl 2012). Topologische Defekte in der Pia-Kontaktfläche (z.B. Löcher durch Bildartefakte), die sphärische Verzerrung verhindern, werden korrigiert und es wird ein Deformation berechnet, welche die Pia-Oberfläche anschließend auf einer Kugel abbildet (Fischl et al. 2001, 2012).

Freesurfer parzelliert den Kortex basierend auf einem ebenfalls sphärischen, Oberflächen-definierten Atlas. Dabei wird die globale Wahrscheinlichkeit berücksichtigt, dass sich an einer Koordinate eine bestimmte Struktur befindet, sowie lokale anatomische Beziehungen der Strukturen untereinander (z.B. dass der Gyrus praecentralis niemals posterior zum Gyrus postcentralis liegt, Fischl et al. 2004). Der Atlas selbst basiert auf 24 manuell segmentierten T1-gewichteten 1,5T-MRT-Datensätzen von gesunden Probanden (18-25 Jahre alt, 12 Frauen). Er erlaubt mit hoher Reliabilität die automatische Segmentierung 74 Sulci und Gyri, die in Duvernoys Nomenklatur aufgeführt werden (Destrieux et al. 2010).

1.4.6 NEUROPSYCHOLOGISCHE DATEN

Sowohl in der Genetics of Nicotine Dependence and Neurobiological Phenotypes-Studie als auch im BioCog-Projekt wurden umfangreichen neuropsychologische Testungen durchgeführt. Analysiert wurden sowohl Einzeltests der exekutiven Funktion (TMT und Stroop-Test) wie auch die globale kognitive Leistungsfähigkeit.

Das Konzept einer globalen kognitiven Leistungskomponente „g“ beruht auf dem Befund, dass Ergebnisse aus verschiedensten kognitiven Tests miteinander korrelieren, sodass sich ein globales

„g“ aus Ergebnissen einer kompletten Testbatterie ableiten lässt (Johnson et al. 2004, 2008). In dieser Arbeit wurde eine Principal Component Analysis (PCA) durchgeführt, um „g“ aus den Einzeltests der kognitiven Testbatterie zu extrahieren (Staff et al. 2006, Shenkin et al. 2009). In der PCA wurden über lineare Kombinationen der ursprünglichen Variablen, also der Ergebnisse aus einzelnen Test der gesamten Testbatterie, ebenso viele Hauptkomponenten konstruiert. Dazu wurden die Variablen zunächst standardisiert, d.h. um den Mittelwert zentriert und auf eine Standardabweichung skaliert, sodass alle Variablen den Mittelwert 0 und Standardabweichung 1 haben. Einzelne Variablen wurden transformiert, damit sie sich einer Normalverteilung annähern. Dann wurde die erste Hauptkomponente (prinicipal component) so konstruiert, dass ihre Varianz maximiert wird. Anschließend wurden ebenso weitere Hauptkomponenten konstruiert, die orthogonal zur ersten ausfielen. Das bedeutet, dass Hauptkomponenten nicht miteinander korreliert sind und eine Komponente stets weniger Varianz in den Testergebnissen erklärt als die zuvor konstruierte. Folglich entspricht die erste Hauptkomponente der globalen kognitiven Komponente „g“, da sie die meiste Varianz in den Einzeltestergebnissen erklärt. Die Relevanz der einzelnen Hauptkomponenten wurde anhand von Eigenwert und am Anteil der erklärten Varianz beurteilt. Der Eigenwert ist die Varianz der Hauptkomponente. Wenn sie größer als 1 ist, erklärt die Komponente mehr Varianz als eine Ursprungsvariable, also das Ergebnis in einem einzelnen Test. Eigenwerte für alle Hauptkomponenten wurden im Cattell-Scree-Plot dargestellt. Die erste Hauptkomponente bildet „g“ dann gut ab, wenn ihr Eigenwert einerseits einen hohen Wert hat und andererseits ein großer Abstand zwischen dem ersten Eigenwert und den nachfolgenden besteht, d.h. die übrigen Komponenten nur sehr wenig Varianz in den kognitiven Testdaten erklären. Zudem muss die erste Hauptkomponente „g“ mit allen Ursprungsvariablen gut korrelieren, also hohe „component loadings“ haben (Keho 2012).

1.5 ERGEBNIS

In dieser Arbeit wurde die Assoziation von Subregionen des Nucleus basalis Meynert und exekutiver Funktion in einer Gruppe junger, gesunder Probanden untersucht. Das Volumen des linken NBM ist mit der Leistungsfähigkeit im TMT assoziiert, aber nicht mit dem Stroop-Effekt. Dieser Effekt folgt einem U-förmigen Zusammenhang, sodass geringe wie auch sehr große Volumina mit schlechteren Testergebnissen assoziiert sind. In einer supplementären Analyse wurde zusätzlich untersucht, ob das Ergebnis durch die Inklusion von Rauchern und Niemals-Rauchern beeinflusst wurde. Die Gruppen unterscheiden sich nicht hinsichtlich des NBM-Volumens, noch beeinflusste er die Assoziation zwischen Kognition und Volumen.

Zusätzlich wurde der Zusammenhang von BFCS-Volumen, Hirnvolumen und BPF mit globaler und testspezifischer Kognition bei gesunden, älteren Probanden untersucht. Das BFCS-Volumen ist mit globaler Kognition „g“ assoziiert, jedoch ist dieser Zusammenhang abhängig von einer stärkeren Assoziation zwischen globaler Kognition und Hirnvolumen. Das BFCS-Volumen ist zudem mit dem Ergebnis diverser Einzeltests assoziiert, jedoch sind diese Zusammenhänge schwächer verglichen mit „g“. Bei zwei Tests der allgemeinen Reaktionszeit und der Motorfunktion ist die Stärke des Zusammenhangs abhängig vom Leistungsniveau der untersuchten Gruppe. Die Assoziation ist bei Gruppen mit niedrigerem Leistungsniveau stärker. BPF ist ebenfalls mit der globalen Kognition assoziiert. Dieser Effekt ist unabhängig vom BFCS-Volumen.

In der dritten Arbeit wurde der Zusammenhang zwischen globaler und lokaler grauer Substanz, der BPF und exekutiver Funktion in Teil B des TMT bei gesunden älteren Probanden untersucht. Das globale Volumen der grauen Substanz ist stärker mit exekutiver Funktion assoziiert als lokale Volumina der einzelnen Lobi. Die BPF ist nur in einzelnen Modellen unabhängig von lokalen Volumina signifikant mit dem Ergebnis im TMT-B assoziiert. In einer supplementären Analyse wurde zusätzlich die Assoziation mit der Differenz der Zeiten zur Vervollständigung von Teil A und B des TMT untersucht. Diese wird in allen Modellen auch signifikant von der BPF beeinflusst. Zudem zeigte sich, dass das Temporallappenvolumen stärker mit der Zeitdifferenz assoziiert ist als das Volumen der globalen grauen Substanz.

1.6 DISKUSSION

In der ersten Publikation dieser Arbeit wurden zum ersten Mal Assoziationen zwischen dem Volumen des NBM, einer Kernregionen des BFCS, und exekutiver Funktion bei jungen gesunden Probanden untersucht. Die Assoziation gilt für beide Teile des TMT, sodass die Effekte vermutlich über Einflüsse auf visuelle Funktionen wie Suchgeschwindigkeit statt exekutiver Funktionen vermittelt werden (Crowe 1998). Zusätzlich messen beide Teile motorische Funktionen, aber da die cholinerge Innervation des Motorkortex spärlich ist, scheint eine Beeinflussung durch das Volumen cholinerger Systeme unwahrscheinlicher (Mesulam et al. 1983). Der Zusammenhang zwischen Volumen und Testergebnis ist parabelförmig, sodass anzunehmen ist, dass sowohl ein Mangel wie auch ein Überschuss an Acetylcholin die kognitive Leistungsfähigkeit beeinträchtigen (Holley et al. 1995, Bentley et al. 2011).

Bisherige Arbeiten untersuchten meist ältere Populationen (Grothe et al. 2010, 2016, Choi et al. 2012, Wolf et al. 2014). Butler (et al. 2012) beschrieb zwar eine ähnliche junge Population, suchte jedoch explizit nach Assoziationen des medialen Septumvolumens mit Gedächtnisfunktion. Damit ist unsere Studie bisher einzigartig und bedarf der Bestätigung durch zukünftige Arbeiten. Dabei sollte berücksichtigt werden, dass die hier untersuchte Stichprobe relativ klein und inhomogen ist, da sie aus einer Gruppe von Rauchern sowie Probanden besteht, die niemals geraucht haben. Damit ist die Übertragbarkeit auf die allgemeine Bevölkerung eingeschränkt und der Raucherstatus ein potentieller Störfaktor. Supplementäre Analysen, die das Rauchverhalten berücksichtigten, ergaben jedoch keinen Hinweis darauf, dass das Ergebnis verzerrt wurde. Die Studienteilnehmer wurden zudem über Melderegister zufällig aus der Allgemeinbevölkerung rekrutiert, was für eine Generalisierbarkeit der Ergebnisse spricht.

In einer zweiten Publikation wurden Assoziationen des BFCS-Volumens mit globaler Kognition und Ergebnissen in Einzeltests einer umfangreichen neuropsychologischen Testung untersucht. Ähnliche Untersuchungen bei gesunden älteren Probanden wurden bereits von Wolf (et al. 2014) durchgeführt, dessen Ergebnisse aufgrund der kleinen Stichprobe und des hohen Intelligenzquotienten von 138±16 kaum auf die Allgemeinbevölkerung anwendbar sind. Dennoch decken sich die Ergebnisse von Wolf und dieser Studie in dem Punkt, dass eine Assoziation zwischen BFCS-Volumen und globaler Kognition besteht. Weitere Studien von Grothe (et al. 2010, 2016) untersuchten die Assoziation mit diversen Einzeltests, ohne jedoch einen Nachweis bei gesunden Probanden erbringen zu können. Erklärungen können einerseits eine zu geringe statistische Power für die Vielzahl neuropsychologischer Tests sein, andererseits muss

berücksichtigt werden, dass in Grothes Arbeiten die Analysen separat für gesunde Probanden und Patienten mit MCI durchgeführt wurden. Es ist also wahrscheinlich, dass Grothes Kontrollgruppen stets aus einer Subgruppe mit überdurchschnittlich gut erhaltener kognitiver Leistungsfähigkeit bestanden, und übrige Probanden der MCI-Gruppe zugeordnet wurden. Damit ist die Spannweite der kognitiven Leistung in diesen Kontrollgruppen möglicherweise zu gering, um einen Effekt nachweisen zu können. In der BioCog-Studie wurde zwar ein Demenz-Screening zum Studieneinschluss durchgeführt, aber da keine umfassende MCI-Diagnostik durchgeführt wurde, umfasst die hier präsentierte Studie ein breiteres Spektrum der alterstypischen kognitiven Leistungsfähigkeit. Grothe beschrieb jedoch signifikante Zusammenhänge von BFCS-Volumen und Kognition bei MCI-Patienten, die durch diese Arbeit untermauert werden konnten. In dieser Arbeit wurde zum ersten Mal Quantilenregression zur Analyse dieser Fragestellung eingesetzt: Hierdurch zeigte sich, dass die Assoziation von Kognition und BFCS-Volumen auch bei gesunden Probanden stärker war, wenn sie schlechter in einigen Tests abschnitten.

Zusätzlich erbrachte diese Arbeit neue Erkenntnisse hinsichtlich des Zusammenhangs von globalen und lokalen Hirnvolumina sowie globaler Kognition und spezifischen Tests. So ist dies die erste Arbeit, die zeigt, dass die Assoziation zwischen BFCS-Volumen und einzelnen kognitiven Tests hauptsächlich von einem unspezifischen Zusammenhang von Hirnvolumen und globaler Kognition abhängt. Auch ist dies die erste Arbeit, die einen Zusammenhang von BPF und globaler Kognition zeigen konnte. Damit widerspricht sie dem Ergebnis von Shenkin (et al. 2009), was auf Unterschiede im Messverfahren von BPF, aber auch der größeren Altersspanne in der BioCog-Studie mit einer möglicherweise breiteren Spanne altersabhängiger Verluste der kognitiven Leistungsfähigkeit zusammenhängen könnte.

In beiden Publikationen wurde der Trail-Making-Test als Test der exekutiven Funktionen untersucht. Der nicht-lineare Zusammenhang zwischen Volumen und exekutiver Funktion bei jungen Probanden kann darauf zurückgeführt werden, dass neben einem Mangel an kortikalem Acetylcholin auch ein Überschuss zu kognitiver Dysfunktion führen könnte. Dieser Befund ließ sich in der Stichprobe älterer Probanden nicht reproduzieren. Dies ist dadurch erklärbar, dass durch altersabhängige zerebrale Atrophie kaum Patienten eingeschlossen wurden, deren BFCS-Volumen groß genug war, einen Überschuss zu produzieren. Zusätzlich unterschieden sich die Analysemethoden zwischen beiden Arbeiten. So wurde in der ersten Arbeit zur jungen Population das Volumen des NBM entsprechend des Gesamthirnvolumens adjustiert, wohingegen in der zweiten Arbeit das nicht adjustierte BFCS-Volumen untersucht wurde. Es ist möglich, dass das adjustierte Volumen eine Tendenz zum Acetylcholin-Überschuss anzeigt, da es das Verhältnis von Acetylcholinproduktion zum Bedarf gemessen am Hirnvolumen besser reflektiert.

Zuletzt zeigt sich beim Vergleich der Ergebnisse aus beiden Publikationen, dass bei es bei älteren Probanden wenig Hinweise auf spezifische Assoziationen zwischen cholinergen Kernvolumina und einzelnen kognitiven Funktionen gibt, wohingegen sich bei jungen Probanden ein spezifischer Zusammenhang zwischen lokalen Volumina und der exekutiven Funktion zeigte, der unabhängig vom gesamten Hirnvolumen ist. Eine Erklärung hierfür ist, dass neben dem cholinergen System auch andere Regionen im Alter von Atrophie betroffen sind, sodass einzelne lokale Biomarker nur schlecht mit die Funktion des gesamten zentralen Nervensystems abbilden.

In der dritten Publikation wurden die Assoziationen von globaler und lokaler grauer Substanz, der BPF und exekutiver Funktion in einer älteren Population untersucht. Dabei ist dies die erste Arbeit, die Assoziationen zwischen Trail-Making-Test, BPF und grauer Substanz untersucht. Ähnlich wie beim BFCS scheint die globale graue Substanz stärker mit dem Testergebnis assoziiert zu sein als Hirnlappenvolumina. Dies stützt die Hypothese aus der vorherigen Publikation, dass lokale Volumina komplexe kognitive Funktionen nur schlecht abbilden. Die BPF ist nur sehr schwach mit dem Ergebnis im TMT-B assoziiert. Supplementäre Analysen der Differenz der Testergebnisse der Teile A und B zeigten jedoch eine stärkere, sowie vom Volumen der grauen Substanz unabhängige Assoziation der BPF. Die Differenz wird berechnet, um Effekte rein motorischer und visueller Fähigkeiten auf das Testergebnis zu korrigieren (Lamberty et al. 1994, Crowe 1998). Das Ergebnis legt nahe, dass Hirnatrophie einen stärkeren Einfluss auf komplexe kognitive Fähigkeiten als Motorik und einfache visuelle Funktionen im Alter hat. Auch zeigte sich, dass der Temporallappen stärker mit der Ergebnisdifferenz im TMT assoziiert ist als das Gesamtvolumen der grauen Substanz. Eine Erklärung hierfür ist, dass Teil B des TMT motorische, visuelle und exekutive Funktionen prüft, worin eine Vielzahl kortikaler Areale involviert sind. Da in der Ergebnisdifferenz der beiden Teile des TMT Motorik und visuelle Effekte kaum Einfluss haben, können hier eher spezifische Effekte einzelner kortikaler Areale auf die exekutive Funktion beobachtet werden.

Shenkin (et al. 2009) untersuchte diese Fragestellung mit dem Moray House Test Nr. 12 als Test der exekutiven Funktion, jedoch mit dem Ergebnis, dass Assoziationen zwischen Lappenvolumina und exekutiver Funktion vom intrakraniellen Volumen abhingen und kaum spezifische Effekte hätten. Ebenso berichtete die Studie nicht über einen Einfluss der BPF. Neben den unterschiedlichen neuropsychologischen Tests gelten jedoch auch hier die bereits angeführten Kritikpunkte.

1.7 LITERATURVERZEICHNIS

Anand, P., Singh, B., 2013. A review on cholinesterase inhibitors for Alzheimer's disease. Arch. Pharm. Res. 36, 375–399.

Ashburner, J., 2007. A fast diffeomorphic image registration algorithm. NeuroImage 38, 95–113.

Ashburner, J., Friston, K.J., 2005. Unified segmentation. NeuroImage 26, 839–851.

Baldanzi, S., Cecchi, P., Fabbri, S., Pesaresi, I., Simoncini, C., Angelini, C., Bonuccelli, U., Cosottini, M., Siciliano, G., 2016. Relationship between neuropsychological impairment and grey and white matter changes in adult-onset myotonic dystrophy type 1. Neuroimage Clin 12, 190–197.

Bentley, P., Driver, J., Dolan, R.J., 2011. Cholinergic modulation of cognition: insights from human pharmacological functional neuroimaging. Prog. Neurobiol. 94, 360–388.

Bernstein, M.A., King, K.F., Zhou, X.J., 2004. Handbook of MRI Pulse Sequences. Elsevier Science & Technology, San Diego, UNITED STATES.

Bettcher, B.M., Mungas, D., Patel, N., Elofson, J., Dutt, S., Wynn, M., Watson, C.L., Stephens, M., Walsh, C.M., Kramer, J.H., 2016. Neuroanatomical Substrates of Executive Functions: Beyond Prefrontal Structures. Neuropsychologia 85, 100–109.

Birks, J.S., Grimley Evans, J., 2015. Rivastigmine for Alzheimer's disease. Cochrane Database Syst Rev CD001191.

Birks, J.S., Harvey, R.J., 2018. Donepezil for dementia due to Alzheimer's disease. Cochrane Database Syst Rev 6, CD001190.

Butler, T., Blackmon, K., Zaborszky, L., Wang, X., DuBois, J., Carlson, C., Barr, W.B., French, J., Devinsky, O., Kuzniecky, R., Halgren, E., Thesen, T., 2012. Volume of the human septal forebrain region is a predictor of source memory accuracy. J Int Neuropsychol Soc 18, 157–161.

Butler, T., Harvey, P., Deshpande, A., Tanzi, E., Li, Y., Tsui, W., Silver, C., Fischer, E., Wang, X., Chen, J., Rusinek, H., Pirraglia, E., Osorio, R.S., Glodzik, L., de Leon, M.J., 2018. Basal forebrain septal nuclei are enlarged in healthy subjects prior to the development of Alzheimer's disease. Neurobiol. Aging 65, 201–205.

Cai, L., Gibbs, R.B., Johnson, D.A., 2012. Recognition of novel objects and their location in rats with selective cholinergic lesion of the medial septum. Neurosci. Lett. 506, 261–265.

Callahan, B.L., Ramirez, J., Berezuk, C., Duchesne, S., Black, S.E., for the Alzheimer's Disease Neuroimaging Initiative, 2015. Predicting Alzheimer's disease development: a comparison of cognitive criteria and associated neuroimaging biomarkers. Alzheimer's Research & Therapy 7, 68.

Cantero, J.L., Zaborszky, L., Atienza, M., 2017. Volume Loss of the Nucleus Basalis of Meynert is Associated with Atrophy of Innervated Regions in Mild Cognitive Impairment. Cereb Cortex 27, 3881–3889.

Choi, S.H., Jung, T.M., Lee, J.E., Lee, S.-K., Sohn, Y.H., Lee, P.H., 2012. Volumetric analysis of the substantia innominata in patients with Parkinson's disease according to cognitive status. Neurobiol. Aging 33, 1265–1272.

Collins, D.L., Holmes, C.J., Peters, T.M., Evans, A.C., 1995. Automatic 3-D model-based neuroanatomical segmentation. Human Brain Mapping 3, 190–208.

Crowe, S.F., 1998. The differential contribution of mental tracking, cognitive flexibility, visual search, and motor speed to performance on parts A and B of the Trail Making Test. J Clin Psychol 54, 585–591.

Cruz-Gómez, Á.J., Ventura-Campos, N., Belenguer, A., Ávila, C., Forn, C., 2014. The link between resting-state functional connectivity and cognition in MS patients. Mult. Scler. 20, 338–348.

Dale, A.M., Fischl, B., Sereno, M.I., 1999. Cortical surface-based analysis. I. Segmentation and surface reconstruction. Neuroimage 9, 179–194.

Damoiseaux, J.S., Rombouts, S.A.R.B., Barkhof, F., Scheltens, P., Stam, C.J., Smith, S.M., Beckmann, C.F., 2006. Consistent resting-state networks across healthy subjects. Proc Natl Acad Sci U S A 103, 13848–13853.

Davis, P.J.M., Wright, E.A., 1977. A New Method for Measuring Cranial Cavity Volume and Its Application to the Assessment of Cerebral Atrophy at Autopsy. Neuropathology and Applied Neurobiology 3, 341–358.

Deloire, M.S.A., Salort, E., Bonnet, M., Arimone, Y., Boudineau, M., Amieva, H., Barroso, B., Ouallet, J.-C., Pachai, C., Galliaud, E., Petry, K.G., Dousset, V., Fabrigoule, C., Brochet, B., 2005. Cognitive impairment as marker of diffuse brain abnormalities in early relapsing remitting multiple sclerosis. J. Neurol. Neurosurg. Psychiatry 76, 519–526.

Destrieux, C., Fischl, B., Dale, A., Halgren, E., 2010. Automatic parcellation of human cortical gyri and sulci using standard anatomical nomenclature. Neuroimage 53, 1–15.

Difiglia, M., 1987. Synaptic organization of cholinergic neurons in the monkey neostriatum. Journal of Comparative Neurology 255, 245–258.

Fischl, B., 2012. FreeSurfer. NeuroImage, 20 YEARS OF fMRI 62, 774–781.

Fischl, B., Dale, A.M., 2000. Measuring the thickness of the human cerebral cortex from magnetic resonance images. PNAS 97, 11050–11055.

Fischl, B., Liu, A., Dale, A.M., 2001. Automated manifold surgery: constructing geometrically accurate and topologically correct models of the human cerebral cortex. IEEE Transactions on Medical Imaging 20, 70–80.

Fischl, B., van der Kouwe, A., Destrieux, C., Halgren, E., Ségonne, F., Salat, D.H., Busa, E., Seidman, L.J., Goldstein, J., Kennedy, D., Caviness, V., Makris, N., Rosen, B., Dale, A.M., 2004. Automatically parcellating the human cerebral cortex. Cereb. Cortex 14, 11–22.

Friston, K.J., 2004. Human brain function editors, Richard S.J. Frackowiak ... [et. al.]., 2nd ed. ed. Elsevier Academic Press, Amsterdam ; Boston.

Grothe, M., Heinsen, H., Teipel, S., 2013. Longitudinal measures of cholinergic forebrain atrophy in the transition from healthy aging to Alzheimer's disease. Neurobiol. Aging 34, 1210–1220.

Grothe, M., Zaborszky, L., Atienza, M., Gil-Neciga, E., Rodriguez-Romero, R., Teipel, S.J., Amunts, K., Suarez-Gonzalez, A., Cantero, J.L., 2010. Reduction of basal forebrain cholinergic system parallels cognitive impairment in patients at high risk of developing Alzheimer's disease. Cereb. Cortex 20, 1685–1695.

Grothe, M.J., Heinsen, H., Amaro, E., Grinberg, L.T., Teipel, S.J., 2016. Cognitive Correlates of Basal Forebrain Atrophy and Associated Cortical Hypometabolism in Mild Cognitive Impairment. Cereb Cortex 26, 2411–2426.

Harati, H., Barbelivien, A., Cosquer, B., Majchrzak, M., Cassel, J.-C., 2008. Selective cholinergic lesions in the rat nucleus basalis magnocellularis with limited damage in the medial septum specifically alter attention performance in the five-choice serial reaction time task. Neuroscience 153, 72–83.

Hohol, M.J., Guttmann, C.R.G., Orav, J., Mackin, G.A., Kikinis, R., Khoury, S.J., Jolesz, F.A., Weiner, H.L., 1997. Serial Neuropsychological Assessment and Magnetic Resonance Imaging Analysis in Multiple Sclerosis. Arch Neurol 54, 1018–1025.

Holley, L.A., Turchi, J., Apple, C., Sarter, M., 1995. Dissociation between the attentional effects of infusions of a benzodiazepine receptor agonist and an inverse agonist into the basal forebrain. Psychopharmacology (Berl.) 120, 99–108.

Holmes, C.J., Hoge, R., Collins, L., Woods, R., Toga, A.W., Evans, A.C., 1998. Enhancement of MR Images Using Registration for Signal Averaging. Journal of Computer Assisted Tomography 22, 324.

Janssen, M.A.M., Meulenbroek, O., Steens, S.C.A., Góraj, B., Bosch, M., Koopmans, P.P., Kessels, R.P.C., 2015. Cognitive functioning, wellbeing and brain correlates in HIV-1 infected patients on long-term combination antiretroviral therapy. AIDS 29, 2139–2148.

Johnson, W., Bouchard, T.J., Krueger, R.F., McGue, M., Gottesman, I.I., 2004. Just one g: consistent results from three test batteries. Intelligence 32, 95–107.

Johnson, W., Nijenhuis, J. te, Bouchard, T.J., 2008. Still just 1 g: Consistent results from five test batteries. Intelligence 36, 81–95.

Keho, Y., 2012. The Basics of Linear Principal Components Analysis. Principal Component Analysis.

Kilimann, I., Grothe, M., Heinsen, H., Alho, E.J.L., Grinberg, L., Amaro Jr., E., Santos, D., Bento, G.A., Silva, D., Emídio, R., Mitchell, A.J., Frisoni, G.B., Bokde, A.L.W., Fellgiebel, A., Filippi, M., Hampel, H., Klöppel, S., Teipel, S.J., 2014. Subregional Basal Forebrain Atrophy in Alzheimer's Disease: A Multicenter Study. Journal of Alzheimer's Disease 40, 687–700.

Kilimann, I., Hausner, L., Fellgiebel, A., Filippi, M., Würdemann, T.J., Heinsen, H., Teipel, S.J., 2017. Parallel Atrophy of Cortex and Basal Forebrain Cholinergic System in Mild Cognitive Impairment. Cereb. Cortex 27, 1841–1848.

Klein, A., Andersson, J., Ardekani, B.A., Ashburner, J., Avants, B., Chiang, M.-C., Christensen, G.E., Collins, D.L., Gee, J., Hellier, P., Song, J.H., Jenkinson, M., Lepage, C., Rueckert, D., Thompson, P., Vercauteren, T., Woods, R.P., Mann, J.J., Parsey, R.V., 2009. Evaluation of 14 nonlinear deformation algorithms applied to human brain MRI registration. Neuroimage 46, 786–802.

Kuperman, V., 2000. Magnetic Resonance Imaging: Physical Principles and Applications. Elsevier Science & Technology, Burlington, UNITED STATES.

Lamberty, G.J., Putnam, S.H., Chatel, D.M., Bieliauskas, L.A., 1994. Derived Trail Making Test indices: A preliminary report. Neuropsychiatry, Neuropsychology, & Behavioral Neurology 7, 230–234.

Lindenberg, A., Brinkmeyer, J., Dahmen, N., Gallinat, J., Millas, W. de, Mobascher, A., Wagner, M., Schulze-Rauschenbach, S., Gründer, G., Spreckelmeyer, K.N., Clepce, M., Thürauf, N., Goltz, C. von der, Kiefer, F., Steffens, M., Holler, D., Díaz-Lacava, A., Wienker, T., Winterer, G., 2011. The German multi-centre study on smoking-related behavior—description of a population-based case-control study. Addiction Biology 16, 638–653.

MacLullich, A.M.J., Ferguson, K.J., Deary, I.J., Seckl, J.R., Starr, J.M., Wardlaw, J.M., 2002. Intracranial capacity and brain volumes are associated with cognition in healthy elderly men. Neurology 59, 169–174.

Matsumae, M., Kikinis, R., Mórocz, I.A., Lorenzo, A.V., Sándor, T., Albert, M.S., Black, P.M., Jolesz, F.A., 1996. Age-related changes in intracranial compartment volumes in normal adults assessed by magnetic resonance imaging. Journal of Neurosurgery 84, 982–991.

McDaniel, M.A., 2005. Big-brained people are smarter: A meta-analysis of the relationship between in vivo brain volume and intelligence. Intelligence 33, 337–346.

Mesulam, M.M., Mufson, E.J., Levey, A.I., Wainer, B.H., 1983. Cholinergic innervation of cortex by the basal forebrain: cytochemistry and cortical connections of the septal area, diagonal band nuclei, nucleus basalis (substantia innominata), and hypothalamus in the rhesus monkey. J. Comp. Neurol. 214, 170–197.

Mori, S., Zhang, J., 2006. Principles of diffusion tensor imaging and its applications to basic neuroscience research. Neuron 51, 527–539.

Mugler, J.P., Brookeman, J.R., 1991. Rapid three-dimensional T1-weighted MR imaging with the MP-RAGE sequence. J Magn Reson Imaging 1, 561–567.

Parikh, V., Kozak, R., Martinez, V., Sarter, M., 2007. Prefrontal acetylcholine release controls cue detection on multiple timescales. Neuron 56, 141–154.

Pfefferbaum, A., Mathalon, D.H., Sullivan, E.V., Rawles, J.M., Zipursky, R.B., Lim, K.O., 1994. A quantitative magnetic resonance imaging study of changes in brain morphology from infancy to late adulthood. Arch. Neurol. 51, 874–887.

Risacher, S., Shen, L., West, J., Kim, S., McDonald, B., Beckett, L., Harvey, D., Jack, C., Weiner, M., Saykin, A., 2010. Longitudinal MRI atrophy biomarkers: Relationship to conversion in the ADNI cohort. Neurobiol Aging 31, 1401–1418.

Rudick, R.A., Fisher, E., Lee, J.C., Simon, J., Jacobs, L., 1999. Use of the brain parenchymal fraction to measure whole brain atrophy in relapsing-remitting MS. Multiple Sclerosis Collaborative Research Group. Neurology 53, 1698–1704.

Seiler, M., Schwab, M.E., 1984. Specific retrograde transport of nerve growth factor (NGF) from neocortex to nucleus basalis in the rat. Brain Res. 300, 33–39.

Shenkin, S.D., Rivers, C.S., Deary, I.J., Starr, J.M., Wardlaw, J.M., 2009. Maximum (prior) brain size, not atrophy, correlates with cognition in community-dwelling older people: a cross-sectional neuroimaging study. BMC Geriatr 9, 12.

Simić, G., Mrzljak, L., Fucić, A., Winblad, B., Lovrić, H., Kostović, I., 1999. Nucleus subputaminalis (Ayala): the still disregarded magnocellular component of the basal forebrain may be human specific and connected with the cortical speech area. Neuroscience 89, 73–89.

Staff, R.T., Murray, A.D., Deary, I.J., Whalley, L.J., 2006. Generality and specificity in cognitive aging: a volumetric brain analysis. Neuroimage 30, 1433–1440.

Talairach, J., 1993. Referentially oriented cerebral MRI anatomy: an atlas of stereotaxic anatomical correlations for gray and white matter. Thieme ua, Stuttgart u.a.

Teipel, S.J., Flatz, W.H., Heinsen, H., Bokde, A.L.W., Schoenberg, S.O., Stöckel, S., Dietrich, O., Reiser, M.F., Möller, H.-J., Hampel, H., 2005. Measurement of basal forebrain atrophy in Alzheimer's disease using MRI. Brain 128, 2626–2644.

Torelli, F., Moscufo, N., Garreffa, G., Placidi, F., Romigi, A., Zannino, S., Bozzali, M., Fasano, F., Giulietti, G., Djonlagic, I., Malhotra, A., Marciani, M.G., Guttmann, C.R.G., 2011. Cognitive profile and brain morphological changes in obstructive sleep apnea. NeuroImage 54, 787–793.

Vågberg, M., Granåsen, G., Svenningsson, A., 2017. Brain Parenchymal Fraction in Healthy Adults —A Systematic Review of the Literature. PLOS ONE 12, e0170018.

Varjacic, A., Mantini, D., Demeyere, N., Gillebert, C.R., 2018. Neural signatures of Trail Making Test performance: Evidence from lesion-mapping and neuroimaging studies. Neuropsychologia, Special Issue: Lesions and Brain Mapping 115, 78–87.

White, P., Hiley, C.R., Goodhardt, M.J., Carrasco, L.H., Keet, J.P., Williams, I.E., Bowen, D.M., 1977. Neocortical cholinergic neurons in elderly people. Lancet 1, 668–671.

Winterer, G., Androsova, G., Bender, O., Boraschi, D., Borchers, F., Dschietzig, T.B., Feinkohl, I., Fletcher, P., Gallinat, J., Hadzidiakos, D., Haynes, J.D., Heppner, F., Hetzer, S., Hendrikse, J., Ittermann, B., Kant, I.M.J., Kraft, A., Krannich, A., Krause, R., Kühn, S., Lachmann, G., van Montfort, S.J.T., Müller, A., Nürnberg, P., Ofosu, K., Pietsch, M., Pischon, T., Preller, J., Renzulli, E., Scheurer, K., Schneider, R., Slooter, A.J.C., Spies, C., Stamatakis, E., Volk, H.D., Weber, S., Wolf, A., Yürek, F., Zacharias, N., 2018. Personalized risk prediction of postoperative cognitive impairment – rationale for the EU-funded BioCog project. European Psychiatry, Workshop on Schizophrenia and other mental disorders - S. Frangou (Editor in Chief), A. Del Guerra, S. Galderisi (Guest Editors) 50, 34–39.

Wolf, D., Grothe, M., Fischer, F.U., Heinsen, H., Kilimann, I., Teipel, S., Fellgiebel, A., 2014. Association of basal forebrain volumes and cognition in normal aging. Neuropsychologia 53, 54–63.

Yuan, P., Raz, N., 2014. Prefrontal cortex and executive functions in healthy adults: A meta-analysis of structural neuroimaging studies. Neuroscience & Biobehavioral Reviews 42, 180–192.

Zaborszky, L., Hoemke, L., Mohlberg, H., Schleicher, A., Amunts, K., Zilles, K., 2008. Stereotaxic probabilistic maps of the magnocellular cell groups in human basal forebrain. Neuroimage 42, 1127–1141.

Zhang, H., Trollor, J.N., Wen, W., Zhu, W., Crawford, J.D., Kochan, N.A., Slavin, M.J., Brodaty, H., Reppermund, S., Kang, K., Mather, K.A., Sachdev, P.S., 2011. Grey matter atrophy of basal forebrain and hippocampus in mild cognitive impairment. J. Neurol. Neurosurg. Psychiatry 82, 487–493.

2 Anteilserklärungen

2.1 Nucleus Basalis Meynert volume on the Trail-Making-Test are restricted to the left hemisphere

Lammers, F., Mobascher, A., Musso, F., Shah, N.J., Warbrick, T., Zaborszky, L., Winterer, G., 2016. Effects of Ncl. Basalis Meynert volume on the Trail-Making-Test are restricted to the left hemisphere. Brain Behav 6, e00421. https://doi.org/10.1002/brb3.421

Die Genetics of Nicotine Dependence and Neurobiological Phenotypes-Studie, die zu dieser Publikation geführt hat, war zu Beginn der Promotion bereits abgeschlossen. Daher lagen kognitive Daten und MRT-Rohdaten bereits vollständig vor. Im Rahmen dieser ersten Arbeit sollte die Kernmethode, also die MRT-basierte Volumetrie der cholinergen Kerngebiete im basalen Vorderhirn (basal forebrain cholinergic system, BFCS), etabliert werden. Die Hypothese, die auf Basis der Daten geprüft wurde, haben mein Betreuer Prof. Winterer und ich gemeinsam entwickelt. Die Methode zur Volumetrie wurde in unserer Arbeitsgruppe durch mich etabliert. Dies bedeutete im Detail, die notwendige Software zusammenzustellen und die probabilistische Karte des BFCS zu akquirieren und mich in die Methodik selbstständig einzuarbeiten. Ich habe alle Daten selbst ausgewertet und interpretiert. Das Manuskript und alle Grafiken zur Publikation wurden von mir geschrieben und erstellt.

2.2 Basal forebrain cholinergic system volume is associated with general cognitive ability in the elderly

Lammers, F., Borchers, F., Feinkohl, I., Hendrikse, J., Kant, I.M.J., Kozma, P., Pischon, T., Slooter, A.J.C., Spies, C., van Montfort, S.J.T., Zacharias, N., Zaborszky, L., Winterer, G., BioCog consortium, 2018. Basal forebrain cholinergic system volume is associated with general cognitive ability in the elderly. Neuropsychologia 119, 145–156. https://doi.org/10.1016/j.neuropsychologia.2018.08.005

Die Daten zu dieser Publikation stammen aus der BioCog-Studie, die ich von Beginn an als Doktorand begleitet habe. Die Rohdaten wurden zu einem substantiellen Teil von mir am MRT gesammelt, zunächst als assistierender Basic-User, später eigenverantwortlich als Advanced User. (Anmerkung: Im Berlin Center for Advanced Neuroimaging, wo die MRT-Messung durchgeführt werden, gilt die Bestimmung, das Basic-User nur gemeinsam mit einer medizintechnischen Assistentin das MRT nutzen dürfen, während Advanced User die volle Eigenverantwortung für die Messdurchführung übernehmen und daher auch selbstständig den MRT-Scanner zu Forschungszwecken nutzen können.)

Die Hypothese haben Prof. Winterer und ich gemeinsam entwickelt. Mein besonderes Interesse galt dabei dem Aspekt der steigenden Relevanz des BFCS-Volumens in Populationen mit im Alter sinkender kognitiver Leistungsfähigkeit im Gegensatz zur gesamten Stichprobe mit zum Teil sehr gut erhaltener kognitiven Leistungsfähigkeit. Daher habe ich mich in die zusätzliche statistische Methode der Quantilenregression eingearbeitet, um speziell diese Fragestellung in dieser Arbeit beantworten zu können. Die volumetrische Auswertung der MRT-Rohdaten habe ich vollständig

selbst durchgeführt. Alle statistischen Analysen und Interpretationen der Daten habe ich selbst durchgeführt. Das Manuskript mit allen Grafiken habe ich selbst erstellt.

2.3 Size matters: Grey matter brain reserve predicts executive functioning in the elderly

Laubach, M., Lammers, F., Zacharias, N., Feinkohl, I., Pischon, T., Borchers, F., Slooter, A.J.C., Kühn, S., Spies, C., Winterer, G., BioCog Consortium, 2018. Size matters: Grey matter brain reserve predicts executive functioning in the elderly. Neuropsychologia 119, 172–181. https://doi.org/10.1016/j.neuropsychologia.2018.08.008

Die MRT-Rohdaten dieser Arbeit stammen ebenfalls aus der BioCog-Studie und wurden daher zu einem substantiellen Teil von mir erhoben, häufig auch als technisch verantwortlicher Advanced User.

Zur Arbeit selbst stammen einige Anregungen von mir. So habe ich das Konzept der Brain Parenchymal Fraction (BPF), einem Atrophie-Marker, für BioCog vorgeschlagen. Auch habe ich vorgeschlagen, die Interaktion zwischen Volumina und Alter zu testen sowie alternative Maße der exekutiven Funktion im Trail-Making-Test (z.B. die Differenz zwischen den Ergebnissen von Teil A und B) zu berücksichtigen. Dies war mir möglich, weil ich mich bereits in Publikation 1 (Brain and Behavior 2016) mit Interaktionen und Tests der exekutiven Funktion beschäftigt hatte. So habe ich auch die statistische Analyse beratend unterstützt und schließlich bei der Überarbeitung des Manuskripts mitgewirkt.

Unterschrift, Datum und Stempel des betreuenden Hochschullehrers Prof. Georg Winterer

Unterschrift des Doktoranden Florian Lammers

3 Eidesstattliche Versicherung

Ich, Florian Lammers, versichere an Eides statt durch meine eigenhändige Unterschrift, dass ich die vorgelegte Dissertation mit dem Thema: „Strukturelle Determinanten kognitiver Funktionen im MRT“ selbstständig und ohne nicht offengelegte Hilfe Dritter verfasst und keine anderen als die angegebenen Quellen und Hilfsmittel genutzt habe.

Alle Stellen, die wörtlich oder dem Sinne nach auf Publikationen oder Vorträgen anderer Autoren beruhen, sind als solche in korrekter Zitierung kenntlich gemacht. Die Abschnitte zu Methodik (insbesondere praktische Arbeiten, Laborbestimmungen, statistische Aufarbeitung) und Resultaten (insbesondere Abbildungen, Graphiken und Tabellen werden von mir verantwortet.

Meine Anteile an etwaigen Publikationen zu dieser Dissertation entsprechen denen, die in der untenstehenden gemeinsamen Erklärung mit dem/der Betreuer/in, angegeben sind. Für sämtliche im Rahmen der Dissertation entstandenen Publikationen wurden die Richtlinien des ICMJE (International Committee of Medical Journal Editors; www.icmje.og) zur Autorenschaft eingehalten. Ich erkläre ferner, dass mir die Satzung der Charité – Universitätsmedizin Berlin zur Sicherung Guter Wissenschaftlicher Praxis bekannt ist und ich mich zur Einhaltung dieser Satzung verpflichte.

Die Bedeutung dieser eidesstattlichen Versicherung und die strafrechtlichen Folgen einer unwahren eidesstattlichen Versicherung (§156,161 des Strafgesetzbuches) sind mir bekannt und bewusst.

Datum, Unterschrift des Doktoranden Florian Lammers

4 Druckexemplare

Brain and Behavior

Open Access

Effects of Ncl. Basalis Meynert volume on the Trail-Making-Test are restricted to the left hemisphere

Florian Lammers[1], Arian Mobascher[2], Francesco Musso[3], Nadim Jon Shah[4,5], Tracy Warbrick[4], Laszlo Zaborszky[6] & Georg Winterer[7,8]

[1]Department of Anaesthesiology and Surgical Intensive Care Medicine, Charité – University Medicine Berlin, Berlin, Germany
[2]Department of Psychiatry, University Hospital Mainz, Mainz, Germany
[3]Department of Psychiatry, Heinrich-Heine University, Düsseldorf, Germany
[4]Institute of Neuroscience & Medicine, Research Centre Jülich, Jülich, Germany
[5]Department of Neurology, Faculty of Medicine, RWTH Aachen University, Aachen, Germany
[6]Centre for Molecular and Behavioral Neuroscience, Rutgers The State University of New Jersey, Newark, New Jersey 07102
[7]Experimental and Clinical Research Centre (ECRC), Charité – University Medicine Berlin, Berlin, Germany
[8]Pharmaimage Biomarker Solutions GmbH, Biotech Park Berlin-Buch, Robert-Rössle-Str. 10, 13125 Berlin, Germany

Keywords
Acetylcholine, attention, magnetic resonance imaging (MRI), neuroimaging

Correspondence
Florian Lammers, Experimental and Clinical Research Centre (ECRC), Charité – University Medicine Berlin, Lindenberger Weg 80, 13125 Berlin, Germany. Tel: 0049 3045 0540 759 or 0049 1769 9072 547; Fax: 0049 3045 0754 0767;
E-mail: florian.lammers@charite.de

Funding Information
This study was conducted within the framework of the Priority Program SPP1226 of the German Research Foundation (DFG, Deutsche Forschungsgemeinschaft): "Nicotine: Molecular and Physiological Effects in CNS" (www.nicotine-research.com), grant Wi1316/7-1. Laszlo Zaborszky was supported by the NIH grant NIH/NINDS NS023945 for his work on the maximum probability map of the basal forebrain cholinergic system.

Received: 17 July 2015; Revised: 17 September 2015; Accepted: 3 November 2015

***Brain and Behavior*, 2016; 6(1), e00421, doi: 10.1002/brb3.421**

Abstract

Background: Cortical acetylcholine released from cells in the basal forebrain facilitates cue detection and improves attentional performance. Cholinergic fibres to the cortex originate from the CH4 cell group, sometimes referred to as the Nucleus basalis of Meynert and the Nucleus subputaminalis of Ayala. The aim of this work was to investigate the effects of volumes of cholinergic nuclei on attention and executive function. **Methods:** The volumes of CH4 and CH4p subregions were measured in a subgroup of 38 subjects (33.5 ± 11 years, 20 females) from a population-based cohort study of smokers and never-smokers who have undergone additional MR imaging. To define regions of interest, we applied a DARTEL-based procedure implemented in SPM8 and a validated probabilistic map of the basal forebrain. Attention and executive function were measured with Trail-Making Test (TMT A+B) and Stroop-Task. **Results:** We found a quadratic effect of the left CH4 subregion on performance of the TMT. Extremely small as well as extremely large volumes are associated with poor test performance. **Conclusions:** Our results indicate that a small CH4 volume predisposes for a hypocholinergic state, whereas an extremely large volume predisposes for a hypercholinergic state. Both extremes have detrimental effects on attention. Comparable nonlinear effects have already been reported in pharmacological studies on the effects cholinergic agonists on attention.

Introduction

Neurophysiological experiments demonstrated that successful cue detection specifically elicits cholinergic transients in the medial prefrontal cortex (Parikh et al. 2007). In Alzheimer's dementia (AD), which is frequently accompanied by cholinergic deficiency, attention and executive ability decline during early disease stages (White

et al. 1977; Haxby et al. 1990). Acetylcholine-esterase (AChE) inhibitors are thought to delay cognitive decline, but also to improve attentional deficits in individuals at high risk of developing dementia (Winblad et al. 2001; Salloway et al. 2004).

The magnocellular cell clusters in the basal forebrain are the main origin of cholinergic fibres to the cortex, which in its main part compromises the Ncl. basalis of Meynert (NBM or CH4, Mesulam et al. 1983). Some authors describe another cell cluster in the primate brain projecting to the cortex, the Nucleus subputaminalis of Ayala (NSP), although other authors refer to it as a part of the NBM or CH4 (Simić et al. 1999; Boban et al. 2006; Zaborszky et al. 2008).

Selective lesioning of the NBM in rats leads to attentional deficits (Harati et al. 2008). Studies with the objective to investigate the function of the NBM in humans are mainly restricted to research on AD. In AD as well as mild cognitive impairment (MCI), where its degeneration is thought to play a key role, smaller NBM volume predicts cognitive decline (Grothe et al. 2010, 2013).

Whereas the NBM is thought to be the main origin of cholinergic innervation to the whole cortex, the NSP is thought to project to frontal and cingular areas, brain regions that are especially involved in performance of the Stroop-Task (Mesulam et al. 1983; Simić et al. 1999; Banich et al. 2000). The NSP is thought to be human-specific and may thus play a pivotal role for higher cognitive functions (Simić et al. 1999). Studies on ageing populations have reported an association of the NSP with IQ, but no specific hypotheses about its function in young individuals have yet been made (Wolf et al. 2014).

In this study we hypothesized that NBM volumes predict cognitive performance, in particular in attention and executive function in young individuals, referring to evidence from fundamental and clinical studies. We further hypothesized that the NSP might have a similar relevance for higher cognitive functions.

Although we had no specific a priori hypothesis on interactions of the cholinergic system including smoking status with demographic variables, we considered them potentially relevant with regard to a role of the NBM for cognitive decline during healthy ageing and neurodegenerative diseases (Fratiglioni et al. 1991; Wolf et al. 2014).

Materials and Methods

Participants

We investigated a subsample of $N = 38$ healthy subjects ($N = 20$ females) from the German multi-centric cohort study "Genetics of Nicotine Dependence and Neurobiological Phenotypes", who underwent additional neuroimaging investigations (for details see Lindenberg et al. 2011). All participants were randomly selected from the general population. All participants from our subsample were recruited at the Helmholtz Research Centre in Jülich.

Subjects with a history of medical, neurological or axis 1-psychiatric illness (according to DSM-IV) or alcohol-/drug abuse within the last 6 months as assessed by medical interview and examination, routine laboratory tests, an electrocardiogram, drug screening and standardized psychiatric interview were excluded from the study.

All participants gave written informed consent. The study was approved by the local ethics committee and conducted according to the declaration of Helsinki.

Mean age was 33.5 ± 11 years (range: 19–55 years). Median school and professional education was 15 years (range: 9–22 years).

Only never-smokers ($N = 18$) and current smokers ($N = 20$) according to DSM-IV were included in this study. Never-smoking status was defined by lifetime consumption of less than 20 cigarettes. Smokers were included if their score in the Fagerström test for nicotine dependence (FTND) was at least 4. Further details on smoking behavior in our study sample are given in the supplement.

Results of the TMT Part A were available for all the participants, but for TMT Part B and the Stroop-Task, results were missing for one individual.

Neuropsychological assessment

Trail-Making-Test (TMT) Part A and B as well as the Stroop-Task were administered to each participant by research assistants as part of a comprehensive test battery taking at maximum 75 min for completion. Assessment took place from 10:00 AM to 01:00 PM. Both smokers and never-smokers were assigned equally to the mid-morning or midday test session to avoid bias due to an effect of the circadian rhythm on cognitive performance. To avoid nicotine withdrawal effects on test performance in smokers, tests were completed within 3 h after the last cigarette.

The TMT Part A demands the participant to sequentially search and connect numbers, which are distributed on the test sheet in a semi-randomized manner. Part B additionally requires connecting a set of letters in alphabetical order, switching attention by alternating between numbers and letters. Time for completion of the tests was measured (Reitan 1979).

During the Stroop-Task the participant is presented color words printed in colored ink and asked to name the color of the letters. We subtracted the time needed to name the color of line from the time needed to name the color of incongruent words to calculate a measure of the interference effect. The incongruent stimuli (e.g. the word

"red" printed in green) demand the subject to concentrate attention selectively on a single feature of the stimulus (Stroop 1935; Bäumler 1985).

Trail-Making Test is a common measure of visual search, and especially Pt. B demands additional attentional resources, whereas the Stroop-Task is a common paradigm in research on selective attention (Crowe 1998; Banich et al. 2000). Stroop-Task as well as TMT Pt. B have been used to detect early decline of attentional deficits in progression of Alzheimer's dementia (Haxby et al. 1990).

Image acquisition

T1-weighted, 3D structural scans (magnetization prepared rapid gradient echo: repetition time/echo time = 2250/3.03 msec, flip angle = 9°, 176 sagittal slices, field of view = 200 × 200 mm, 64 × 64 mm matrix, voxel size = 1 × 1 × 1 mm) of the participants were acquired using a 3T scanner (TIM-Trio, Siemens, Erlangen, Germany). All scans were acquired with the same MR scanner at the Helmholtz Research Centre in Jülich.

Image processing and volume measurement

The volumes of the NBM as well as its subregions were quantified using a validated tissue probability map of cholinergic cores in the basal forebrain (Butler et al. 2014). For a detailed description of the creation of the probabilistic map, we refer to Zaborszky et al. (2008). Ten brains of body donors with no record of neurological or psychiatric disease (five female, age range 37–75 years) were obtained at autopsy and fixed in formaldehyde or Bodian fixative. MR images of the brains were obtained using a 1.5 T Siemens Magnetron SP scanner and a 3D Flash sequence. A modified silver staining method of Gallyas was used for histological delineation of cholinergic cell groups. The cell groups were traced out in the MR images of the subjects and combined into a probabilistic map by normalizing all brain scans to the single subject T1-weighted MNI reference brain. The probabilistic map distinguishes four different cell clusters which were specified with a modified version of Mesulam's nomenclature. A voxel was assigned to a structure which it represented in at least 40% of the brains. In case the cell clusters from different brains showed overlap in one voxel, the voxel was assigned to the structure with the highest probability.

Image processing was carried out using SPM8 (Wellcome Trust Centre for Neuroimaging, http://www.fil.ion.ucl.ac.uk/spm/software/spm8/) in a MATLAB R2013a environment (The Mathworks, Inc., Natick, MA).

The images were manually aligned to each other and partitioned into grey and white matter using the SPM segmentation routine. Subsequently, the DARTEL Toolbox was applied to create a mean template from all images and calculate flow fields. DARTEL was run a second time to calculate the flow field needed to match the reference brain (http://www.bic.mni.mcgill.ca/ ServicesAtlases/Colin27) used by Zaborszky et al. to the template.

The probability map was then warped to fit the image of each participant. As such, a deformation was applied to each individual image composed of the flow field of the reference brain in a backward deformation and the flow field of each individual image in a forward deformation.

In this way individual tissue maps of each participant were created. Finally, 3DSlicer 4.3.0 (http://www.slicer.org/) was used to calculate the volume of each labelled region in the map.

To achieve volume normalization of the subregions (V_{norm}), we calculated the quotient of core volume (V_{CH}) and total brain volume (V_{tB}). Subsequently, this quotient was multiplied with the average volume of all brains (V_{avB}) to scale each subregion volume to an average-sized brain: $V_{norm} = (V_{CH}/V_{tB}) \times V_{avB}$.

Statistical analysis

Our probabilistic map distinguishes two subregions of the basal forebrain with projections to the cortex. These are named CH4 and CH4p according to a modified version of Mesulam's nomenclature, first introduced by Zaborszky et al. (2008). CH4 corresponds to the Nucleus basalis Meynert, but CH4p also covers the Nucleus subputaminalis of Ayala.

Since the normalized volumes of the four cholinergic subregions were expected to correlate with each other, we decided to design a general linear model for the effect of each subregion volume (CH4 and CH4p in each hemisphere) on each of the three test scores, yielding twelve analyses in total. $P < 0.05$ was set as the level of significance. Since the three test scores were correlated, we report significant main effects after a Bonferroni-correction for testing four different subregions. Performance in the TMT Part A correlated with the TMT Part B at $R = 0.653$ ($P < 0.001$) and with the Stroop-Effect at $R = 0.468$ ($P = 0.004$).

Age (in years), sex and education (school and professional, measured in years) were included in each model as covariates. Interactions of the cholinergic nuclei with these covariates were considered in the model if they showed at least trend for significance at $P < 0.1$. To minimize effects of multicollinearity, all independent variables were centered around their mean. Male and female sex were coded as 0.5 and −0.5, respectively. Additionally, the variance inflation factors were checked if they exceeded a threshold of 2.5. The literature considers a value of >5 as critical (Urban and Mayerl 2011).

During inspection of partial regression plots we found evidence for a quadratic rather than a linear effect of the left CH4 volume on performance in the TMT Part A and B. Referring to a report on the finding that hypoperfusion of the left hemisphere is associated with postoperative low performance in the Trail-Making-Test, we considered a focus on this subregion appropriate (Messerotti Benvenuti et al. 2012; Zanatta et al. 2012). Holley et al. (1995) modulated the activity of cholinergic basal forebrain cells in a rat model of sustained attention using a $GABA_A$-receptor antagonist. They report that an "increase in false alarms may model a critical component of the cognitive dysfunctions that are associated with abnormally high activity of cortical cholinergic inputs" with the implication of an inverse u-shaped effect of cortical acetylcholine on attention. We thus performed a quadratic regression analysis for the effect of the left CH4 volume on TMT performance.

In a post hoc exploratory analysis, we also considered an effect of smoking on test performance and relevant core volumes (see supplement).

We used partial regression plots to assess the direction of main effects and report B-coefficients from the general linear model equation to interpret the effects of interaction terms. When an interaction term of core volume with a covariate had the same direction like the main effect of core volume, this indicated a stronger effect of the core volume on test performance for larger values of the confounding variable.

Before analysis, data were checked for normal distribution using the Kolmogorov–Smirnov-test and the assumption of normal distribution was accepted if $P > 0.05$. Homoscedasticity was visually controlled by plotting standardized residuals against standardized predicted values.

IBM SPSS Statistics 21 (IBM Corporation, Armonk, NY) was used for all statistical analyses.

Results

Segmentation results for one subject are shown in Figure 1. According to the Kolmogorov-Smirnov-test, we could not reject the assumption of normal distribution for test performance ($p_{TMT\text{-}A} = 0.976$, $p_{TMT\text{-}B} = 0.728$, $p_{Stroop} = 0.336$). VIFs were below the threshold of 2.5 in all analyses.

The linear models showed no significant main effects of the cholinergic subregions on TMT or Stroop-Task. However, significant interactions of the left CH4 region

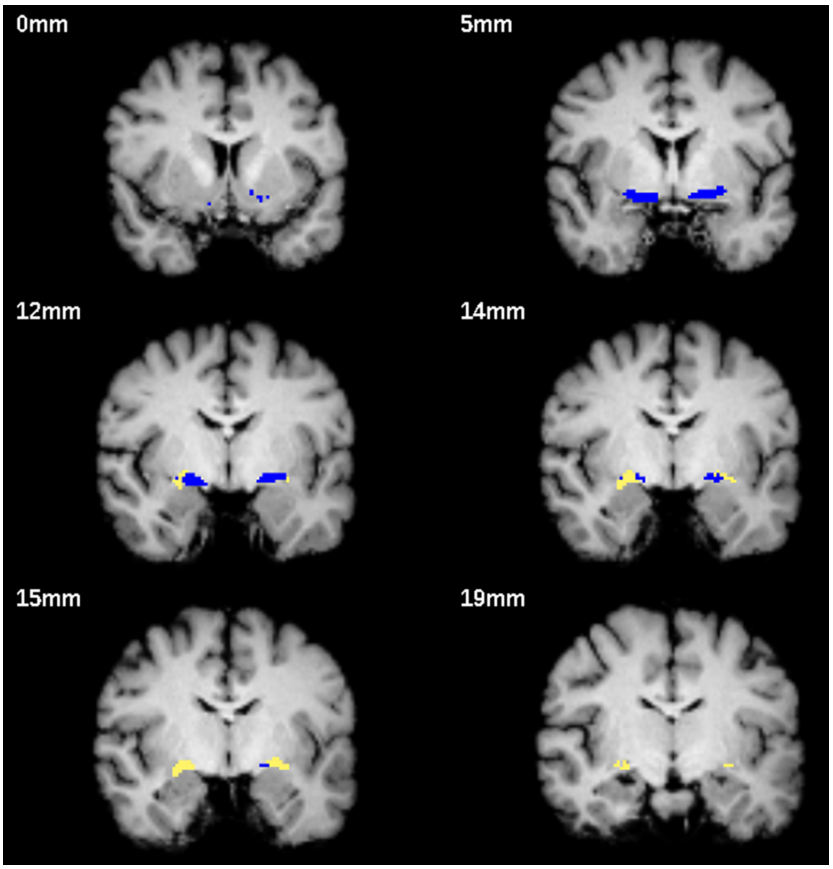

Figure 1. Segmentation example for one brain. The blue ROI refers to CH4, CH4p is shown in yellow. Slices were chosen with the intention to show that CH4p covers a cell cluster often referred to as the Nucleus subputaminalis of Ayala which is rostrolateral extension of the NBM (at 12, 14 and 15 mm). Slice positions are indicated with reference to the most anterior slice on the top left.

Table 1. Linear effects of normalized cholinergic subregion volumes on task performance.

Independent variable	TMT Part A B ± SE (*P*)	TMT Part B B ± SE (*P*)	Stroop-effect B ± SE (*P*)
Left CH4	0.026 ± 0.027 (0.343)	0.075 ± 0.064 (0.251)	0.034 ± 0.047 (0.484)
Left CH4 × Sex	0.162 ± 0.056 (0.007*)	0.380 ± 0.127 (0.005*)	0.195 ± 0.090 (0.038*)
Left CH4 × Age	−0.003 ± 0.002 (0.077)	– (n.s.)	– (n.s.)
Right CH4	0.025 ± 0.029 (0.399)	0.117 ± 0.079 (0.149)	0.015 ± 0.052 (0.782)
Right CH4 × Sex	0.161 ± 0.054 (0.006*)	– (n.s.)	– (n.s.)
Left CH4p	−0.037 ± 0.089 (0.683)	−0.184 ± 0.235 (0.439)	−0.023 ± 0.141 (0.874)
Right CH4p	−0.003 ± 0.057 (0.958)	0.048 ± 0.147 (0.744)	−0.036 ± 0.089 (0.691)

TMT, Trail-Making Test.

*Indicates any effect significant at $P < 0.05$ without Bonferroni correction, (n.s.) indicates an insignificant term which was rejected from the model. Unstandardized B-coefficients with standard errors (SE) as well as the respective *P*-values are also shown.

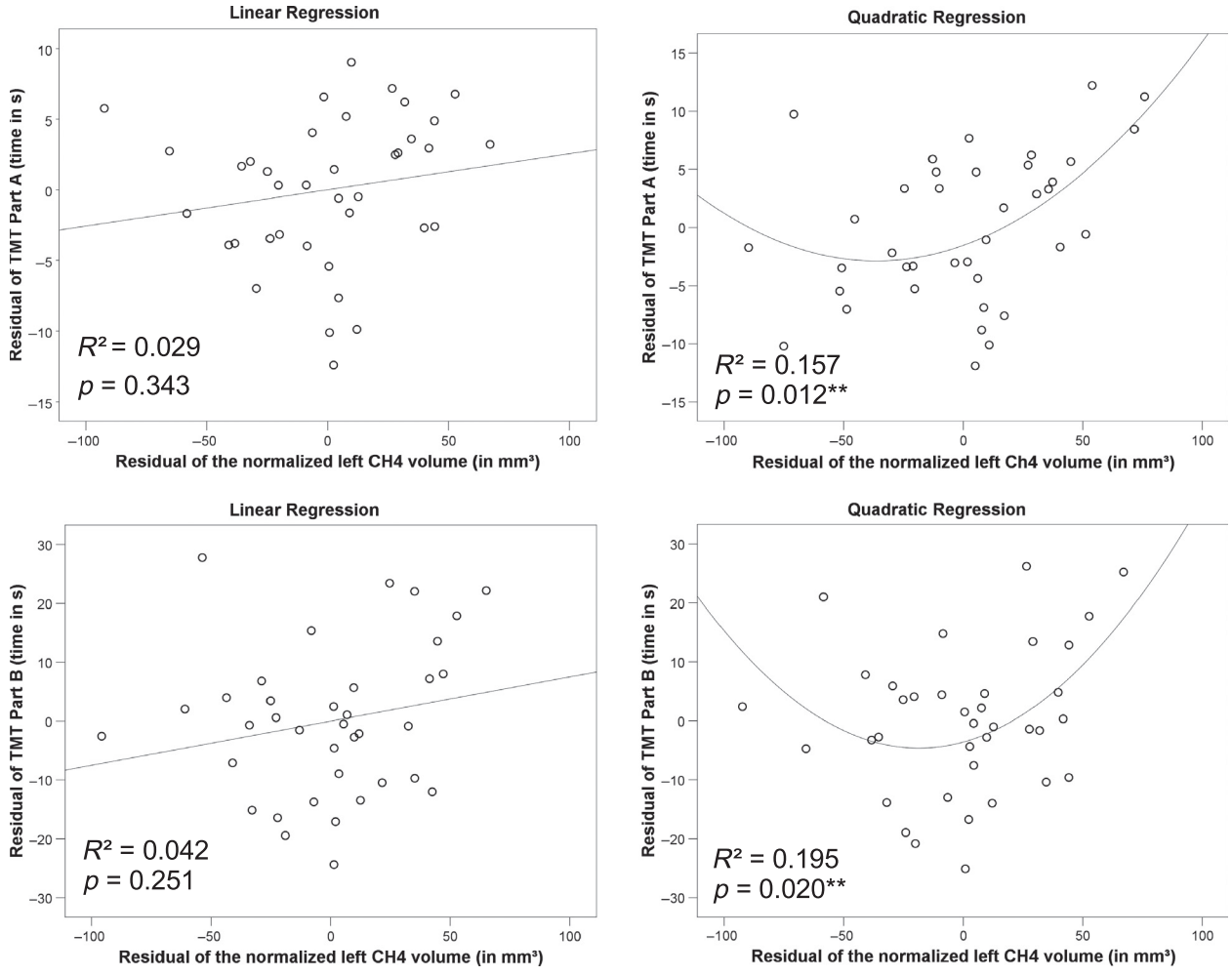

Figure 2. Effects of the left CH4 volume on Trail-Making Test (TMT) performance analysed in a linear (left) and quadratic (right) regression. The proportion of variance in TMT performance explained exclusively by the left CH4 volume is shown on the bottom left of each plot (R^2). ** indicates a significant corrected P-value for the quadratic term. The adjusted R^2 for each test was larger for the quadratic (adj. $R^2_{TMT\text{-}A} = 0.361$, adj. $R^2_{TMT\text{-}B} = 0.571$) than the linear model (adj. $R^2_{TMT\text{-}A} = 0.332$, adj. $R^2_{TMT\text{-}B} = 0.423$), indicating an improvement of the model by using quadratic regression.

and sex were found for all three tests (Stroop-Task and TMT Part A and B). Sex moderated the effect of the right CH4 region on performance in TMT Part A. Details of main effects of subregion volumes on test performance as well as interactions with covariates are shown in Table 1. Partial regression plots pointed to a quadratic relationship of the left CH4 volume and performance in the TMT (see Fig. 2).

The detailed analysis of a quadratic relationship of the left CH4 and the TMT revealed significant quadratic and linear effects of this subregion on Part A (Fig. 2). The latter was moderated by age (Table 2). Performance in Part B was only significantly influenced by the squared term, and the linear effect was moderated by age (Table 3 and Fig. 2).

We further analysed the relationship of CH4 volume and smoking. CH4 volumes did not differ between smokers and never-smokers. The effect of the left CH4 volume on TMT performance was not restricted to either the group of smokers or never-smokers (see supplement for details.)

Table 2. Effects of normalized left CH4 volume and covariates on TMT Part A in the quadratic regression analysis.

Independent variable	B-coefficient ± SE	Standardized β-coefficient	*P*
Squared volume	0.001 ± 0.000	0.534	0.012**
Volume	0.062 ± 0.023	0.418	0.040**
Volume × Age	−0.005 ± 0.002	−0.377	0.022*
Sex	−4.058 ± 2.130	−0.300	0.066
Age	0.076 ± 0.093	0.121	0.421
Education	−0.813 ± 0.360	−0.312	0.031*
Intercept	23.153 ± 1.214		<0.001*

TMT, Trail-Making Test; SE, standard error.
*Indicates any effect significant at $P < 0.05$ without correction, whereas **indicates a significant effect of core volume on test performance after Bonferroni correction.

Table 3. Effects of normalized left CH4 volume and covariates on TMT Part B in the quadratic regression analysis.

Independent variable	B-coefficient ± SE	Standardized β-coefficient	*P*
Squared volume	0.004 ± 0.001	0.507	0.020**
Volume	0.116 ± 0.058	0.302	0.216
Volume × Age	−0.012 ± 0.004	−0.389	0.006*
Volume × Sex	0.249 ± 0.135	0.301	0.076
Sex	0.115 ± 5.213	0.003	0.983
Age	0.057 ± 0.203	0.035	0.773
Education	−1.099 ± 0.853	−0.161	0.761
Intercept	51.050 ± 2.704		<0.001*

TMT, Trail-Making Test; SE, standard error.
*Indicates any effect significant at $P < 0.05$ without correction, whereas **indicates a significant effect of core volume on test performance after Bonferroni correction.

Discussion

Effects of NBM volumes on attention and executive functions

In the present study we found a non-linear effect of the left CH4 volume on performance in the TMT, but not on the Stroop-Effect. This may indicate a comparatively higher sensitivity of the TMT to the effects of central cholinergic system parameters on cognition. Notably, the cohort study from which our sub-sample was drawn showed that smokers performed worse on the TMT, but not on the Stroop-Task (Wagner et al. 2013).

The effect of the volume on performance was u-shaped (quadratic), predicting good performance for individuals with core volumes close to the average, whereas extremely small or large volumes were associated with poor results in the TMT. The finding that small cholinergic core volumes are associated with poor performance is in line with studies on the cholinergic system in ageing and neurodegenerative diseases (e.g. Alzheimer's disease) as well as animal studies on NBM lesions (Harati et al. 2008; Grothe et al. 2013; Wolf et al. 2014). We assume that a small volume might be associated with a relative hypocholinergic state in healthy young individuals. On the other hand, we suggest that an extremely large volume predisposes an individual for hypercholinergic states. Studies on AChE inhibitor application in healthy participants showed a cognitive impairment rather than an enhancement and a bell-shaped dose-response curve has been proposed for the effects of several cholinergic receptor agonists on cognition (Kennedy et al. 2003; Kitagawa et al. 2003; Beglinger et al. 2004, 2005). Holley et al. (1995) modulated the activity of cholinergic cells in the basal forebrain of rats during a cue detection task using an $GABA_A$-receptor agonist or antagonist. They found that inhibition of ACh release decreased the number of detected cues, whereas dis-inhibition of the cholinergic cells increased the number of false rejection of distractor cues.

Several studies showed a lateralization effect toward the left hemisphere during performance of the TMT Part B (Moll et al. 2002; Zakzanis et al. 2005). These studies suggest a relevance of left frontal, cingular and motion-related regions to set shifting. These areas are structurally and functionally connected to the CH4 region, and thus an effect of its volume on the TMT seems reasonable (Mesulam et al. 1983; Li et al. 2014). The CH4p region is thought to project to the speech-area in the inferior frontal gyrus as well auditory areas in the temporal lobe,

which explains the low impact of its volume on visually attention-demanding tasks (Mesulam et al. 1983; Simić et al. 1999; Zaborszky et al. 2008). Both parts of the TMT, especially Part A, require visual search (Crowe 1998). Although the attention network has been thought to be right-lateralized, activation in circumscribed regions in left frontal and parietal areas has been attributed to several subdomains of visual search (Weidner et al. 2009). Additionally, performance in the TMT has been found to be specifically affected by hypoperfusion of the left hemisphere, which is in line with our finding of the left CH4 region specifically affecting TMT performance (Messerotti Benvenuti et al. 2012; Zanatta et al. 2012).

The effect of the left CH4 on TMT performance was moderated by age, and our data suggest, that with increasing age, even a large core volume would less likely cause impairment of test performance. Thus, the risk of shifting into a hypercholinergic state is decreased during ageing. This is in line with the epidemiology of AD, a disease of elderly patients, which is associated with a hypocholinergic state (Fratiglioni et al. 1991). Decreasing ACh synthesis and release by the cholinergic neurons might be accountable for this finding, since choline-acetyltransferase and ACh-esterase activity have been shown to decrease early during the lifespan (Perry et al. 1992; Sparks et al. 1992).

Although the linear model did not show a main effect of cholinergic subregions on attention in the first approach, results suggest an interaction of subregion volumes with sex. Men and women have been suggested to use different strategies and cognitive systems in tasks of visual attention, which may be differentially be influenced by acetylcholine (Rubia et al. 2010). The direction of the interaction effect suggested that among individuals with above-average CH4 volumes, women would outperform men in attention demanding tasks. Since men recruit especially left-sided cortical regions involved in saliency-dependent processes for attention allocation, they might be at risk for high levels of ACh to induce false-rejection errors (Rubia et al. 2010).

Limitations

Our study sample included regular smokers in addition to never-smokers. Since smokers have cognitive deficits especially in the domain of attention, the generalizability of our results may be limited (Wagner et al. 2013). To estimate the extent to which the inclusion of smokers in our study affects our results, we performed an additional analysis, which is described in detail in the supplement of this article. The results from our study suggest that the high fraction of smokers does not affect the generalizability of our results.

The TMT was part of a comprehensive test battery and we do not know how preceding tests interfere with its assessment. Sustaining attention during the whole neuropsychological examination might facilitate a hypercholinergic state by ACh accumulation especially in individuals with a large nucleus.

TMT and Stroop-Task are common tests used for the examination of attention, but include different subcomponents of attention, such as visual search in TMT Parts A and B, but divided attention and set-shifting especially in TMT Part B (Crowe 1998). These subcomponents are also constituent part in other cognitive domains, which could be affected by acetylcholine, but are not attention-related in the strict sense.

Conclusions

We describe an association of an NBM subregion volume with performance in tests of attention and executive functions. Cholinergic innervation seems to be especially important for performance in visual search tasks. Extremely small as well as extremely large volumes are associated with poor test performance, indicating that either hypocholinergic or hypercholinergic states impair cognition.

Conflict of interest

This publication is part of Florian Lammers' doctorate. All authors have no conflicting financial interests.

References

Banich, M. T., M. P. Milham, R. Atchley, N. J. Cohen, A. Webb, T. Wszalek, et al. 2000. fMri studies of Stroop tasks reveal unique roles of anterior and posterior brain systems in attentional selection. J Cogn Neurosci 12:988–1000.

Bäumler, G. 1985. Farbe–Wort–Interferenztest (FWIT) nach J.W. Stroop. Hogrefe, Göttingen.

Beglinger, L. J., B. L. Gaydos, D. A. Kareken, O. Tangphao-Daniels, E. R. Siemers, and R. C. Mohs. 2004. Neuropsychological test performance in healthy volunteers before and after donepezil administration. J. Psychopharmacol. (Oxford) 18:102–108. doi:10.1177/0269881104040248.

Beglinger, L. J., O. Tangphao-Daniels, D. A. Kareken, L. Zhang, R. Mohs, and E. R. Siemers. 2005. Neuropsychological test performance in healthy elderly volunteers before and after donepezil administration: a randomized, controlled study. J. Clin. Psychopharmacol. 25:159–165.

Boban, M., I. Kostovic, and G. Simic. 2006. Nucleus subputaminalis: neglected part of the basal nucleus of Meynert. Brain 129:E42; author reply E43. doi:10.1093/brain/awl025.

Butler, T., L. Zaborszky, E. Pirraglia, J. Li, X. H. Wang, Y. Li, et al. 2014. Comparison of human septal nuclei MRI measurements using automated segmentation and a new manual protocol based on histology. NeuroImage 97:245–251. doi:10.1016/j.neuroimage.2014.04.026.

Crowe, S. F. 1998. The differential contribution of mental tracking, cognitive flexibility, visual search, and motor speed to performance on parts A and B of the Trail Making Test. J. Clin. Psychol. 54:585–591.

Fratiglioni, L., M. Grut, Y. Forsell, M. Viitanen, M. Grafström, K. Holmén, et al. 1991. Prevalence of Alzheimer's disease and other dementias in an elderly urban population: relationship with age, sex, and education. Neurology 41:1886–1892.

Grothe, M., L. Zaborszky, M. Atienza, E. Gil-Neciga, R. Rodriguez-Romero, S. J. Teipel, et al. 2010. Reduction of basal forebrain cholinergic system parallels cognitive impairment in patients at high risk of developing Alzheimer's disease. Cereb. Cortex 20:1685–1695. doi:10.1093/cercor/bhp232.

Grothe, M., H. Heinsen, and S. Teipel. 2013. Longitudinal measures of cholinergic forebrain atrophy in the transition from healthy aging to Alzheimer's disease. Neurobiol. Aging 34:1210–1220. doi:10.1016/j.neurobiolaging.2012.10.018.

Harati, H., A. Barbelivien, B. Cosquer, M. Majchrzak, and J.-C. Cassel. 2008. Selective cholinergic lesions in the rat nucleus basalis magnocellularis with limited damage in the medial septum specifically alter attention performance in the five-choice serial reaction time task. Neuroscience 153:72–83. doi:10.1016/j.neuroscience.2008.01.031.

Haxby, J. V., C. L. Grady, E. Koss, B. Horwitz, L. Heston, M. Schapiro, et al. 1990. Longitudinal study of cerebral metabolic asymmetries and associated neuropsychological patterns in early dementia of the Alzheimer type. Arch. Neurol. 47:753–760.

Holley, L. A., J. Turchi, C. Apple, and M. Sarter. 1995. Dissociation between the attentional effects of infusions of a benzodiazepine receptor agonist and an inverse agonist into the basal forebrain. Psychopharmacology 120:99–108.

Kennedy, D. O., G. Wake, S. Savelev, N. T. J. Tildesley, E. K. Perry, K. A. Wesnes, et al. 2003. Modulation of mood and cognitive performance following acute administration of single doses of Melissa officinalis (Lemon balm) with human CNS nicotinic and muscarinic receptor-binding properties. Neuropsychopharmacology 28:1871–1881. doi:10.1038/sj.npp.1300230.

Kitagawa, H., T. Takenouchi, R. Azuma, K. A. Wesnes, W. G. Kramer, D. E. Clody, et al. 2003. Safety, pharmacokinetics, and effects on cognitive function of multiple doses of GTS-21 in healthy, male volunteers. Neuropsychopharmacology 28:542–551. doi:10.1038/sj.npp.1300028.

Li, C. R., J. S. Ide, S. Zhang, S. Hu, H. H. Chao, and L. Zaborszky. 2014. Resting state functional connectivity of the basal nucleus of Meynert in humans: in comparison to the ventral striatum and the effects of age. NeuroImage 97:321–332. doi:10.1016/j.neuroimage.2014.04.019.

Lindenberg, A., J. Brinkmeyer, N. Dahmen, J. Gallinat, W. de Millas, A. Mobascher, et al. 2011. The German multi-centre study on smoking-related behavior-description of a population-based case-control study. Addict. Biol. 16:638–653. doi:10.1111/j.1369-1600.2011.00322.x.

Messerotti Benvenuti, S., P. Zanatta, C. Longo, A. P. Mazzarolo, and D. Palomba. 2012. Preoperative cerebral hypoperfusion in the left, not in the right, hemisphere is associated with cognitive decline after cardiac surgery. Psychosom. Med. 74:73–80. doi:10.1097/PSY.0b013e3182383a94.

Mesulam, M. M., E. J. Mufson, A. I. Levey, and B. H. Wainer. 1983. Cholinergic innervation of cortex by the basal forebrain: cytochemistry and cortical connections of the septal area, diagonal band nuclei, nucleus basalis (substantia innominata), and hypothalamus in the rhesus monkey. J. Comp. Neurol. 214:170–197. doi:10.1002/cne.902140206.

Moll, J., R. de Oliveira-Souza, F. T. Moll, I. E. Bramati, and P. A. Andreiuolo. 2002. The cerebral correlates of set-shifting: an fMRI study of the trail making test. Arq. Neuropsiquiatr. 60:900–905.

Parikh, V., R. Kozak, V. Martinez, and M. Sarter. 2007. Prefrontal acetylcholine release controls cue detection on multiple timescales. Neuron 56:141–154. doi:10.1016/j.neuron.2007.08.025.

Perry, E. K., M. Johnson, J. M. Kerwin, M. A. Piggott, J. A. Court, P. J. Shaw, et al. 1992. Convergent cholinergic activities in aging and Alzheimer's disease. Neurobiol. Aging 13:393–400. doi:10.1016/0197-4580(92)90113-C.

Reitan, R. M. 1979. Trail Making Test (TMT). Beltz, Weinheim.

Rubia, K., Z. Hyde, R. Halari, V. Giampietro, and A. Smith. 2010. Effects of age and sex on developmental neural networks of visual-spatial attention allocation. NeuroImage 51:817–827. doi:10.1016/j.neuroimage.2010.02.058.

Salloway, S., S. Ferris, A. Kluger, R. Goldman, T. Griesing, D. Kumar, et al. 2004. Efficacy of donepezil in mild cognitive impairment: a randomized placebo-controlled trial. Neurology 63:651–657.

Simić, G., L. Mrzljak, A. Fucić, B. Winblad, H. Lovrić, and I. Kostović. 1999. Nucleus subputaminalis (Ayala): the still disregarded magnocellular component of the basal forebrain may be human specific and connected with the cortical speech area. Neuroscience 89:73–89.

Sparks, D. L., J. C. Hunsaker, J. T. Slevin, S. T. DeKosky, R. J. Kryscio, and W. R. Markesbery. 1992. Monoaminergic and cholinergic synaptic markers in the nucleus basalis of Meynert (nbM): normal age-related changes and the effect of heart disease and Alzheimer's disease. Ann. Neurol. 31:611–620. doi:10.1002/ana.410310608.

Stroop, J. R. 1935. Studies of interference in serial verbal reactions. J. Exp. Psychol. 18:643–662.

Urban, D., and J. Mayerl. 2011. Regressionsanalyse: Theorie, Technik und Anwendung, 4., vüberarb. und erw. Aufl. ed, Studienskripten zur Soziologie. VS, Verl. für Sozialwiss, Wiesbaden.

Wagner, M., S. Schulze-Rauschenbach, N. Petrovsky, J. Brinkmeyer, C. von der Goltz, G. Gründer, et al. 2013. Neurocognitive impairments in non-deprived smokers–results from a population-based multi-center study on smoking-related behavior. Addict. Biol. 18:752–761. doi:10.1111/j.1369-1600.2011.00429.x.

Weidner, R., J. Krummenacher, B. Reimann, H. J. Müller, and G. R. Fink. 2009. Sources of top-down control in visual search. J. Cogn. Neurosci. 21:2100–2113. doi:10.1162/jocn.2008.21173.

White, P., C. R. Hiley, M. J. Goodhardt, L. H. Carrasco, J. P. Keet, I. E. Williams, et al. 1977. Neocortical cholinergic neurons in elderly people. Lancet 1:668–671.

Winblad, B., K. Engedal, H. Soininen, F. Verhey, G. Waldemar, A. Wimo, et al. 2001. A 1-year, randomized, placebo-controlled study of donepezil in patients with mild to moderate AD. Neurology 57:489–495.

Wolf, D., M. Grothe, F. U. Fischer, H. Heinsen, I. Kilimann, S. Teipel, et al. 2014. Association of basal forebrain volumes and cognition in normal aging. Neuropsychologia 53:54–63. doi:10.1016/j.neuropsychologia.2013.11.002.

Zaborszky, L., L. Hoemke, H. Mohlberg, A. Schleicher, K. Amunts, and K. Zilles. 2008. Stereotaxic probabilistic maps of the magnocellular cell groups in human basal forebrain. NeuroImage 42:1127–1141. doi:10.1016/j.neuroimage.2008.05.055.

Zakzanis, K. K., R. Mraz, and S. J. Graham. 2005. An fMRI study of the Trail Making Test. Neuropsychologia 43:1878–1886. doi:10.1016/j.neuropsychologia.2005.03.013.

Zanatta, P., S. Messerotti Benvenuti, C. Valfrè, F. Baldanzi, and D. Palomba. 2012. The role of asymmetry and the nature of microembolization in cognitive decline after heart valve surgery: a pilot study. Perfusion 27:199–206. doi:10.1177/0267659112437776.

Supporting Information

Additional supporting information may be found in the online version of this article:

Table S1. Demographic data of smokers and never-smokers.

SUPPLEMENT

1 Nicotine dependence and the cholinergic system

Affection of the central cholinergic system is considered to play a role in the pathogenesis of nicotine dependence (Winterer et al. 2010). An fMRI study on visual attention revealed increased activation of the basal forebrain in smokers, suggesting an affection of the NBM in particular (Vossel et al. 2011). We considered it therefore possible, that the effect of NBM volume on attention is modulated by a history of nicotine dependence.
On the other hand, the sample composition in our study (heavy and never-smokers) might affect the generalisability of our results.
The study, from which this sub-sample was drawn, has shown that smokers have cognitive deficits that are not attributable to withdrawal. These deficits especially concern the performance in the TMT and other tests of visual attention (Wagner et al. 2013).
We performed additional statistical analyses to address the questions if (1) smoking habits affects CH4 volumes and (2) the effect of the left CH4 volume on test performance interacts with the effect of nicotine dependence.

2 Baseline data according to smoking habits

Baseline data did not differ significantly between smokers and never-smokers. Table S1 provides details about the demographic data in both groups.
Smokers consumed at least two and up to 35 cigarettes per day with an average of 15.5 at the time of data acquisition. They reported a smoking history of up to 41.2 packyears, with a mean of 12.5±13.9 packyears.
Blood samples for measurement of cotinine plasma levels were taken at the end of the test day, two hours after the participant had smoked a second cigarette. Plasma samples were kept at -80°C pending the chemical analysis. Mean cotinine levels in smokers were 85.2±96.3ng/mL, levels in never-smokers were below the detection threshold.

TABLE S1: Demographic data of smokers and never-smokers.

	Smokers	Never-smokers	p	Test procedure
Age (mean±SD)	*35.65±11.07yrs*	*31.17±10.64yrs*	*0.212*	Student's t-test df=36, t=-1.270
Sex (female/male)	*8/10*	*12/8*	*0.746*	Chi-Square-test df=1, χ=0.105
Years of Education (median, range)	*15, 9-22yrs*	*15.5, 11-18yrs*	*0.906*	Mann-Whitney-U-test U=176

3 Statistical Analysis

The left and the right normalised CH4 volume were used as the dependent variables in two analyses of covariance (ANCOVA) of which each included current smoking (yes/no) as the covariate of interest, and age and sex as covariates of no interest. Interactions among the independent variables were rejected from the model, if they were insignificant at $p \geq 0.1$.
To check effects of smoking on our analysis of TMT performance, we added smoking (yes/no) and the interaction effect of smoking and left CH4 volume and squared left CH4 volume to the regression model. Smokers were coded as 0.5, never-smokers as -0.5.
We report significant results at an uncorrected threshold of $p<0.05$.

4 Results

Smoking affected neither the left (F=0.006, df=33, p=0.940), nor the right CH4 volume (F=0.225, df=33, p=0.638).
For Part A of the TMT, there was a significant interaction of smoking and the squared volume (B=-0.002±0.001, p=0.031), but the main effects of the volume also remained significant (quadratic: B=0.001±0.000, p=0.003; linear: B=0.069±0.022, p=0.004). There was no significant interaction of the linear effect of left CH4 volume with smoking (p=0.578).
For Part B of the TMT, we found no significant interactions of smoking and the left CH4 volume (quadratic: p=0.165; linear: p=0.482). In the regression analysis of the TMT Part B, the VIFs exceeded the threshold of 2.5 (3.118 maximum).

5 Conclusions

The results of our additional analyses showed no effect of nicotine dependence on the normalised CH4 volumes.
Results from the analysis of interaction terms of smoking and the left CH4 volume are somewhat difficult to interpret: There was an interaction of the quadratic volume effect and smoking on TMT Part A, indicating that volume differences in smokers affected performance in Part A less than in never-smokers, which might reflect decreased sensitivity of smokers to ACh release. Decreased ACh sensitivity has been suggested to predispose to nicotine dependence due to its effect on cognitive performance (Ernst et al. 2001). Nevertheless, we could not reproduce this finding in the analysis of TMT Part B, although one would expect that performance in both tests depends on similar cognitive mechanisms. To fully elucidate this point will need further studies. Since VIFs slightly exceeded the threshold value in the analysis of TMT Part B, multicollinearity might have affected our results.
Since smokers did not differ in regards of CH4 volumes, and interactions of left CH4 volume that could affect TMT performance were either insignificant (Part B) or did not affect the significance of main effects (Part A), we conclude that our results can be generalised for other populations.

6 References

Ernst, M., Heishman, S.J., Spurgeon, L., London, E.D., 2001. Smoking history and nicotine effects on cognitive performance. Neuropsychopharmacology 25, 313–319. doi:10.1016/S0893-133X(01)00257-3

Vossel, S., Warbrick, T., Mobascher, A., Winterer, G., Fink, G.R., 2011. Spatial and sustained attention in relation to smoking status: behavioural performance and brain activation patterns. J. Psychopharmacol. (Oxford) 25, 1485–1495. doi:10.1177/0269881110391830

Wagner, M., Schulze-Rauschenbach, S., Petrovsky, N., Brinkmeyer, J., von der Goltz, C., Gründer, G., Spreckelmeyer, K.N., Wienker, T., Diaz-Lacava, A., Mobascher, A., Dahmen, N., Clepce, M., Thuerauf, N., Kiefer, F., de Millas, J.W., Gallinat, J., Winterer, G., 2013. Neurocognitive impairments in non-deprived smokers--results from a population-based multi-center study on smoking-related behavior. Addict Biol 18, 752–761. doi:10.1111/j.1369-1600.2011.00429.x

Winterer, G., Mittelstrass, K., Giegling, I., Lamina, C., Fehr, C., Brenner, H., Breitling, L.P., Nitz, B., Raum, E., Müller, H., Gallinat, J., Gal, A., Heim, K., Prokisch, H., Meitinger, T., Hartmann, A.M., Möller, H.-J., Gieger, C., Wichmann, H.-E., Illig, T., Dahmen, N., Rujescu, D., 2010. Risk gene variants for nicotine dependence in the CHRNA5-CHRNA3-CHRNB4 cluster are associated with cognitive performance. Am. J. Med. Genet. B Neuropsychiatr. Genet. 153B, 1448–1458. doi:10.1002/ajmg.b.31126

Neuropsychologia 119 (2018) 145–156

Contents lists available at ScienceDirect

Neuropsychologia

journal homepage: www.elsevier.com/locate/neuropsychologia

Basal forebrain cholinergic system volume is associated with general cognitive ability in the elderly

Florian Lammers[a,b,*], Friedrich Borchers[a], Insa Feinkohl[c], Jeroen Hendrikse[d], Ilse M.J. Kant[e], Petra Kozma[a], Tobias Pischon[c,f,g], Arjen J.C. Slooter[e], Claudia Spies[a], Simone J.T. van Montfort[e], Norman Zacharias[a,b], Laszlo Zaborszky[h], Georg Winterer[a,b], The BioCog consortium

[a] Department of Anaesthesiology, Charité – Universitätsmedizin Berlin, Corporate Member of Freie Universität Berlin, Humboldt-Universität zu Berlin and Berlin Institute of Health, Augustenburger Platz 1, 13353 Berlin, Germany
[b] Pharmaimage Biomarker Solutions GmbH, Robert-Rössle-Straße 10, 13125 Berlin, Germany
[c] Max-Delbrück-Center for Molecular Medicine in the Helmholtz Association (MDC), Robert-Rössle-Straße 10, 13125 Berlin, Germany
[d] Department of Radiology and Brain Center Rudolf Magnus, University Medical Centre Utrecht, Utrecht University Heidelberglaan 100, 3584 CX Utrecht, Netherlands
[e] Department of Intensive Care Medicine and Brain Center Rudolf Magnus, University Medical Center Utrecht, Utrecht University Heidelberglaan 100, 3584 CX Utrecht, Netherlands
[f] Charité – Universitätsmedizin Berlin, Corporate Member of Freie Universität Berlin, Humboldt-Universität zu Berlin and Berlin Institute of Health, Germany
[g] MDC/BIH Biobank, Max-Delbrück Center for Molecular Medicine in the Helmholtz Association (MDC), and Berlin Institute of Health (BIH), Berlin, Germany
[h] Center for Molecular and Behavioral Neuroscience, Rutgers The State University of New Jersey, 197 University Avenue, Newark, NJ 07102, USA

A B S T R A C T

Objective: At the present, it is unclear whether association of basal forebrain cholinergic system (BFCS) volume with cognitive performance exists in healthy as well as in cognitively impaired elderly subjects. Whereas one small study reported an association of BFCS volume with general cognitive ability 'g' in healthy ageing, effects on specific cognitive domains have only been found in subjects with cognitive decline. Here we aim to clarify whether an association of BFCS volume and 'g' is present in a larger sample of elderly subjects without obvious symptoms of dementia and whether similar associations can also be observed in specific cognitive domains.

Methods: 282 pre-surgical patients from the BioCog study (aged 72.7 ± 4.9 years with a range of 65–87 years, 110 women) with a median MMSE score of 29 points (range 24–30) were investigated. BFCS and brain volume as well as brain parenchymal fraction were assessed in T1-weighted MR images using SPM12 and a probabilistic map of the BFCS. Neuropsychological assessment comprised the CANTAB cognitive battery and paper-and-pencil based tests. For data analysis, generalised linear models and quantile regression were applied.

Results: Significant associations of BFCS volume with 'g' and several cognitive domains were found, with the strongest association found for 'g'. BFCS volume explained less variance in cognitive performance than brain volume. The association was not confounded by brain parenchymal fraction. Furthermore, the association of BFCS volume and 'g' was similar in high- and low-performers.

Conclusion: Our results extend previous study findings on BFCS volume associations with cognition in elderly subjects. Despite the observed associations of BFCS volume and cognitive performance, this association seems to reflect a more general association of brain volume and cognition. Accordingly, a specific association of BFCS volume and cognition in non-demented elderly subjects is questionable.

1. Introduction

The basal forebrain is the main source of acetylcholine (ACh) for hippocampal and neocortical structures. The basal forebrain cholinergic system (BFCS) comprises the medial septum nuclei (Ch1), Broca's diagonal (Ch2) and horizontal nuclei (Ch3) as well as the Nucleus basalis of Meynert (Ch4) and the Nucleus subputaminalis of Ayala (Mesulam et al., 1983; Simić et al., 1999). Its main neurotransmitter acetylcholine is well known to play a role in cognition which has been shown in several neurophysiological experiments and lesion studies of the BFCS (Parikh et al., 2007; Harati et al., 2008; Cai et al., 2012).

In patients with Alzheimer's Dementia (AD), the number of cholinergic neurons in the human brain is diminished (White et al., 1977; Kilimann et al., 2014). Furthermore, MRI studies have shown that cholinergic atrophy parallels cognitive decline as the disease process is progressing (Grothe et al., 2013). Current treatment strategies of Alzheimer's dementia aim at compensation for the cholinergic deficit by administration of ACh-esterase inhibitors (Birks 2006; Winblad et al., 2001). These drugs increase neurotransmitter persistence in the synaptic cleft by pharmacological inhibition of its degradation,

* Correspondence to: Lindenberger Weg 80, 13125 Berlin, Germany.
E-mail address: florian.lammers@charite.de (F. Lammers).

https://doi.org/10.1016/j.neuropsychologia.2018.08.005
Received 28 April 2018; Received in revised form 2 August 2018; Accepted 6 August 2018
Available online 07 August 2018

ameliorating cognitive symptoms (Anand and Singh, 2013).

Atrophy of cholinergic cells in the basal forebrain is also seen in healthy elderly subjects without clinical evidence of dementia (Grothe et al., 2012, 2013; Teipel et al., 2015). Post mortem studies reported a decrease of histological markers of ACh-synthesis and cholinergic synapses during normal ageing which is accelerated in AD patients (Sparks et al., 1992; Perry et al., 1992). However, it is still controversial whether cholinergic deficits are also associated with age-associated cognitive decline in subjects without evidence of dementia development. Wolf et al. (2014) recently reported an association of BFCS volume with cognitive performance in a small group of healthy elderly subjects without evidence of dementia. On the other hand, ACh-esterase-inhibitors have not been proven effective in elderly patients with memory complaints without dementia (mild cognitive impairment) and cholinergic cell loss seems to occur at advanced stages of AD (Russ and Morling, 2012; Gilmor et al., 1999). Furthermore, histological studies suggested that 30% of cholinergic neurons in the basal forebrain need to be lost until relevant cognitive deficits manifest (Mini-Mental State Examination/MMSE < 24) which is questioning an association of cognition and basal forebrain volume in healthy ageing (Schliebs and Arendt, 2006).

Associations of BFCS subregion volumes and cognitive domains (episodic memory, executive functions) were reported for patients with mild cognitive impairment (MCI). This association was not observed in the healthy control group (Grothe et al., 2010, 2016). Since these studies were designed to investigate differences between healthy elderly and patients with mild cognitive impairment, one needs to take into account that the control group was strictly defined as a highly functional ("hypernormal") control group without the slightest suspicion for cognitive impairment. Thus, Grothe et al. (2016) used a control group from the Alzheimer's Disease Neuroimaging Initiative (ADNI-2) comprising individuals without any memory complaints, normal memory function according to the Wechsler Memory Scale-R and a Clinical Dementia Rating Scale (CDR) score of 0. In addition, subjects with significant systemic illness or unstable medical condition were not included in the control group. Since multimorbidity has been shown to be associated with age and cognitive impairment, exclusion of participants due to non-neurocognitive medical conditions affects the prevalence of age-associated cognitive decline in the sample (Barnett et al., 2012; Vassilaki et al., 2015).

The aim of the present study is the analysis of BFCS volume associations with cognitive performance in a natural rather than a "hypernormal" cohort of elderly pre-surgical patients (≥ 65 years) without obvious symptoms of clinical dementia (MMSE score median 29 points, range 24–30, Folstein et al., 1975).

2. Methods

2.1. Participants

Participants were recruited as part of the BioCog project (Biomarker Development for Postoperative Cognitive Impairment in the Elderly study, www.biocog.eu), which is a prospective multicentre cohort study with the aim to develop a biomarker-based algorithm for risk prediction of post-operative cognitive disorders. Only patients ≥ 65 years of age presenting for an elective major surgery were recruited (for further inclusion and exclusion criteria see Table 1).

All patients gave written informed consent to participate in the study. The study protocol was approved by the local ethics committees and conducted in accordance with the declaration of Helsinki. The study was registered at clinicaltrials.gov (NCT02832193).

In line with the study protocol, the first 400 out of 1033 participants recruited at two study centres in Berlin, Germany (N = 291) and Utrecht, Netherlands (N = 109) were selected for this interim analysis. In total, 2733 patients were screened for inclusion in the interim sample in both study centres. 297 out of 400 patients underwent anatomical neuroimaging. Two patients were excluded due to brain pathology interfering with the segmentation procedure. Thirteen datasets were incomplete with regard to demographic data or patients did not perform cognitive testing at all. Finally, data from 282 participants are included in the analysis (N = 204 from Berlin, N = 78 from Utrecht). Neuropsychological data were incomplete for several participants reducing the final sample size for test analysis.

2.2. Neuropsychological assessments

One day before surgery, all participants underwent a comprehensive computerised neuropsychological test battery (CANTAB, Cambridge Cognition Ltd., UK), comprising the Paired Associate Learning (PAL), Verbal Recognition Memory (VRM), Spatial Span Length (SSP) and Simple Reaction Time (SRT). Additionally, pen-and-paper versions of the Trail-Making-Test (TMT, Parts A and B) and a manual dexterity test called the Grooved Pegboard Task (GPT) were conducted. Testing was performed by trained doctoral students and study nurses based on a standard operating procedure which was consented with two neuropsychologists.

PAL: The participant is shown different patterns in fixed locations on a screen in a randomised order. Subsequently, the patterns are obscured and the participant is asked to indicate the location where a particular pattern has been shown previously. In case of an error, the participant is asked to repeat the task for a maximum of ten trials. The task is then repeated on another stage with increased difficulty level. The first trial memory score is calculated as the number of patterns correctly allocated at first attempt for all completed stages. The PAL memory score assesses explicit visuospatial memory and has been found to indicate dementia, especially of Alzheimer's type (Lee et al., 2003).

VRM: The participant is shown a list of twelve words and asked to recall freely as many items as possible. Subsequently, the participant is shown a second list including the previously presented words as well as distractors and is asked to choose the items he or she recognises. The recognition procedure is repeated after twenty minutes. The number of items recognised after delay is analysed, since recognition memory has been shown to be associated with medial septal volume in the BFCS in younger participants (Butler et al., 2012). Furthermore, two studies suggest associations of BFCS volume with delayed recall in memory tasks (Grothe et al., 2010, 2016).

SSP: The participant is shown colour changing boxes on a screen. He or she is then asked to indicate the correct sequence by which the boxes have changed colours. The parameter of interest analysed is the longest sequence of boxes recalled (span length), which is thought to represent visual working memory (Monaco et al., 2013).

SRT: The participant is shown a square on a computer screen. He or she is asked to respond to this stimulus by selecting a button as fast as possible. Mean response latency (reaction time) is the parameter of interest. Reaction time is considered to be a marker of fluid intelligence and age-associated decline in cognitive ability (Der and Deary, 2018).

TMT: The participant is asked to connect dots marked with ascending numbers in Part A or alternating numbers and letters (e.g. 1-A-2-B-3…) in Part B. When a mistake is made, the participant is asked to correct it. Time for completion of both parts is the parameter of interest. Values above commonly used cut-off thresholds (180s for TMT-A, 300s for TMT-B) were excluded during a plausibility check before data analysis. Part A is considered to be a measure of visual search and motor speed, whereas part B measures executive functions including cognitive alternation, working memory and attention (Bowie and Harvey, 2006; Crowe, 1998).

GPT: The participant is asked to insert 25 pegs with a key alongside into wholes in a board. The key slots are rotated randomly, demanding visual-motor coordination skills and manual dexterity (Otten et al., 2012). Test parameter of interest is the time for completion with the dominant hand. Data from participants who exceeded a limit of 300 s for this task were excluded during the plausibility check.

Table 1
Inclusion and exclusion criteria of the BioCog study.

Inclusion criteria	Exclusion criteria
• Age ≥ 65 years • European descent (Caucasian) • Major elective surgery with planned operation time ≥ 60 min • Ability to give informed consent	• MMSE score ≤ 23 points at inclusion • Neuropsychiatric morbidity (including addiction), which limits the conduction of the neurocognitive testing • Anacusis or hypacusis, which limits the conduction of the neurocognitive testing • Centrally acting medication (e.g. antidepressants or tranquillizers) • Homelessness or inability to reach patient for follow-up • Participation in another prospective interventional clinical study during hospital stay • Accommodation in an institution due to an official or judicial order • Missing informed consent for saving and handing out pseudonymous data

Global cognitive ability 'g': The global cognitive component is derived from performance on the neurocognitive battery (above) using Principal Component Analysis (PCA) in line with previous literature (Staff et al., 2006, Shenkin et al., 2009). The first unrotated factor was extracted from data of 303 participants enrolled at both study centres in Berlin and Utrecht with complete neurocognitive assessment. The first factor had an eigenvalue of 2.3 and explained 38.33% of the variance in test performance and is considered the global cognitive ability. In our study the factor is derived from TMT-B (factor loading 0.76), PAL (factor loading: 0.71), GPT (factor loading: 0.68), SSP (factor loading: 0.55), SRT (factor loading: 0.49) and VRM (factor loading: 0.46). Due skewed distributions, time for completion of TMT-B and GPT as well as SRT mean latency were reversed and underwent logarithmic transformation prior to PCA. The test outcomes used for extraction of 'g' are those stated above except for the VRM: The number of words correctly remembered in the free recall has been used for calculation of g, but based on existing literature, the delayed recognition task seemed more relevant for analysis of BFCS volume associations with VRM performance (Butler et al., 2012; Grothe et al., 2010, 2016).

2.3. MR image acquisition

MR imaging was conducted on the same day the neurocognitive assessments took place. In Berlin, data were collected at the Berlin Center for Advanced Neuroimaging using a 3 T Magnetom Trio MR scanner (Siemens) with a 32-channel head coil. T1-weighted 3D structural brain scans were acquired using a MPRAGE sequence (magnetisation prepared rapid gradient echo in 192 sagittal slices, FOV: 256·256 mm^2, voxel size: 1·1 mm^2 at 1 mm slice thickness, TR: 2500 ms, TE: 4.77 ms, 7° flip angle). In Utrecht, data were collected with an Achieva 3 T MRI scanner (Phillips) equipped with an 8-channel head coil. For technical reasons, the scanner at this study site had to be exchanged with an identical machine equipped with a 32-channel head coil during the study. A similar T1w sequence was recorded here (192 sagittal slices, FOV: 256·232 mm^2, voxel size 1·1 mm^3 at 1 mm slice thickness, TR: 7.9 ms, TE: 4.5 ms, 8° flip angle).

A board-certified neuroradiologist screened all MR images for incidental findings with clinical relevance.

2.4. MRI processing

2.4.1. Segmentation of brain volume and brain parenchyma fraction

T1-weighted MR images were partitioned into grey and white matter as well as cerebrospinal fluid using the standard SPM12 segmentation routine (http://www.fil.ion.ucl.ac.uk/spm/software/spm12/) in a MATLAB environment (The Mathworks, Inc., Natick, MA). Partition volume was defined as the sum of all voxels with at least 50% probability to correspond to the respective partition. Total brain volume is calculated as the sum of grey and white matter. Intracranial volume (ICV) is defined as the sum of brain volume and cerebrospinal fluid volume. Brain parenchyma fraction (BPF) is defined as the ratio of brain volume and intracranial volume which is a global marker for age related neurodegeneration. BPF decreases during ageing and has been associated with disease related cognitive impairment in Multiple Sclerosis (Blatter et al., 1995; Hohol et al., 1997; Matsumae et al., 1996; Smith et al., 2008). ICV is thought to be driven by brain growth during childhood and does not undergo shrinkage in ageing (Davis and Wright, 1977; Pfefferbaum et al., 1994). We thus consider ICV a biomarker for archaeological maximum brain size and the BPF a marker of preserved brain volume and the degree of age related atrophy (Shenkin et al., 2009).

2.4.2. Segmentation of the BFCS

We have previously described the segmentation method we used for the volumetry of the BFCS (Lammers et al., 2016). Butler et al. (2014) described a similar method and they were able to show that the results are comparable to manual segmentation techniques.

Segmentation of the BFCS was performed using a probabilistic map of the basal forebrain presented by Zaborszky et al. (2008) which has been used in several previous imaging studies (Grothe et al., 2010; Butler et al., 2012, 2013, 2014; Li et al., 2014a; Kline et al., 2016; Cantero et al., 2017). Zaborszky and colleagues used histological slices and corresponding MR images of ten post-mortem body-donor brains (five female, age 37–75 years) without known neurological or psychiatric disease to define four cholinergic subregions in the basal forebrain. Brain sections were stained for cell bodies using a modified silver method of Gallyas. A comprehensive description of the BFCS delineation is found in the original publication (Zaborszky et al., 2008). The probabilistic map uses a modified version of the Mesulam nomenclature. Furthermore, apart from dense cell aggregates, also scattered magnocellular neurons in adjacent structures (e.g. the basal ganglia) were included. Studies identified these neurons as cholinergic, suggesting that these are displaced cells of the Nucleus basalis Meynert (Saper and Chelimsky, 1984; Mesulam and Geula, 1988). It is a point of discussion whether researchers should refer to these scattered neurons as a part of the Ch1-Ch4 system (Mesulam and Geula, 1988; Halliday et al., 1993).

A voxel in this map was assigned to one of the subregions which it represented in at least four out of ten brains. The final map was referenced to the anatomical MNI (Montreal Neurological Institute) space (Holmes et al., 1998).

SPM12 was used to segment MR images as well as the anatomical MNI reference brain. The DARTEL (Diffeomorphic Anatomical Registration using Exponentiated Lie algebra) toolbox was then used to create DARTEL flow fields describing deformations from the MNI reference brain to a participant's individual brain (Ashburner, 2007). These deformations were applied to the probabilistic map of the basal forebrain resulting in individual labelling of cholinergic subregions in a participant's brain scan. Volumes of cholinergic subregions in the basal forebrain were determined by counting all voxels labelled as corresponding to this regions. Fig. 1 shows the segmented regions in MR images of one subject.

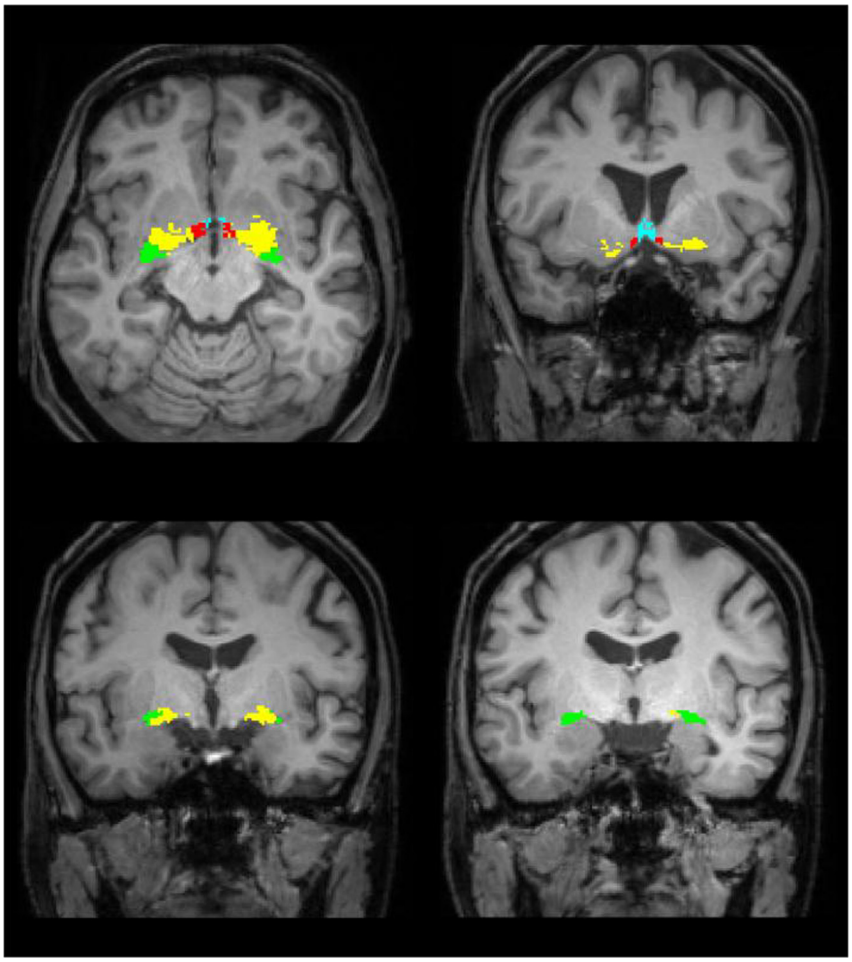

Fig. 1. Location of the BFCS in one individual. The Ch1/2 region is displayed in blue, Ch3 in red. Ch4 is shown in yellow and Ch4p corresponds to the green area. We refer to a modified version of the Mesulam-nomenclature (Zaborszky et al., 2008). (For interpretation of the references to colour in this figure legend, the reader is referred to the web version of this article.)

2.5. Statistical analysis

2.5.1. Analysis pipeline

We first analysed the association of BFCS volume with the global cognitive component 'g' (primary parameter of interest). We report unadjusted and adjusted associations (for age, sex and education) in generalised linear models. To assess confounding effects of global volumes, the goodness of fit of a model including BFCS volume was compared with models including brain volume and BPF. We further analysed the associations of BFCS volume with 'g' after addition of these confounder variables into the model. We repeated the analysis correcting for scanner and centre effects. Since adjustment for these did not change the results, nor significant effects were found, the variables were dropped for post-hoc analysis of test performance analysis.

In addition, subsequent descriptive analyses were conducted to assess associations of BFCS volume and performance on each of the individual tests of the neurocognitive battery (secondary, post-hoc parameters of interest). If test performance was significantly associated with BFCS volume without adjustment, it was considered for further analysis of adjusted effects. To further assess if associations of BFCS volume with test performance are specific for a cognitive domain, we adjusted the linear model for 'g'.

In a final step, cognitive performance was analysed for quantile-dependent effects of BFCS on 'g' and performance on individual cognitive tests. This allows assessment of associations of BFCS volume with cognitive functions which are specific for low- and high-performers.

All statistical analyses were run in R3.4.1 (https://www.R-project.org/, R Core Team, 2017). The level of significance was set at $p < 0.05$. No corrections for multiple comparisons were made.

2.5.2. Descriptive analysis

We report test performance including median performance, interquartile range and minimum-maximum range. Demographic and neuropsychological data have been compared between centres. Neuroimaging data have also been compared between MR scanners. We used the ANOVA F-test for continuous normal, the Kruskal-Wallis-test for continuous non-normal distributions and the χ^2-test for nominal data. Correlations among independent variables are reported as Pearson's correlation coefficient R.

2.5.3. Generalised linear model

We analysed the associations of BFCS volume and its subregions (in mm^3 and per one standard deviation/SD) with cognitive performance. If a significant association of BFCS volume with subtest performance was found, we adjusted the generalised linear model (GLM) for education (classified according to ISCED/International standard classification of education in three categories), age and sex. For 'g', TMT, SRT latency, PAL memory score and GPT a Gaussian distribution was assumed, for SSP and VRM a quasi-Poisson distribution was selected. TMT, SRT and GPT scores were log-transformed before analysis. For Gaussian-distributed data, R^2 is reported and for quasi-Poisson distributed tests, D^2 is reported (Guisan and Zimmermann, 2000): D^2 = (Null deviance – Residual Deviance)/Null Deviance and partial D^2 = (Residual $\text{Deviance}_{\text{Reduced Model}}$ – Residual $\text{Deviance}_{\text{Full Model}}$)/

Residual Deviance$_{\text{Reduced Model}}$.

2.5.4. Quantile regression analysis

In a second approach, cognitive performance was analysed using quantile regression (Koenker and Hallock, 2001). The rationale for quantile regression is robustness against heteroscedasticity and outliers in neuropsychological data. Rather than analysing the conditional mean as it is done with ordinary least squares (OLS) regression in GLM, quantile regression calculates conditional quantiles. E.g. quantile regression at the 0.5 quantile yields the median of a distribution of the dependent variable for a given value of the independent variable, whereas OLS regression returns the corresponding mean. Furthermore, the analysis of quantiles other than the 0.5th allows assessment of effects at the upper or lower boundaries of a distribution. This approach has appealing properties, when relevant covariates exit, but cannot be included in the regression model (Cade and Noon, 2003). On the other hand, quantile regression allows analysis of associations in high- and low-performing strata of the study sample.

Regression coefficients for different quantiles can be compared and tested for a statistically significant difference (referred to as heterogeneity of slopes). Heterogeneity of slopes suggests that volume affects the shape of a distribution rather than a central shift.

No transformations were applied to these variables prior to quantile regression analysis, but since count data are not eligible for quantile regression, span length was jittered to approximate a continuous distribution (Machado and Silva, 2005).

The Barrodale and Roberts algorithm implemented in the quantreg package was used for computation of quantile regression coefficients (https://CRAN.R-project.org/package=quantreg, Koenker, 2017). We report quantile regression results in scatter plots with quantile regression lines and quantile-coefficent plots (Q-C plots) for nine even spaced quantiles (0.1–0.9) with 95% confidence intervals (CI). Heterogeneity of slopes between the 0.5th and the lowest performing quantile (0.1th or 0.9th, respectively) was analysed using ANOVA. CI and p-values are based on the assumption of non-identical standard errors (called “nid” in the quantreg code).

3. Results

Fig. 2 is the Consort Diagram for the sample. Demographic information on the study participants is provided in Table 2. Neuropsychological test performance including the respective number of analysed datasets is reported in Table 3. Only TMT-B performance (median [IQR]: Berlin 101.98 s [86.25–136.5 s], Utrecht 104.1 s [75–118.8 s], $\chi^2 = 6.35$, $p = 0.0118$) and educational status (ISCED1–2 and ≥5: Berlin 21.1% and 34.3%, Utrecht: 28.2% and 44.9%, $\chi^2 = 6.64$, $p = 0.0361$) differ significantly between centres. Significant between-centre differences are found for BFCS volume ($F_{1,279} = 8.65$, $p = 0.0036$, $\Delta = 93\,mm^3$), total brain volume ($F_{1,279} = 5.37$, $p = 0.0212$, $\Delta = 43\,cm^3$) and BPF ($F_{1,279} = 6.69$, $p = 0.0102$, $\Delta = 0.014$, Table 4). Mean volumes are higher in the Utrecht sample. Between-scanner effects for the study centre in Utrecht are not significant.

BFCS volume correlates with age ($R = -0.26$, $p < 0.0001$), total brain volume ($R = 0.83$, $p < 0.0001$) and BPF ($R = 0.25$, $p < 0.0001$). BFCS volume ($F_{1,280} = 75.69$, $p < 0.0001$), total brain volume ($F_{1,280} = 77.06$, $p < 0.0001$) and BPF ($F_{1,280} = 11.02$, $p = 0.0010$) differ by sex. BFCS and brain volume are larger in men, while BPF is higher in women. Differences by education are found for BFCS volume ($F_{2,279} = 3.27$, $p = 0.0397$), total brain volume ($F_{2,279} = 7.95$, $p = 0.0004$), but not for BPF ($F_{2,279} < 0.01$, $p = 0.85$). BFCS and brain volumes are larger in more educated subjects.

3.1. Associations of BFCS volume with global cognitive ability

Our primary hypothesis is an association of BFCS volume with global cognitive ability: BFCS volume is significantly associated with ‘g’ ($R^2 = 0.061$, $p = 0.0001$, see Fig. 3). This association is largely independent of age, education and sex and remains significant after adjustment for these variables ($R^2 = 0.287$, partial $R^2 = 0.041$, $B = 0.204 \pm 0.064$ per SD, $p = 0.0017$, see Table 5).

Association of BFCS subregions (CH1/2, CH3, CH4, CH4p) with global cognition are also assessed. After correction for age, sex and education, all subregions are significantly associated with ‘g’, and the association of BFCS with general cognition was slightly inferior to the association of ‘g’ and the most posterior subregion CH4p. According to R^2, CH4p ($R^2 = 0.290$, partial $R^2 = 0.045$, $p = 0.0009$) is slightly more relevant for ‘g’ than more rostral regions CH1/2 ($R^2 = 0.281$, partial $R^2 = 0.032$, $p = 0.0057$), CH3 ($R^2 = 0.271$, partial $R^2 = 0.019$, $p = 0.0352$) and CH4 ($R^2 = 0.276$, partial $R^2 = 0.026$, $p = 0.0127$).

Associations of confounding global anatomical volumes (brain

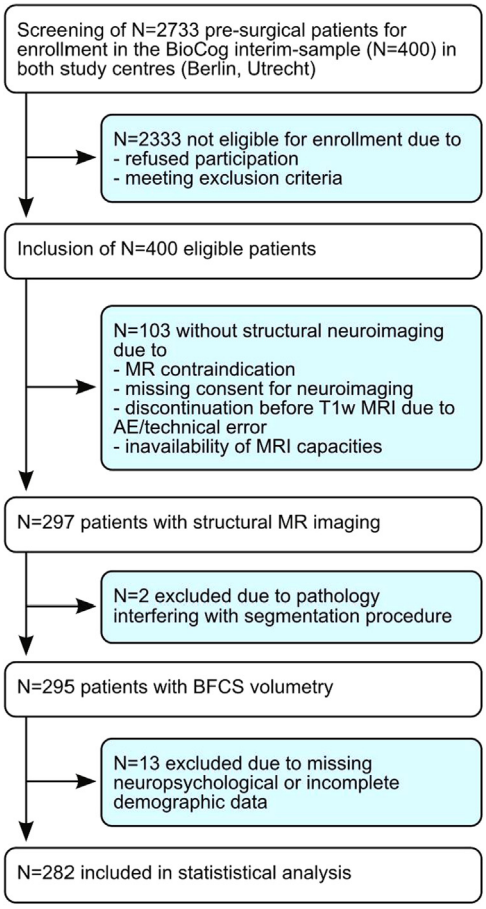

Fig. 2. Consort diagram. For this cross-sectional analysis, datasets have been included which have been defined as drop-outs for longitudinal analysis due to missing primary endpoints (assessment of post-operative delirium). AE refers to adverse event.

Table 2
Demographic description of the study sample. ISCED refers to the International standard classification of education.

		Median	Interquartile Range	Range
Age	(years)	72	68–76	65–87
MMSE	(points)	29	28–30	24–30
		N	%	
Sex	Female	110	39%	
Education	ISCED 1 and 2	65	23%	
	ISCED 3 and 4	110	39%	
	ISCED 5 and higher	107	38%	

Table 3
Summary of cognitive performance: Number of available datasets (N), median, full and interquartile range of performance.

Test	Parameter of interest	N	Median	Interquartile Range	Range
SRT	Mean correct latency (ms)	282	290.2	252.1–348.6	200.8–801.4
TMT-A	Time for completion (s)	267	45	36.02–57.50	19–132
TMT-B	Time for completion (s)	250	100	81–113.04	25.39–298
GPT	Time for completion (s)	270	93	80–110	50–254.27
SSP	Span length	280	5	4–5	3–8
PAL	Memory score	280	13	11–17	0–25
VRM	Number of correctly recognised items after delay	221	22	20–23	0–24
Global cognition	'g'	243	0.10	-0.50–0.74	-2.70–2.35

Table 4
Summary of volumetric data: Median, full and interquartile range.

	Median	Interquartile Range	Range
BFCS volume (mm^3)	2201	2035–2350	1600–2875
Brain volume (cm^3)	999.9	921.7–1077.4	720.6–1280.7
BPF (fraction)	0.68	0.65–0.71	0.47–0.81

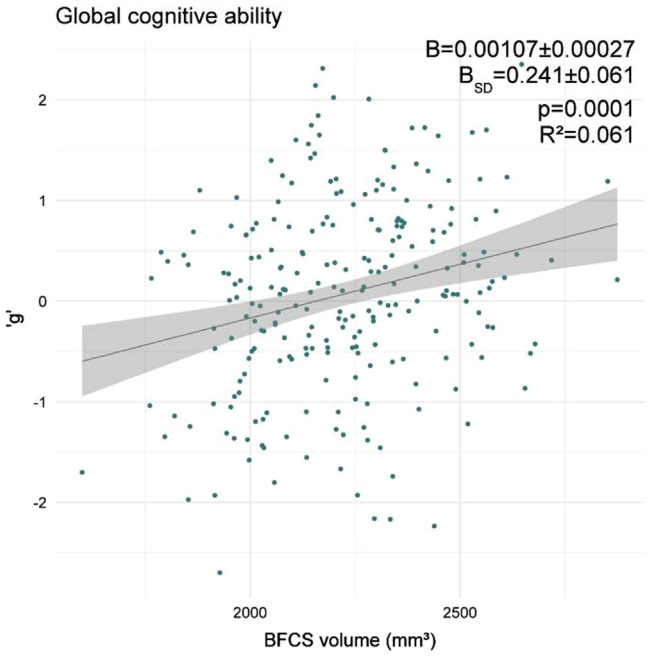

Fig. 3. Association of BFCS volume with global cognitive ability. B indicates the change in 'g' per 1 mm^3 and one standard deviation (B-SD) change in BFCS volume. Regression coefficients (B), p-value and R^2 correspond to the unadjusted model.

Table 5
General linear model (GLM) describing BFCS volume associations with global cognitive abilities. Regression coefficients are indicated as B with standard error (SE) and the corresponding p-value. SD refers to standard deviation.

Independent variable	B ± SE	p
BFCS volume in mm^3 (change per SD)	0.00090 ± 0.00028 (0.204 ± 0.064)	0.0017
Age in years	− 0.059 ± 0.011	< 0.0001
Male sex	− 0.347 ± 0.129	0.0075
ISCED level 1 + 2	− 0.449 ± 0.138	0.0013
ISCED level 5 and higher	0.497 ± 0.122	< 0.0001

volume, BPF) and global cognitive abilities are tested in general linear models adjusting for age, sex and education. A considerable improvement is achieved by using a model which includes total brain volume (R^2 = 0.311, partial R^2 = 0.073, B = 0.280 ± 0.065 per SD, p < 0.0001). The association of global cognitive ability and BPF is significant, but was inferior to the model including brain volume (R^2 = 0.300, partial R^2 = 0.058, B = 0.235 ± 0.062 per SD, p = 0.0002).

BFCS volume and each one of the potentially confounding volume measures are then added concurrently into two further general linear models of 'g'. When total brain volume and BFCS are included in the same model alongside with age, sex and educational status, only the association of total brain volume with global cognitive ability remains significant (partial R^2 = 0.033, B = 0.274 ± 0.096 per SD, p = 0.0047), but not for BFCS (partial R^2 < 0.001, B = 0.008 ± 0.093 per SD, p = 0.93). A model including BFCS volume and BPF shows that BFCS and BPF are independently associated with global cognitive ability (partial R^2_{BFCS} = 0.023, B_{BFCS} = 0.154 ± 0.065 per SD, p_{BFCS} = 0.0191; partial R^2_{BPF} = 0.040, B_{BPF} = 0.198 ± 0.063 per SD, p_{BPF} = 0.0019).

There is no significant effect of MR scanner or study centre, nor does adjustment for these alter the results.

3.2. Associations of BFCS volume with test performance

In the unadjusted analyses, BFCS volume is significantly and positively associated with performance in all tests, except delayed recognition in the VRM.

The strongest associations are seen for TMT-B and SRT latency (R^2 = 0.073 and 0.048, respectively). Somewhat weaker associations are also found for PAL memory score, TMT-A, GPT (see Fig. 4) and the SSP (D^2 = 0.030, B = 0.00015 ± 0.00005, B_{SD} = 0.034 ± 0.012, p = 0.0034, not presented in Fig. 4). Using a Bonferroni-corrected level of significance p′ to account for testing associations with seven cognitive tests (p′ = 0.05/7 ≈ 0.0071), only the unadjusted associations of BFCS volume with TMT-A and -B, SRT as well as SSP remained significant. Adjusting for age, education and sex yields similar associations of BFCS volume with PAL memory score, SRT latency, TMT-B and GPT. R^2 for these models was lower than for the model of 'g'. Associations with TMT-A performance and span length are no longer significant after adjustment for age, sex and education (see Table 6).

VRM is the only test without significant association with BFCS volume (D^2 = 0.005, B_{SD} = 0.011 ± 0.009, p = 0.22). The result for the VRM does not change after rejection of two outlying subjects (D^2 = 0.003, B_{SD} = 0.0060 ± 0.0068, p = 0.38).

After adjustment for global cognitive abilities, only TMT-B performance was significantly associated with BFCS volume (partial R^2 = 0.018, p = 0.0378). This association was no longer significant after further adjustment for age, sex and education (partial R^2 = 0.007, p = 0.19).

3.3. Quantile regression analysis

Fig. 5A and B are a graphical summary of quantile regression results of global cognitive ability and test performance. ANOVA for heterogeneity of slopes indicates that differences between associations of BFCS volume and cognitive performance between 0.5th and 0.9th quantile exist for SRT latency and GPT, but neither for the other tests

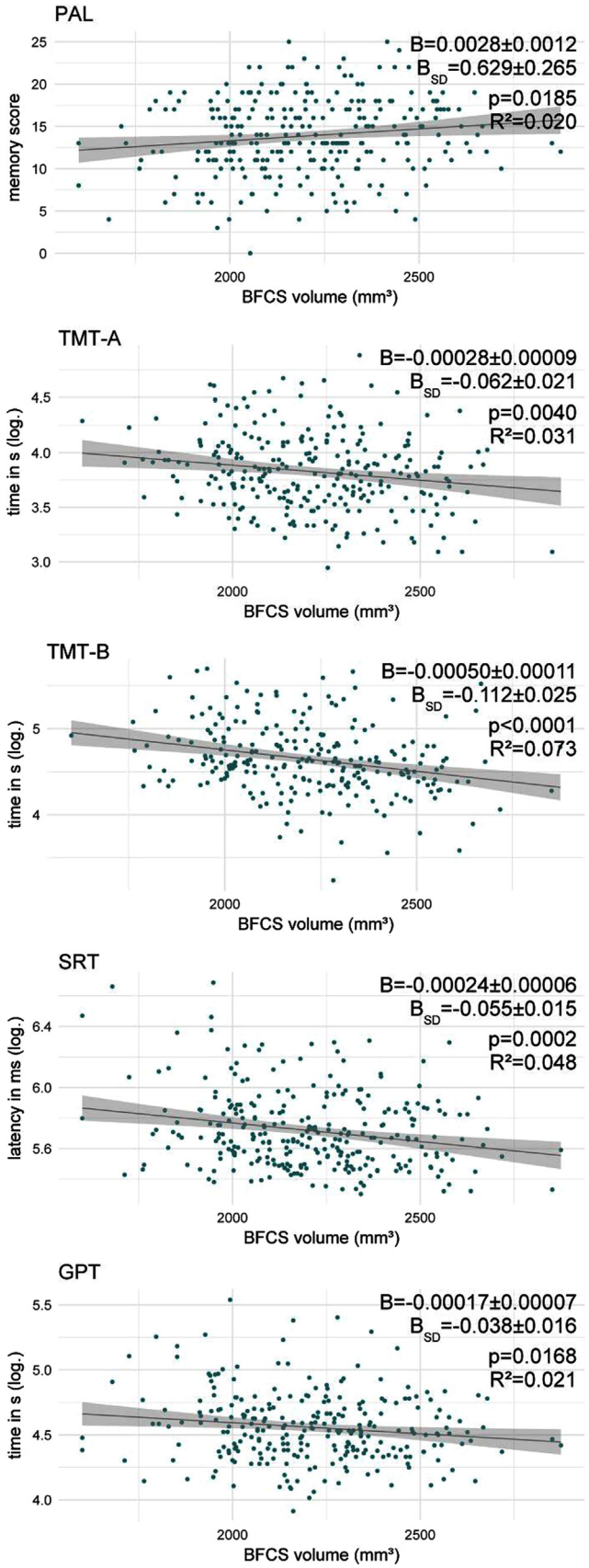

Fig. 4. Association of BFCS volume with test performance. B indicates the change in the test parameter per 1 mm^3 and one standard deviation (B-SD) change in BFCS volume. Regression coefficients (B), p-value and R^2 correspond to the unadjusted model.

Table 6
Adjusted GLM for associations of BFCS volume with test parameters. All GLM are adjusted for age, sex and education. Associations are listed as regression coefficients (B) with standard errors per one SD (standard deviation) change of BFCS volume. P-values, R^2 and partial R^2 for BFCS volume are indicated, except for the SSP: These values marked with an asterisk (*) correspond to D^2. p-values have not been corrected for multiple tests. p-values marked with a double asterisk (**) are significant after Bonferroni correction for independent tests ($p' < 0.0071$).

Test	B ± SE for BFCS volume per SD	(p)	Partial R^2 (D^2)	R^2 (D^2)
PAL	0.632 ± 0.294	(0.0325)	0.017	0.146
TMT-A (log)	− 0.030 ± 0.024	(0.22)	0.006	0.129
TMT-B (log)	− 0.084 ± 0.028	(0.0030**)	0.036	0.241
SRT (log)	− 0.039 ± 0.017	(0.0245)	0.018	0.075
GPT (log)	− 0.046 ± 0.017	(0.0085)	0.026	0.192
SSP	0.016 ± 0.013	(0.22)	0.005*	0.115*

nor 'g'.

For the global component, results from the GLM are reproduced in quantile regression. The association of BFCS volume and 'g' showed no quantile-dependent trend, with significance found for all quantiles in the unadjusted model. After adjustment, significance was restricted to quantiles close to the median ($B = 0.0010 \pm 0.0003$, $B_{SD} = 0.220 \pm 0.076$, $p = 0.0043$).

For TMT-A and -B, PAL and SSP median regression coefficients were acceptably close to the OLS estimate. Neither ANOVA nor inspection of plots suggested systematic quantile-dependent associations, especially not after adjustment for age, sex and education. With regard to significance, differences between the analysis methods occurred. On the one hand, parametric methods can be more efficient than alternative methods when data are normally distributed, explaining the more optimistic results of the GLM for the association with PAL (Kitchen, 2009). On the other hand, GLM standard errors are sensitive to outliers and skewed distributions, yielding more favourable results of quantile regression (Wilcox, 2012).

Results for the SRT and GPT differ from GLM results. For these tests, BFCS volume association with test performance differs significantly between the 0.5th and 0.9th quantile with a stronger association for the low-performance quantiles (0.9th, see Fig. 5B). In the adjusted models regression coefficients for the 0.1th to the 0.7th quantile are close to zero, but significant effects are found at higher quantiles for SRT latency (0.9th quantile: $B = -0.198 \pm 0.042$, $B = -44.6 \pm 9.5$ per SD, $p < 0.0001$) and GPT completion time (0.9th quantile: $B = -0.053 \pm 0.018$, $B = -12.0 \pm 4.0$ per SD, $p = 0.0031$).

4. Discussion

In the current study, we analysed the associations of BFCS volume with global cognitive ability and performance on several age-sensitive cognitive tests in a sample of elderly pre-surgical patients. We found significant positive associations of BFCS volume with global cognition and tests of visual memory, manual dexterity, processing speed and executive functions. BFCS volume explains more variance in the global component than in any of the cognitive test outcomes. E.g., independent of age, sex and educational status, BFCS volume explains 4.1% of the variance in 'g', but only 3.6% or less variance in test performance. This result suggests that BFCS volume is associated with better overall cognitive function in ageing rather than affecting a specific cognitive domain. This conclusion is further supported by our finding that performance in cognitive tests was no longer independently associated with BFCS volume when analyses were adjusted for 'g', suggesting that global cognitive abilities mediate the associations with test performance. However, the association of BFCS volume with global

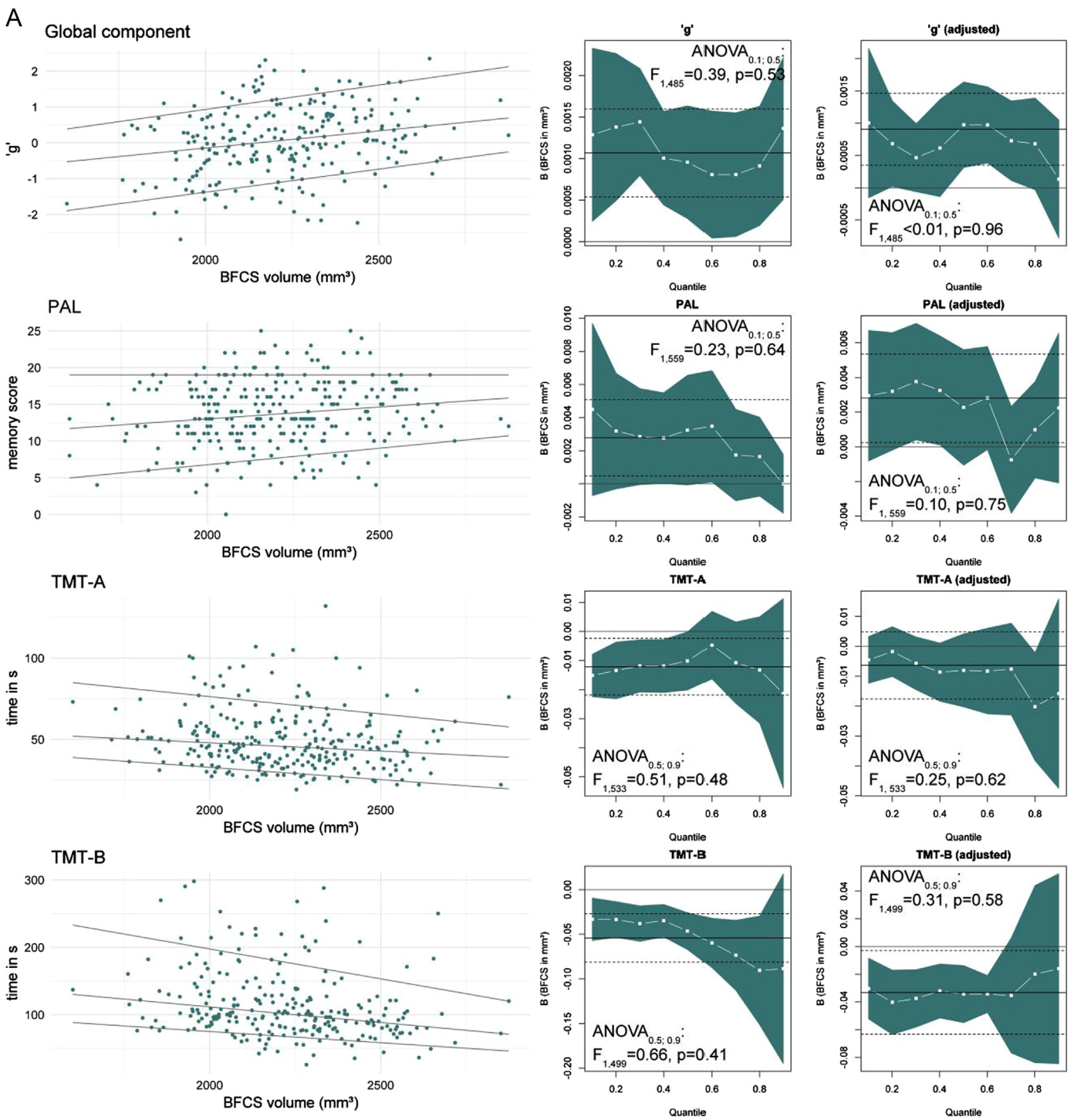

Fig. 5. A: Quantile regression results of 'g' and test performance. The left column shows scatter plots with regression lines for the 0.1th, 0.5th (median) and 0.9th quantile. The columns on the right display quantile-coefficient plots for simple (unadjusted, middle) and multiple quantile regression adjusting for age, sex and education (right). The regression coefficient for BFCS volume (white –■–) are displayed for each quantile (x-axis) with 95% CI (blue area). Solid and dashed lines mark the OLS regressions result with 95% CI. ANOVA results correspond to analysis for slope heterogeneity between median and lowest-performing quantile. (For interpretation of the references to colour in this figure legend, the reader is referred to the web version of this article.)

cognitive ability is driven by a more general association of total brain volume and cognition. BPF and BFCS volume are independently associated with cognition, suggesting BFCS volume has a beneficial function for cognitive reserve in atrophy-related cognitive decline. We further found that whereas the association of BFCS volume and global cognition is stable for all levels of performance, the association with SRT and GPT performance is only found for low-performing participants.

Our study needs to be discussed in the context of results reported by Wolf et al. (2014) and Grothe et al. (2016). The former work analysed associations of BFCS subregion volumes with global cognition and test performance in 43 healthy adults aged 60–85 years with a very high IQ. After correction for intracranial volume, age and education they reported a significant association with global cognitive ability, but not with performance in single cognitive domains. Wolf's results support our findings with regard to an association of BFCS volume with global cognition rather than single test performance. Furthermore, we found a

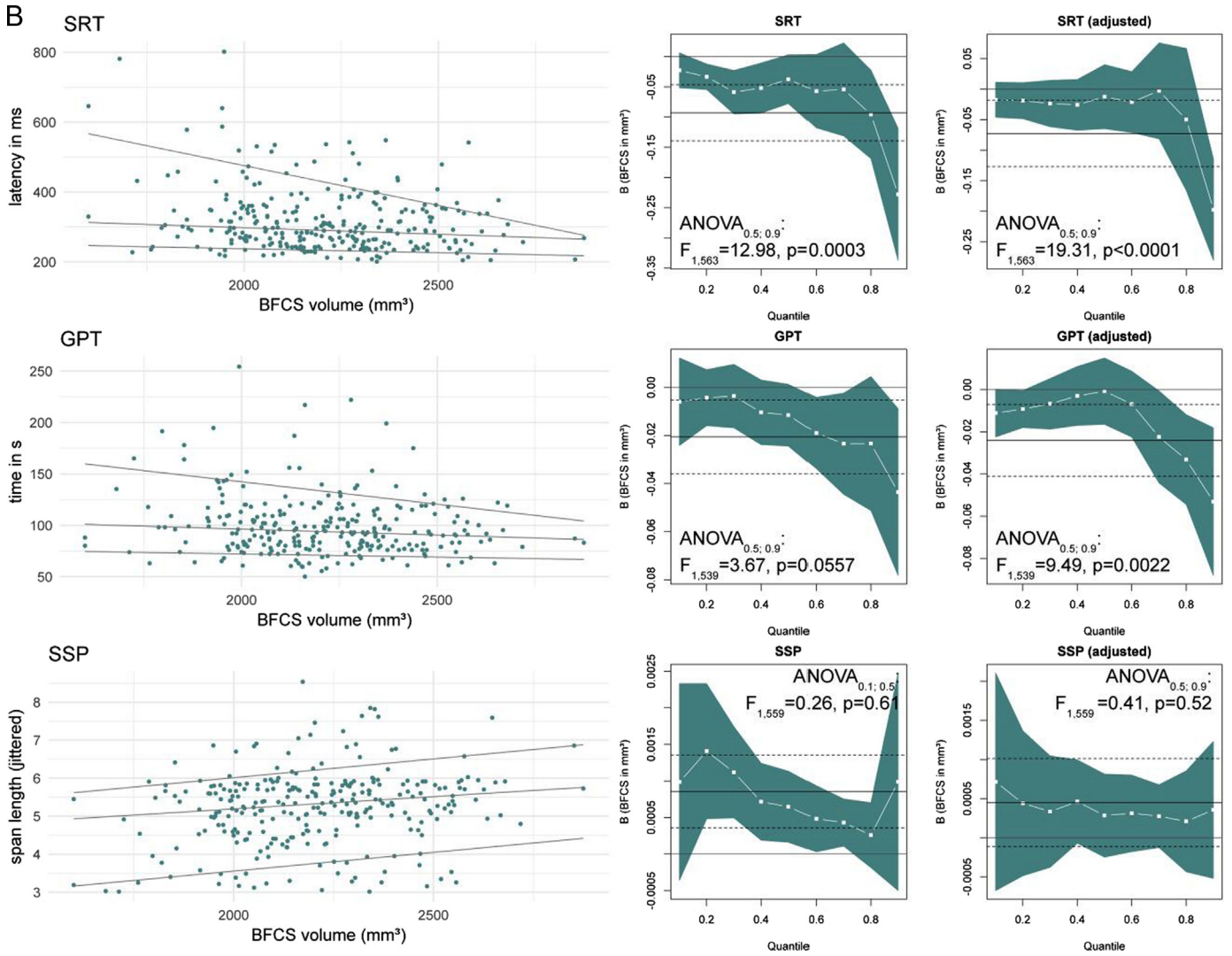

Fig. 5. (*continued*)

similar pattern of BFCS subregion contribution to global cognition: Total BFCS volume and posterior compartments (Ch4p) seem to be more relevant than anterior sections. In our study, the association of BFCS volume with 'g' was stronger than with performance in any cognitive test. Thus it is likely that this study missed associations with test performance due to lower statistical power.

Grothe et al. (2016) analysed the association of BFCS volume and test performance in 132 MCI subjects and 177 "hypernormal" healthy controls enrolled in the ADNI project. After controlling for age, sex and education, no significant associations with subtest performance were found in the healthy control group. Instead, significant associations with memory and attentional control were only found in the MCI group. Although the authors did not report analyses of global cognitive ability, our positive findings on BFCS volume associations with performance in single tests from the neurocognitive battery disagree with the results by Grothe and colleagues. We think that to some extent these differences can be explained by clinical differences in the analysed groups. Whereas the respective studies analysed unusually high performing elderly individuals, cognitive performance in our cohort had greater variance and most likely includes subjects with preclinical cognitive impairment. For instance, comparison of TMT performance, which is reported in all aforementioned studies, suggests that Wolf et al. (TMT mean time: A 36.6 s, B 91.1 s) and Grothe et al. (TMT mean time: A 33.7 s, B 80.3 s) analysed subject groups with better performance compared to the BioCog cohort (TMT mean time: A 48.8 s, B 113.0 s). Tombaugh (2004) presented age-stratified normative data for the TMT. The average performance in Wolf's and Grothe's samples were better than 50% and 70% of the reference group (70–74 years) in Tombaugh's data, whereas the BioCog cohort mean corresponds to the 30th percentile of this reference group. We further compared TMT performance in our sample to reference data stratified by prevalence and future incidence of dementia in a sample of patients aged over 70 years (Holtzer et al., 2008). Although TMT performance of 75% of the BioCog cohort is close to the reference value of the group without prevalent dementia or future conversion (TMT mean time: A 56.7 s, B128.8 s), the TMT completion time in the worst performing quartile of our sample is closer to the groups with incident (TMT mean time: A 87 s, B 186 s), or prevalent dementia (TMT mean time: A 112 s, B 208 s) in that study.

Both the sample analysed by Wolf as well as the control subjects from the ADNI project included in the study by Grothe underwent additional dementia screening (Clinical Dementia Rating Scale, Stamm Screening Questionnaire and International Checklist of ICD-10 and DSM-IV). Dementia screening in the BioCog study is restricted to consultation of medical records and patient interview for neuropsychiatric diseases as well as MMSE assessment. The MMSE score was designed originally as a bedside screening tool for dementia, but is not generally recommended as a diagnostic criterion for dementia (Folstein et al., 1975; Tombaugh and McIntyre, 1992). Comparisons of the MMSE score with the Clinical Dementia Rating Scale (CDR) in a memory clinic suggested that among patients with score of 26–29 points, about 40%

have a CDR score of 0.5 or 1, corresponding to probable or mild dementia (Perneczky et al., 2006). The authors further reported CDR scores of at least 0.5 (probable dementia) for all patients with MMSE scores below 26. This study reports the limited ability of the MMSE score to exclude patients with pre-existing cognitive impairment, which might also apply to the BioCog study (MMSE cut-off at 24 points). Furthermore, the BioCog study only includes elderly pre-operative patients with an indication for surgery and the overall morbidity of the cohort is probably higher compared to the groups analysed by Grothe et al. (2016) and Wolf et al. (2014). Vassilaki et al. (2015) reported associations of multimorbidity and mild cognitive impairment which implies that pre-clinical cognitive decline might occur more often in the clinical sample presented here. Overall, our considerations suggest that a larger proportion of patients with (mild) cognitive impairments in the BioCog group contributes to the significant associations of cognitive performance with BFCS volume compared to the group analysed by Grothe et al. (2016).

To further test this assumption in our data, we used quantile regression analysis to assess the association of BFCS volume with test parameters for different levels of performance. Although in this analysis statistical significance was found only for subjects with median global cognitive ability, we found no quantile-dependent association of BFCS and global cognition, suggesting that BFCS volume is associated with better cognitive performance at all stages of age-associated cognitive decline. Since the association seems to be very stable also for high-performing subjects we suggest that this might contribute to the findings by Wolf et al. (2014). Further analysis of SRT and GPT, which are tests of reaction time and visual-motor control, revealed significantly different associations for the 0.5th and the lowest performing quantile. Independent associations have only been found in poorly achieving subjects. These findings suggest that their association with BFCS volume seems to be specific for individuals with low task performance. It is possible that BFCS volume limits minimum performance in these participants, rather than improving performance in average- to high-performers. This might point to a function of BFCS volume as a structural cognitive reserve which is recruited in low performing subjects, but with regard to the different results of the studies mentioned above, it shows that the association of BFCS volume with test performance indeed depends on the overall performance level of the study group. Whereas Wolf and Grothe might have missed significant associations by recruiting only high performing participants, our results might be driven by a higher fraction of subjects with relevant age-related cognitive decline.

As pointed out above, most differences between studies may arise from differences in sample composition. Even so, some additional differences between these studies need to be taken into account. The BFCS volumes we report are considerably larger than those reported by Wolf and Grothe. Furthermore, the MRI derived volumes in our study are larger than the work by Zaborszky et al. (2008) suggest. Thus, it seems unlikely that these differences are caused by varying degrees of BFCS atrophy between the studies. Instead, we need to take into account that we used a probabilistic map of the BFCS which was derived from histological sections of ten brains. The map summarises brain regions with at least 40% overlap from these brains. In contrast to this, Wolf and Grothe report to have used a BFCS map based on one single brain (Kilimann et al., 2014). Thus, our method overestimates absolute BFCS volume. On the other hand, the location of cholinergic cells in the basal forebrain has high inter-individual variability, limiting the generalisability of single-subject based maps for larger populations (Zaborszky et al., 2008). The choice of the appropriate method is thus a point of discussion and the lack of a final recommendation reinforces the need for different studies using complementing approaches.

Our study has greater statistical power by including more participants than Wolf and colleagues and by refusing to correct for multiple independent tests. Especially after a significant association between ‘g’ and BFCS volume has been shown, it is not reasonable to assume independence of the various tests ultimately constituting the basis of global cognitive ability (Johnson et al., 2004, 2008; Deary et al., 2010).

Notably, we found no association of BFCS volume and episodic memory in VRM. Thus our results could not reproduce findings from studies on younger samples and MCI patients (Butler et al., 2012; Grothe et al., 2010, 2016). Apart from differences in sample composition, methodological differences also need to be taken into account to explain these findings. First, only one of these studies has reported a sample size comparable to the dataset presented here. Second, Butler and colleagues reported associations with source memory accuracy and discriminability rather than recognition memory. Finally, the association of BFCS volume and episodic memory seems to be specific for subjects with impairment in the memory domain. For instance, Grothe et al. (2016) suggested that BFCS atrophy effects on cognition are mediated by disease-related cortical dysfunction.

4.1. Limitations

In our study, ‘g’ has been calculated from several cognitive tests using principal component analysis. Thus, analysis of global cognitive abilities and subtest performance is to some extent redundant. We cannot exclude the possibility that our ‘g’ is biased towards measuring cognitive subdomains, e.g. with over-representation of short term memory (PAL, SSP, VRM free recall) and under-representation of long-term memory. As a consequence, we also might overestimate the association of volumes and ‘g’ by including tests of cognitive domains which might have an unusual strong association with BFCS volume. This is of particular relevance, since in the unadjusted models, the association of BFCS volume with TMT-B performance was stronger than the association with ‘g’, which nevertheless was confounded by age, education and sex.

Segmentation of cholinergic cell groups in the basal forebrain cannot be based on visual features of the cells in MR images (Teipel et al., 2015; Wolf et al., 2014). Therefore, we have to assume that volumetric data of the BFCS have relatively more noise contamination than brain volume which can be segmented by voxel intensity. Thus, associations of cognition and brain volume are a priori stronger than associations of cognition and BFCS volume due to noise distribution. Finally, our results are to some extent inconclusive with respect to the relative relevance of BFCS and total brain volume for cognition.

5. Conclusion

We were able to extend previous reports of BFCS volume association with global cognitive performance in a large sample of older adults. Our results suggest that contradictory findings of BFCS volume effects on subtest performance reflect a specific association for low-performing individuals, although these findings need further evidence.

Funding

The research leading to these results has received the funding from the European Community's FP7 under Grant agreement no. 602461. Additional (internal) funding was obtained from the Berlin Institute of Health (BIH, Berlin, Germany). Laszlo Zaborszky was supported by the NIH (USA) Grant NIH/NINDS NS023945 for his work on the maximum probability map of the basal forebrain cholinergic system.

Conflict of interest

This publication is part of Florian Lammers' doctorate. Prof. Winterer is coordinator of the BioCog Consortium and chief executive of the company Pharmaimage Biomarker Solutions GmbH. The company is one of the partners of the BioCog Consortium. None of the other authors declares a conflict of interest.

References

Anand, P., Singh, B., 2013. A review on cholinesterase inhibitors for Alzheimer's disease. Arch. Pharm. Res. 36, 375–399. https://doi.org/10.1007/s12272-013-0036-3.

Ashburner, J., 2007. A fast diffeomorphic image registration algorithm. Neuroimage 38, 95–113. https://doi.org/10.1016/j.neuroimage.2007.07.007.

Barnett, K., Mercer, S.W., Norbury, M., Watt, G., Wyke, S., Guthrie, B., 2012. Epidemiology of multimorbidity and implications for health care, research, and medical education: a cross-sectional study. Lancet 380, 37–43. https://doi.org/10.1016/S0140-6736(12)60240-2.

Blatter, D.D., Bigler, E.D., Gale, S.D., Johnson, S.C., Anderson, C.V., Burnett, B.M., Parker, N., Kurth, S., Horn, S.D., 1995. Quantitative volumetric analysis of brain MR: normative database spanning 5 decades of life. AJNR Am. J. Neuroradiol. 16, 241–251.

Bowie, C.R., Harvey, P.D., 2006. Administration and interpretation of the Trail Making Test. Nat. Protoc. 1, 2277. https://doi.org/10.1038/nprot.2006.390.

Butler, T., Blackmon, K., Zaborszky, L., Wang, X., DuBois, J., Carlson, C., Barr, W.B., French, J., Devinsky, O., Kuzniecky, R., Halgren, E., Thesen, T., 2012. Volume of the human septal forebrain region is a predictor of source memory accuracy. J. Int. Neuropsychol. Soc. 18, 157–161. https://doi.org/10.1017/S1355617711001421.

Butler, T., Zaborszky, L., Pirraglia, E., Li, J., Wang, X.H., Li, Y., Tsui, W., Talos, D., Devinsky, O., Kuchna, I., Nowicki, K., French, J., Kuzniecky, R., Wegiel, J., Glodzik, L., Rusinek, H., deLeon, M.J., Thesen, T., 2014. Comparison of human septal nuclei MRI measurements using automated segmentation and a new manual protocol based on histology. Neuroimage 97, 245–251. https://doi.org/10.1016/j.neuroimage.2014.04.026.

Butler, T., Zaborszky, L., Wang, X., McDonald, C.R., Blackmon, K., Quinn, B.T., DuBois, J., Carlson, C., Barr, W.B., French, J., Kuzniecky, R., Halgren, E., Devinsky, O., Thesen, T., 2013. Septal nuclei enlargement in human temporal lobe epilepsy without mesial temporal sclerosis. Neurology 80, 487–491. https://doi.org/10.1212/WNL.0b013e31827f0ed7.

Cade, B.S., Noon, B.R., 2003. A gentle introduction to quantile regression for ecologists. Front. Ecol. Environ. 1, 412–420. https://doi.org/10.1890/1540-9295(2003)001[0412:AGITQR]2.0.CO;2.

Cai, L., Gibbs, R.B., Johnson, D.A., 2012. Recognition of novel objects and their location in rats with selective cholinergic lesion of the medial septum. Neurosci. Lett. 506, 261–265. https://doi.org/10.1016/j.neulet.2011.11.019.

Cantero, J.L., Zaborszky, L., Atienza, M., 2017. Volume loss of the nucleus basalis of meynert is associated with atrophy of innervated regions in mild cognitive impairment. Cereb. Cortex 27, 3881–3889. https://doi.org/10.1093/cercor/bhw195.

Crowe, S.F., 1998. The differential contribution of mental tracking, cognitive flexibility, visual search, and motor speed to performance on parts A and B of the Trail Making Test. J. Clin. Psychol. 54, 585–591.

Davis, P.J.M., Wright, E.A., 1977. A new method for measuring cranial cavity volume and its application to the assessment of cerebral atrophy at autopsy. Neuropathol. Appl. Neurobiol. 3, 341–358. https://doi.org/10.1111/j.1365-2990.1977.tb00595.x.

Deary, I.J., Penke, L., Johnson, W., 2010. The neuroscience of human intelligence differences. Nat. Rev. Neurosci. 11, 201. https://doi.org/10.1038/nrn2793.

Der, G., Deary, I.J., 2018. Reaction times match IQ for major causes of mortality: Evidence from a population based prospective cohort study. Intelligence 69, 134–145. https://doi.org/10.1016/j.intell.2018.05.005.

Folstein, M.F., Folstein, S.E., McHugh, P.R., 1975. "Mini-mental state". A practical method for grading the cognitive state of patients for the clinician. J. Psychiatr. Res. 12, 189–198.

Gilmor, M.L., Erickson, J.D., Varoqui, H., Hersh, L.B., Bennett, D.A., Cochran, E.J., Mufson, E.J., Levey, A.I., 1999. Preservation of nucleus basalis neurons containing choline acetyltransferase and the vesicular acetylcholine transporter in the elderly with mild cognitive impairment and early Alzheimer's disease. J. Comp. Neurol. 411, 693–704. https://doi.org/10.1002/(SICI)1096-9861(19990906)411:4<693::AID-CNE13>3.0.CO;2-D.

Grothe, M., Heinsen, H., Teipel, S., 2013. Longitudinal measures of cholinergic forebrain atrophy in the transition from healthy aging to Alzheimer's disease. Neurobiol. Aging 34, 1210–1220. https://doi.org/10.1016/j.neurobiolaging.2012.10.018.

Grothe, M., Heinsen, H., Teipel, S.J., 2012. . Atrophy of the cholinergic basal forebrain over the adult age range and in early stages of Alzheimer´s disease. Biol. Psychiatry 71, 805–813. https://doi.org/10.1016/j.biopsych.2011.06.019.

Grothe, M., Zaborszky, L., Atienza, M., Gil-Neciga, E., Rodriguez-Romero, R., Teipel, S.J., Amunts, K., Suarez-Gonzalez, A., Cantero, J.L., 2010. Reduction of basal forebrain cholinergic system parallels cognitive impairment in patients at high risk of developing Alzheimer's disease. Cereb. Cortex 20, 1685–1695. https://doi.org/10.1093/cercor/bhp232.

Grothe, M.J., Heinsen, H., Amaro, E., Grinberg, L.T., Teipel, S.J., 2016. Cognitive Correlates of Basal Forebrain Atrophy and Associated Cortical Hypometabolism in Mild Cognitive Impairment. Cereb. Cortex 26, 2411–2426. https://doi.org/10.1093/cercor/bhv062.

Guisan, A., Zimmermann, N.E., 2000. Predictive habitat distribution models in ecology. Ecol. Model. 135, 147–186. https://doi.org/10.1016/S0304-3800(00)00354-9.

Halliday, G.M., Cullen, K., Cairns, M.J., 1993. Quantitation and three-dimensional reconstruction of Ch4 nucleus in the human basal forebrain. Synapse 15, 1–16. https://doi.org/10.1002/syn.890150102.

Harati, H., Barbelivien, A., Cosquer, B., Majchrzak, M., Cassel, J.-C., 2008. Selective cholinergic lesions in the rat nucleus basalis magnocellularis with limited damage in the medial septum specifically alter attention performance in the five-choice serial reaction time task. Neuroscience 153, 72–83. https://doi.org/10.1016/j.neuroscience.2008.01.031.

Hohol, M.J., Guttmann, C.R.G., Orav, J., Mackin, G.A., Kikinis, R., Khoury, S.J., Jolesz, F.A., Weiner, H.L., 1997. Serial neuropsychological assessment and magnetic resonance imaging analysis in multiple sclerosis. Arch. Neurol. 54, 1018–1025. https://doi.org/10.1001/archneur.1997.00550200074013.

Holmes, C.J., Hoge, R., Collins, L., Woods, R., Toga, A.W., Evans, A.C., 1998. Enhancement of MR images using registration for signal averaging. J. Comput. Assist Tomogr. 22, 324–333.

Holtzer, R., Goldin, Y., Zimmerman, M., Katz, M., Buschke, H., Lipton, R.B., 2008. Robust norms for selected neuropsychological tests in older adults. Arch. Clin. Neuropsychol. 23, 531–541. https://doi.org/10.1016/j.acn.2008.05.004.

Johnson, W., Bouchard, T.J., Krueger, R.F., McGue, M., Gottesman, I.I., 2004. Just one g: consistent results from three test batteries. Intelligence 32, 95–107. https://doi.org/10.1016/S0160-2896(03)00062-X.

Johnson, W., Nijenhuis, J., te, Bouchard, T.J., 2008. Still just 1 g: consistent results from five test batteries. Intelligence 36, 81–95. https://doi.org/10.1016/j.intell.2007.06.001.

Kilimann, I., Grothe, M., Heinsen, H., Alho, E.J.L., Grinberg, L., Amaro, E., Dos Santos, G.A.B., da Silva, R.E., Mitchell, A.J., Frisoni, G.B., Bokde, A.L.W., Fellgiebel, A., Filippi, M., Hampel, H., Klöppel, S., Teipel, S.J., 2014. Subregional basal forebrain atrophy in Alzheimer's disease: a multicenter study. J. Alzheimers Dis. 40, 687–700. https://doi.org/10.3233/JAD-132345.

Kitchen, C.M.R., 2009. Nonparametric versus parametric tests of location in biomedical research. Am. J. Ophthalmol. 147, 571–572. https://doi.org/10.1016/j.ajo.2008.06.031.

Kline, R.L., Zhang, S., Farr, O.M., Hu, S., Zaborszky, L., Samanez-Larkin, G.R., Li, C.-S.R., 2016. The effects of methylphenidate on resting-state functional connectivity of the Basal Nucleus of Meynert, Locus Coeruleus, and ventral tegmental area in healthy adults. Front. Hum. Neurosci. 10. https://doi.org/10.3389/fnhum.2016.00149.

Koenker, R., 2017. quantreg: Quantile Regression. R package version 5.34. 〈https://CRAN.R-project.org/package=quantreg〉. (Accessed 25 January 2018).

Koenker, R., Hallock, K.F., 2001. Quantile regression. J. Econ. Perspect. 15, 143–156. https://doi.org/10.1257/jep.15.4.143.

Lammers, F., Mobascher, A., Musso, F., Shah, N.J., Warbrick, T., Zaborszky, L., Winterer, G., 2016. Effects of Ncl. Basalis Meynert volume on the Trail-Making-Test are restricted to the left hemisphere. Brain Behav. 6https://doi.org/10.1002/brb3.421. (n/a-n/a).

Lee, A.C.H., Rahman, S., Hodges, J.R., Sahakian, B.J., Graham, K.S., 2003. Associative and recognition memory for novel objects in dementia: implications for diagnosis. Eur. J. Neurosci. 18, 1660–1670. https://doi.org/10.1046/j.1460-9568.2003.02883.x.

Li, C.R., Ide, J.S., Zhang, S., Hu, S., Chao, H.H., Zaborszky, L., 2014a. Resting state functional connectivity of the basal nucleus of Meynert in humans: in comparison to the ventral striatum and the effects of age. Neuroimage 97, 321–332. https://doi.org/10.1016/j.neuroimage.2014.04.019.

Machado, J.A.F., Silva, J.M.C.S., 2005. Quantiles for counts. J. Am. Stat. Assoc. 100, 1226–1237. https://doi.org/10.1198/016214505000000330.

Matsumae, M., Kikinis, R., Mórocz, I.A., Lorenzo, A.V., Sándor, T., Albert, M.S., Black, P.M., Jolesz, F.A., 1996. Age-related changes in intracranial compartment volumes in normal adults assessed by magnetic resonance imaging. J. Neurosurg. 84, 982–991. https://doi.org/10.3171/jns.1996.84.6.0982.

Mesulam, M.M., Geula, C., 1988. Nucleus basalis (Ch4) and cortical cholinergic innervation in the human brain: observations based on the distribution of acetylcholinesterase and choline acetyltransferase. J. Comp. Neurol. 275, 216–240. https://doi.org/10.1002/cne.902750205.

Mesulam, M.M., Mufson, E.J., Levey, A.I., Wainer, B.H., 1983. Cholinergic innervation of cortex by the basal forebrain: cytochemistry and cortical connections of the septal area, diagonal band nuclei, nucleus basalis (substantia innominata), and hypothalamus in the rhesus monkey. J. Comp. Neurol. 214, 170–197. https://doi.org/10.1002/cne.902140206.

Monaco, M., Costa, A., Caltagirone, C., Carlesimo, G.A., 2013. Forward and backward span for verbal and visuo-spatial data: standardization and normative data from an Italian adult population. Neurol. Sci. 34, 749–754. https://doi.org/10.1007/s10072-012-1130-x.

Otten, M.L., Mikell, C.B., Youngerman, B.E., Liston, C., Sisti, M.B., Bruce, J.N., Small, S.A., McKhann, G.M., 2012. Motor deficits correlate with resting state motor network connectivity in patients with brain tumours. Brain 135, 1017–1026. https://doi.org/10.1093/brain/aws041.

Parikh, V., Kozak, R., Martinez, V., Sarter, M., 2007. Prefrontal acetylcholine release controls cue detection on multiple timescales. Neuron 56, 141–154. https://doi.org/10.1016/j.neuron.2007.08.025.

Perneczky, R., Wagenpfeil, S., Komossa, K., Grimmer, T., Diehl, J., Kurz, A., 2006. Mapping scores onto stages: mini-mental state examination and clinical dementia rating. Am. J. Geriatr. Psychiatry 14, 139–144. https://doi.org/10.1097/01.JGP.0000192478.82189.a8.

Perry, E.K., Johnson, M., Kerwin, J.M., Piggott, M.A., Court, J.A., Shaw, P.J., Ince, P.G., Brown, A., Perry, R.H., 1992. Convergent cholinergic activities in aging and Alzheimer's disease. Neurobiol. Aging 13, 393–400. https://doi.org/10.1016/0197-4580(92)90113-C.

Pfefferbaum, A., Mathalon, D.H., Sullivan, E.V., Rawles, J.M., Zipursky, R.B., Lim, K.O., 1994. A quantitative magnetic resonance imaging study of changes in brain morphology from infancy to late adulthood. Arch. Neurol. 51, 874–887.

R: The R Project for Statistical Computing [WWW Document], 2017. URL 〈https://www.r-project.org/〉 (Accessed 25 January 2018).

Russ, T.C., Morling, J.R., 2012. Cholinesterase inhibitors for mild cognitive impairment. Cochrane Database Syst. Rev. CD009132. https://doi.org/10.1002/14651858.CD009132.pub2.

Saper, C.B., Chelimsky, T.C., 1984. A cytoarchitectonic and histochemical study of

nucleus basalis and associated cell groups in the normal human brain. Neuroscience 13, 1023–1037. https://doi.org/10.1016/0306-4522(84)90286-0.
Schliebs, R., Arendt, T., 2006. The significance of the cholinergic system in the brain during aging and in Alzheimer's disease. J. Neural Transm. 113, 1625–1644. https://doi.org/10.1007/s00702-006-0579-2.
Shenkin, S.D., Rivers, C.S., Deary, I.J., Starr, J.M., Wardlaw, J.M., 2009. Maximum (prior) brain size, not atrophy, correlates with cognition in community-dwelling older people: a cross-sectional neuroimaging study. BMC Geriatr. 9, 12. https://doi.org/10.1186/1471-2318-9-12.
Simić, G., Mrzljak, L., Fucić, A., Winblad, B., Lovrić, H., Kostović, I., 1999. Nucleus subputaminalis (Ayala): the still disregarded magnocellular component of the basal forebrain may be human specific and connected with the cortical speech area. Neuroscience 89, 73–89.
Smith, E.E., Egorova, S., Blacker, D., Killiany, R.J., Muzikansky, A., Dickerson, B.C., Tanzi, R.E., Albert, M.S., Greenberg, S.M., Guttmann, C.R.G., 2008. Magnetic resonance imaging white matter hyperintensities and brain volume in the prediction of mild cognitive impairment and dementia. Arch. Neurol. 65, 94–100. https://doi.org/10.1001/archneurol.2007.23.
Sparks, D.L., Hunsaker, J.C., Slevin, J.T., DeKosky, S.T., Kryscio, R.J., Markesbery, W.R., 1992. Monoaminergic and cholinergic synaptic markers in the nucleus basalis of Meynert (nbM): normal age-related changes and the effect of heart disease and Alzheimer's disease. Ann. Neurol. 31, 611–620. https://doi.org/10.1002/ana.410310608.
Staff, R.T., Murray, A.D., Deary, I.J., Whalley, L.J., 2006. Generality and specificity in cognitive aging: a volumetric brain analysis. Neuroimage 30, 1433–1440. https://doi.org/10.1016/j.neuroimage.2005.11.004.
Teipel, S.J., Grothe, M.J., Wittfeld, K., Hoffmann, W., Hegenscheid, K., Völzke, H., Homuth, G., Grabe, H.J., 2015. Association of a neurokinin 3 receptor polymorphism with the anterior basal forebrain. Neurobiol. Aging 36, 2060–2067. https://doi.org/10.1016/j.neurobiolaging.2014.12.031.
Tombaugh, T.N., 2004. Trail Making Test A and B: normative data stratified by age and education. Arch. Clin. Neuropsychol. 19, 203–214. https://doi.org/10.1016/S0887-6177(03)00039-8.
Tombaugh, T.N., McIntyre, N.J., 1992. The mini-mental state examination: a comprehensive review. J. Am. Geriatr. Soc. 40, 922–935.
Vassilaki, M., Aakre, J.A., Cha, R.H., Kremers, W.K., St. Sauver, J.L., Mielke, M.M., Geda, Y.E., Machulda, M.M., Knopman, D.S., Petersen, R.C., Roberts, R.O., 2015. Multimorbidity and Risk of Mild Cognitive Impairment. J. Am. Geriatr. Soc. 63, 1783–1790. https://doi.org/10.1111/jgs.13612.
White, P., Hiley, C.R., Goodhardt, M.J., Carrasco, L.H., Keet, J.P., Williams, I.E., Bowen, D.M., 1977. Neocortical cholinergic neurons in elderly people. Lancet 1, 668–671.
Wilcox, R., 2012. Chapter 1 - Introduction. In: Introduction to Robust Estimation and Hypothesis Testing (Third Edition), Statistical Modeling and Decision Science. Academic Press, Boston, pp. 1–22. ⟨https://doi.org/10.1016/B978-0-12-386983-8.00001-9⟩.
Winblad, B., Engedal, K., Soininen, H., Verhey, F., Waldemar, G., Wimo, A., Wetterholm, A.L., Zhang, R., Haglund, A., Subbiah, P., Donepezil Nordic Study Group, 2001. A 1-year, randomized, placebo-controlled study of donepezil in patients with mild to moderate AD. Neurology 57, 489–495.
Wolf, D., Grothe, M., Fischer, F.U., Heinsen, H., Kilimann, I., Teipel, S., Fellgiebel, A., 2014. Association of basal forebrain volumes and cognition in normal aging. Neuropsychologia 53, 54–63. https://doi.org/10.1016/j.neuropsychologia.2013.11.002.
Zaborszky, L., Hoemke, L., Mohlberg, H., Schleicher, A., Amunts, K., Zilles, K., 2008. Stereotaxic probabilistic maps of the magnocellular cell groups in human basal forebrain. Neuroimage 42, 1127–1141. https://doi.org/10.1016/j.neuroimage.2008.05.055.

Neuropsychologia 119 (2018) 172–181

Contents lists available at ScienceDirect

Neuropsychologia

journal homepage: www.elsevier.com/locate/neuropsychologia

Size matters: Grey matter brain reserve predicts executive functioning in the elderly

M. Laubach[a,e,*,1], F. Lammers[a,e], N. Zacharias[a,e], I. Feinkohl[b], T. Pischon[b], F. Borchers[a], A.J.C. Slooter[d], S. Kühn[c,e], C. Spies[a], G. Winterer[a,e], BioCog Consortium

[a] Clinical Neuroscience Research Group, Experimental and Clinical Research Center (ECRC), Dept. of Anesthesiology and Operative Intensive Care Medicine (CCM, CVK), Charité – Universitätsmedizin Berlin, Corporate Member of Freie Universität Berlin, Humboldt-Universität zu Berlin, and Berlin Institute of Health, Berlin, Germany
[b] Molecular Epidemiology Research Group, Max-Delbrueck-Center for Molecular Medicine in the Helmholtz Association (MDC), Berlin, Germany
[c] Clinic and Polyclinic of Psychiatry and Psychotherapy, University Clinic Hamburg-Eppendorf, Hamburg, Germany
[d] Department of Intensive Care Medicine and Brain Center Rudolf Magnus, University Medical Center Utrecht, Utrecht University, the Netherlands
[e] PharmaImage Biomarker Solutions GmbH, Biotech Park Berlin-Buch, Robert-Rössle-Str. 10, 13125 Berlin, Germany

ARTICLE INFO

Keywords:
Executive functioning
Neuroimaging
Elderly
Neuropsychology
Brain reserve
Cognitive reserve

ABSTRACT

Preserved executive functioning (EF) is crucial for daily functioning in the elderly and it appears to predict dementia development. We sought to clarify the role of atrophy-corrected cortical grey matter (GM) volume as a potential brain reserve (BR) marker for EF in the elderly. In total, 206 pre-surgical subjects (72.50 ± 4.95 years; mean MMSE score 28.50) were investigated. EF was primarily assessed using the Trail Making Test B (TMT B). Global/ lobar GM volumes were acquired with T1 MP-RAGE. Adjusting for key covariates including a brain atrophy index (i.e. brain parenchymal fraction), multiple linear regression analysis was used to study associations of GM volumes and TMT B. All GM volumes - most notably of global GM - were significantly associated with TMT B independently of GM atrophy (ß = −0.201 to −0.275, p = 0.001–0.012). Using atrophy-corrected GM volume as an estimate of maximal GM size in youth may serve as a BR predictor for cognitive decline in future studies investigating BR in the elderly.

1. Introduction

The term cognitive reserve (CR) captures the fact that an individual maintains the capability of performing cognitive tasks in the face of neurological disease with a subsequent loss of neuronal function (Stern, 2012). The model of CR states that patients with higher intelligence (IQ) or occupational attainment might have a functional advantage during late life (Stern, 2002). Analogous to the concept of CR, brain reserve (BR), in particular measures of brain structure, refers to the hypothesis that the brain is capable of minimizing clinical manifestations in the face of age-related cerebral effects or the present neuropathology (Bartrés-Faz and Arenaza-Urquijo, 2011; Chen et al., 2017). Several studies reported that subjects with larger head circumference, intracranial volume or brain weight with higher numbers of neurons are less likely to develop dementia (Katzman et al., 1988; Mori et al., 1997; Schofield et al., 1997). Furthermore, larger brain size may constitute a possible morphological advantage with regard to overall cognitive ability in the elderly (Pietschnig et al., 2015; Persson et al., 2016; Feinkohl et al., 2017; Groot et al., 2017; Vibha et al., 2017).

In both, non-demented elderly subjects and patients with mild cognitive impairment (MCI), a preserved superior level of executive functioning (EF) is associated with superior daily functioning and aging well (Schmitter-Edgecombe et al., 2011; Puente et al., 2015; Darby et al., 2017). EF reflects a range of decision-making and higher-order thinking processes like flexible problem-solving, working memory and response inhibition (Stern, 2012; Puente et al., 2015; Darby et al., 2017). In a recent long-term observation study, Chen et al. (2017) reported that subjects with low baseline EF - but notably not with low baseline memory performance - had a higher conversion rate from normal cognition to MCI. Similar observations were made by others (Royall et al., 2004; Johnson et al., 2007). Johnson et al. (2007) undertook a prospective study of 7717 elderly women (mean modified MMSE of 24.8 points), and observed that impaired EF at baseline, measured by the Trail Making Test (TMT) B, rather than global cognitive function was associated with significantly worse daily functioning both in a cross-section manner and over six years. In a three-

* Correspondence to: Department of Anesthesiology, Charité - University Medicine Berlin, Charitéplatz 1, 10117 Berlin, Germany.
E-mail address: markus.laubach@charite.de (M. Laubach).
[1] www.biocog.eu.

https://doi.org/10.1016/j.neuropsychologia.2018.08.008
Received 21 February 2018; Received in revised form 7 August 2018; Accepted 9 August 2018
Available online 10 August 2018

year longitudinal cohort study of 547 non-demented elderly, Royall et al. (2004) showed that EF instead of e.g. the MMSE score was the most accurate predictor of functional status over time. Comparable results were reported by Rozzini et al. (2007), who observed an association of conversion to Alzheimer's disease (AD) with poor global cognitive performance at baseline and with worsening executive functioning, but not with worsening memory performance (one year follow-up period) in a group of amnestic MCI individuals. These findings suggest that EF is a particularly relevant constituent of CR.

Phillips et al. (2008) demonstrated that cognition and behavior in older non-demented adults are highly dependent on EF, which, in turn, is associated with prefrontal brain function. Multiple studies of elderly subjects have demonstrated that the integrity of the different brain lobes, most notably the frontal lobe, are associated with EF (Elderkin-Thompson et al., 2008; Cardenas et al., 2011; Zhang et al., 2011; Dong et al., 2015). More recently, however, Bettcher et al. (2016) reported findings that are not easily reconciled with the hypothesis of an outstanding role of the frontal lobe with respect to EF in the aging process. In their study (N = 202), cortical grey matter (GM) volume of the frontal lobe as well as additional brain lobes were not independently associated with EF performance when statistically corrected for global GM volume. Importantly, all of these studies have in common that they quantify GM volume without distinguishing whether it is the maximal brain size in youth or GM atrophy during later life that predicts EF in elderly subjects. Accordingly, any association between frontal or global GM volume and EF can be interpreted in two different ways. Low EF performance can result from age-associated cortical atrophy, small GM volumes already at a young age (BR) or both. The concept of brain reserve (BR) is mostly attributed to passive individual differences of morphological brain characteristics enduring neuropathological processes (Bartrés-Faz and Arenaza-Urquijo, 2011). Reaching a critical threshold of brain damage might result in clinical and functional deficits becoming apparent (Satz et al., 1993). A number of studies have found impaired EF preceding memory decline in the course of dementia development (Johnson et al., 2007) and the literature has pointed out the need to consider brain morphology associated with EF possibly serving as an early marker of neurodegenerative disease (Chen et al., 2017). Thus, as brain atrophy is suggested to be an early risk indicator, brain imaging might be beneficial by delivering diagnostic and prognostic information to patients in the process of individual personalized medicine (Chen et al., 2017).

In the present study, we sought to clarify, whether maximal GM volume in youth, i.e. the cortical BR, contributes to EF in the elderly. In addition, we addressed the question of whether frontal or global GM volume is associated with EF. For the neuropsychological assessment of EF the commonly used trail-making tests were applied (Reitan, 2004; Rabin et al., 2005) which have been hypothesized to reflect a wide variety of cognitive processes such as visual searching and scanning, flexibility and the ability to execute and modify a plan of action (Salthouse, 2011). In order to estimate cortical GM during youth as a BR marker in our elderly patient group, we adopted a novel strategy which - to the best of our knowledge - has not been previously applied. We calculated a brain atrophy index (brain parenchymal fraction, BPF), i.e. the ratio of the total brain parenchymal volume (BPV), which includes GM and white matter (WM), to the total intracranial volume (ICV). In the past, BPF has been used as a measure of brain atrophy, for instance by the Alzheimer's Disease Neuroimaging Initiative consortium, to predict cognitive decline in dementia patients (Callahan et al., 2015). Literature concerning the application of BPF in healthy individuals is sparse; in particular, evaluation of the course of brain atrophy in healthy adults. Vågberg et al. (2017) investigated cross-sectional data of BPF that are currently available in the literature and highlighted in a systematic review that the BPF values in healthy individuals increase until the age of 40, whereas a progressive rate of atrophy occurs along with further aging. Since ICV is stable throughout adulthood, it represents an "archeological" estimate of maximal brain size in youth (Royle et al., 2013). Thus, we used BPF in our study to correct an individual GM volume for GM atrophy, which lends this measure to the quality of a BR prediction marker even when imaging data are collected at advanced age in a cross-sectional study design. Accordingly, this strategy of data analysis extends recent work using ICV per se as a BR marker for the prediction of dementia development (Guo et al., 2013; Negash et al., 2013; Groot et al., 2017). The rationale of our approach is the well-known inter-individual variability (~ 10%) of the ratio between ICV and cortical GM volume (Ge et al., 2002).

2. Material and methods

2.1. Participants

In total, 206 neuropsychologically healthy adults (aged: 65–87 years), were selected as part of an interim analysis from a cohort study within the framework of the Biomarker Development for Postoperative Cognitive Impairment in the Elderly (BioCog) study (www.biocog.eu). The BioCog study is a prospective 2-center (Charité University Hospital Berlin (Germany) and the University Hospital Utrecht (Netherlands)) observational cohort study with N = 1033 elderly elective surgical patients, aiming to establish valid clinical, neuroimaging and molecular biomarker panels for risk and clinical outcome prediction of postoperative delirium and postoperative cognitive deficits (Winterer et al., 2018). According to the study protocol, pre-operative data of the first 400 enrolled patients can be used for interim analyses (data from N = 291 patients in the Charité University Hospital Berlin (Germany) and N = 109 patients from the University Hospital Utrecht (Netherlands)). In the present study, only data from patients from the clinical center of Berlin, who were recruited in the entire area of the city of Berlin, were used for analyses. Since approximately 50% of all surgical interventions in the Berlin area, with roughly five million inhabitants, are conducted at the Charité University Hospital, the study cohort in Berlin ensures a good coverage of elderly surgical patients in the region (Winterer et al., 2018). The inclusion criteria comprise male and female patients aged ≥ 65 years and of European descent (Caucasian) who are scheduled for elective surgery. Study participants with ≤ 23 points in the Mini-Mental-State-Examination (MMSE), a life-time history of neuropsychiatric disorders or addiction disorders during the past five years or with centrally acting medication were excluded (complete list of eligibility criteria: https://clinicaltrials.gov/ct2/show/NCT02265263?term=biocog&rank=1). The study is registered at ClinicalTrials.gov: NCT02832193. All patients have given written informed consent after receiving spoken and written information on the study. The study was approved by the local ethics committee and conducted according to the declaration of Helsinki.

Magnetic resonance imaging (MRI) data acquisition together with clinical and neurocognitive assessments took place one day before surgery. In total, 218 MRI scans were available for this interim analysis using data from the patients from the clinical center of Berlin (N = 291). Due to the withdrawal of consent by one patient after inclusion and one case with preterm finishing of the FreeSurfer processing pipeline, as well as ten cases with gross anatomical aberrations seen while inspecting the post-processed images, 206 processed MRI scans were finally available for analysis. Of the 206 available MRI scans, TMT B data were available for 174 subjects (for demographics see Table 1).

2.2. Measures

2.2.1. Cognitive assessments

For the assessment of executive functioning, the Trail Making Test (TMT A and TMT B) was applied on the same day as the MRI investigation. The measurement of visuoperceptual abilities, which are speeded (motor) measures, is mainly reflected by part A of the TMT, whereas inhibition and set-shifting ability is reflected by part B (Arbuthnott and Frank, 2000; Strauss et al., 2006; Sánchez-Cubillo

Table 1
Cognitive and neuroimaging characteristics of participants.

Demographics	N	Mean (SD)	Range
Age (years)	206	72.50 (4.95)	65–87
Male Sex (%)	118	57.28	
Education			
ISCED 1997 Level	183	2 A/B: 23.00% 3 A/B/C: 38.20% 4 A/B: 3.20% 5 A/B: 35.60%	
Education (years)	166	13.02 (4.15)	6–24
Executive Functions Measures			
TMT A (sec)	189	50.30 (19.21)	19–132
TMT B (sec)	174	119.56 (51.01)	25–298
Intelligence Test			
IQ score	121	114.07 (14.14)	70–143
MMSE	206	28.50 (1.41)	24–30
Neuroimaging Measures			
Total intracranial volume (mm^3)	206	1.338.010 (203.127)	922.433–2.007.198
Total brain parenchymal volume (mm^3)	206	979.727 (101.958)	705.772–1.222.338
Total cortical GM volume (mm^3)[a,b]	206	310.639 (30.572)	233.497–394.180
Frontal lobe GM volume (mm^3)[a]	206	123.858 (12.543)	93.016–164.200
Parietal lobe GM volume (mm^3)[b]	206	85.802 (8.888)	66.548–111.093
Temporal lobe GM volume (mm^3)	206	61.794 (6.779)	45.140–80.615
Occipital lobe GM volume (mm^3)	206	39.185 (4.760)	28.485–52.202
BPF (BPV/ICV)	206	0.742 (0.088)	0.53–0.99
GMF (GMV/ICV)	206	0.235 (0.028)	0.16–0.30

Key: BPF, Brain Parenchymal Fraction; BPV, Brain Parenchymal Volume; GM, Grey Matter; GMF, Grey Matter Fraction; GMV, Grey Matter Volume; ICV, Intracranial Volume; IQ, Intelligence Quotient; ISCED, International Standard Classification of Education; mm, millimeters; MMSE, Mini-Mental State Examination; SD, standard deviation; sec, seconds; TMT, Trail Making Test.
[a] Excluding primary motor cortex.
[b] Excluding sensory cortex.

et al., 2009). By calculating a difference score (TMT_{Diff} = TMT B – TMT A) the variance attributable to the graphomotor and visual scanning components of the TMT A are minimized (Sánchez-Cubillo et al., 2009; Misdraji and Gass, 2010). While comparing the TMT_{Diff} score to other neuropsychological measures, correlations to memory functioning were found (Corrigan and Hinkeldey, 1987; Sánchez-Cubillo et al., 2009). However, statistically significant effects are inconsistent and more recent investigations showed that the TMT B score might be more strongly associated with working memory than the TMT_{DIFF} score (Sánchez-Cubillo et al., 2009; Fellows et al., 2017). During part A, subjects are required to connect numbers on a sheet of paper in the correct order as quickly as possible. During part B subjects have to draw lines on a sheet of paper sequentially connecting 25 encircled numbers and alternating letters (1, A, 2, B, 3, C, etc.). In the present study, the required time to finish the TMT B is used as the primary dependent variable. Due to the dependence on intelligence, visuomotor coordination and age, literature regarding standard cut-off values for the TMT is sparse (Spreen and Strauss, 1998; Tombaugh, 2004). For reference norm values across age groups, see Tombaugh (2004). For the assessment of the Intelligence Quotient (IQ) score, the multiple choice vocabulary test ("Mehrfachwahl-Wortschatz-Intelligenztest" (MWT-A)) was applied to assess crystallized cognitive ability (Lehrl, 2005). The derived IQ score correlates fairly well with global IQ in healthy adults (Lehrl et al., 1995).

2.2.2. Education

According to the International Standard Classification of Educational Degrees (ISCED-1997) (approved by the United Nations Educational Scientific and Cultural Organization (UNESCO) General Conference at its 29th session in November 1997) and following previous procedures (Kave et al., 2012), the educational level of the subjects was classified into one of seven categories: (0) preprimary education, (1) primary education, (2) lower secondary education, (3) upper secondary education, (4) post-secondary education, (5) first tertiary education and (6) second stage tertiary education. The ISCED 1997 levels of 2 and 3 are sub-classified into a,b,c and levels 4 and 5 in a,b depending on the educational level attained. The ISCED score was initially developed by the UNESO in the early 1970s as a framework to collect, illustrate and compare educational statistics on a national as well as international level.

2.2.3. Structural neuroimaging

MRI scans were obtained on a 3.0 T MRI scanner (Siemens Magnetom Trio) using a 32-channel head coil. Structural imaging yields whole head high-resolution anatomical magnetic resonance images using a 3D T1-weighted magnetization-prepared rapid gradient-echo sequence (MP-RAGE) for studying cortical volume. An axial-oblique 3D Fast Spoiled Gradient Recalled Echo (FSPGR) sequence for the T1-weighted sequence was applied (TR/TE = 2500/4.77 ms, $\alpha = 7°$). A field of view of 256 × 256 mm, with 1 × 1 mm in-plane resolution and 1 mm slice thickness was applied. After acquisition, all MRI images were checked on pathological intracranial processes by a board-certified neuroradiologist.

2.2.3.1. FreeSurfer. The FreeSurfer software package was used in order to allow a direct comparison with earlier studies. Furthermore in order to process T1 MP-RAGE structural MR images, the software FreeSurfer (version 5.30) was used due to its fully automated pipeline and its free availability (http://surfer.nmr.mgh.harvard.edu), as well as a good test-retest reliability (Han et al., 2006; Jovicich et al., 2006). The steps executed were motion correction, the removal of non-brain tissue and automated Talairach transformation (Segonne et al., 2007). The pipeline of FreeSurfer conducts segmentation of the subcortical white matter and deep grey matter into structural volumes (Fischl et al., 2002), intensity normalization (Sled et al., 1998), tessellation of the grey matter into structural volumes (Fischl et al., 2002, 2004), automated topology correction (Fischl et al., 2002) and surface deformation (Dale et al., 1999; Fischl and Dale, 2000). All surfaces of each individual image data were visually inspected post-processing for the accuracy of spatial registration and grey/white matter segmentation (e.g. removal of skull and dura mater and accurate delineation of grey/white matter and pial surfaces). Since all subjects were manually checked by one researcher (M.L.), potentially differing inter-observer interpretations of the accuracy of processed images were avoided. FreeSurfer provides a 3-dimensional segmentation method in order to allocate each voxel to a neuroanatomical label. The global GM volume was calculated by summing up specific GM volumes which were segmented into 68 parcellations using the Desikan-Killiany atlas (Desikan et al., 2006). The individual parcellations were summed up to estimate the frontal, temporal, occipital and parietal lobe GM volumes (Fischl et al., 2004; Desikan et al., 2006). Since the primary motor and the sensory cortex are mainly involved in controlling motor action, respectively receiving input from peripheral mechanoreceptors (Lotze et al., 1999) by excluding the associated cortical volumes from global GM as well as specific lobar volumes, we sought to eradicate the bias of reduced dexterity and somatosensory inaccuracy with respect to the conducted tests. The same approach of excluding the primary motor and the sensory cortex from the calculations of the volumes of the frontal, respectively the parietal lobe, was chosen by Bettcher et al. (2016).

2.2.3.2. Brain parenchymal fraction. Correction for global cerebral atrophy was executed by first calculating the estimated total intracranial volume (eTIV, aka ICV) as well as the total brain parenchymal volume (global GM volume plus total WM volume

excluding ventricles). The software FreeSurfer calculates the total intracranial volume by exploiting the relationship between the ICV and the linear transform to MNI305 space and using an atlas-based spatial normalization procedure (Buckner et al., 2004). The cerebral atrophy index, i.e. the brain parenchymal fraction (BPF), was subsequently derived by dividing the total brain parenchymal volume (BPV) by the total intracranial volume (ICV) (Rudick et al., 1999; Callahan et al., 2015).

2.3. Statistical analysis

For statistical analyses, SPSS (version 25) was used. In total, three sets of analyses were executed. 1) Five separate linear multiple regression analyses for each of the four brain lobes (GM volume) and the global GM volume were executed, each time including age, the BPF and sex as additional independent variables and the TMT B score as the dependent variable (analogous calculation with the dependent variable TMT_{Diff} score). 2) In order to adjust for global GM volume, the GM volume of each of the four different lobes was divided by the global GM volume and the regression analyses with TMT B scores were repeated in the same way. Additionally, multiple regression analyses for the IQ score and the educational level as dependent variables and global GM volume, age, BPF and sex as the independent variables were conducted. Following a recent suggestion by Van Loenhoud et al. (2017), we furthermore repeated our calculations replacing the atrophy index BPF by GMF (Grey Matter Fraction) (GM/ICV). 3) Via linear regression analyses, we tested sex-specific effects on the correlation of age with the TMT B performance for small and large global GM volumes. The critical value for significance was set to $p < 0.05$.

3. Results

The 206 non-demented elderly Caucasian surgical patients investigated had a mean MMSE score of 28.50 points (range 24–30, SD 1.41) and a mean educational attainment of 13 years of education (range 6–24, SD 4.12). The effects of the different GM volumes of the four lobes and the global GM volume on the TMT B score are shown in Table 2.

All volumes of the different lobes and the global GM volume were negatively associated with the TMT B scores (see also Fig. 1).

The model shows that every increase of one standard deviation (SD) of each individual GM volume, as well as the global GM volume, significantly lowers the TMT B score. In other words, faster TMT B performance is associated with larger individual and larger global GM volumes. In detail, an increase of one SD of the frontal GM volume decreases the TMT B score by 0.229 SDs (p = 0.006), the increase of one SD of the parietal GM volume decreases the TMT B score by 0.263 SDs (p = 0.002), the increase of one SD of the temporal GM volume decreases the TMT B score by 0.263 SDs (p = 0.002) and an increase of one SD of the occipital GM volume decreases the TMT B score by 0.201 SDs (p = 0.012); also, an increase of one SD of the global GM volume decreases the TMT B score by 0.275 SDs (p = 0.001). The standardized coefficient (-ß-) of the global GM volume of −0.275 (p = 0.001) is most negatively related to the TMT B score in our model and, thus, is the most accurate predictor of all region-of-interests (GM volumes). Age also has significant explanatory power to predict TMT B performance; higher age is associated with a higher TMT B score (ß = 0.187–0.209, p = 0.007–0.015). No sex-specific tendencies were observed (ß = −0.085 to −0.139, p = 0.096–0.326). Similar results were found when including the primary motor and the sensory cortex in the calculations of the frontal, respectively the parietal lobe as well as the global GM volume (see Table 1 in the Supplement). Furthermore, we found that the TMT B - TMT A score was also accurately predicted by the global GM volume (ß = −0.269, p = 0.002), although the association of the temporal GM volume with the TMT_{DIFF} score was slightly more pronounced (ß = −0.284, p = 0.001) (see Table 2 in the Supplement).

Table 2
Associations of individual lobar and global GM volume, age, the BPF and sex with the score of the TMT B.

Independent Variable	Dependent variable	Estimate	Standard error	p-value
Frontal GM volume (mm^3)[a]	**TMT B**	-0.229	< 0.001	0.006
Age (years)		0.191	0.804	0.014
BPF (BPV/ICV)		-0.151	45.641	0.056
Sex (female)		-0.120	8.669	0.154
Parietal GM volume (mm^3)[b]	**TMT B**	-0.263	< 0.001	0.002
Age (years)		0.199	0.792	0.009
BPF (BPV/ICV)		-0.158	45.340	0.045
Sex (female)		-0.098	8.705	0.245
Temporal GM volume (mm^3)	**TMT B**	-0.263	0.001	0.002
Age (years)		0.190	0.797	0.013
BPF (BPV/ICV)		-0.146	45.368	0.065
Sex (female)		-0.095	8.805	0.270
Occipital GM volume (mm^3)	**TMT B**	-0.201	0.001	0.012
Age (years)		0.209	0.799	0.007
BPF (BPV/ICV)		-0.124	46.220	0.121
Sex (female)		-0.139	8.551	0.096
Global GM volume (mm^3)[a,b]	**TMT B**	-0.275	< 0.001	0.001
Age (years)		0.187	0.796	0.015
BPF (BPV/ICV)		-0.146	45.261	0.063
Sex (female)		-0.085	8.861	0.326

The model consists of the different grey matter volumes, age, the BPF and sex entered as independent variables and the TMT B score (sec) as a dependent variable. Estimates are standardized regression coefficients of this model. The reference of the standardized regression coefficient of sex is female.
Key: BPF, Brain Parenchymal Fraction; BPV, Brain Parenchymal Volume; GM, Grey Matter; ICV, Intracranial Volume; mm, millimeters; sec, seconds; TMT, Trail Making Test
[a] excluding primary motor cortex
[b] excluding sensory cortex

The BPF itself, except for the regression analysis including the parietal lobe (p = 0.045), did not contribute significantly to the prediction of EF measured by the TMT B (p = 0.056–0.121); however, non-significant trends were observed (see Tables 2 and 3). Of note, Fig. 2 shows only slight variance in brain atrophy across the MMSE scores (24–30 points).

As shown in Table 3, when running the multiple regression including the ratio consisting of the lobar GM volumes divided by the global GM volume, no associations of different lobar GM ratios ("adjusted lobar GM volumes") with the TMT B score were found. In this model, consisting of the "adjusted lobar GM volumes", age, BPF and sex as independent variables and the TMT B score as the dependent variable, the lobar GM ratios did not significantly predict performance at the TMT B (beta = −0.019 to 0.062, p = 0.388–0.789). In this model, consisting of adjusted GM volumes (see Table 3), male sex was statistically significantly negatively associated with the prediction of performance in the TMT B (ß-values: −0.222 to −0.230, p = 0.003–0.004). Higher age was observed to significantly predict the TMT B score positively (ß-values: 0.231–0.237, all p = 0.002–0.003).

Replacing the atrophy index BPF by GMF did not markedly change the obtained results (see Table 3 in the Supplement).

As part of a moderation analysis, the moderator effect of small and large global GM volume on the relation between age and the TMT B score was investigated (Fig. 3). We observed that the strength relationship of age and TMT B changes as a function of global GM volume. In the subgroup of larger global GM volume of male participants, the correlation between age and TMT B was weaker (R^2 = 0.106) compared to the smaller global GM volume (R^2 = 0.154). For female

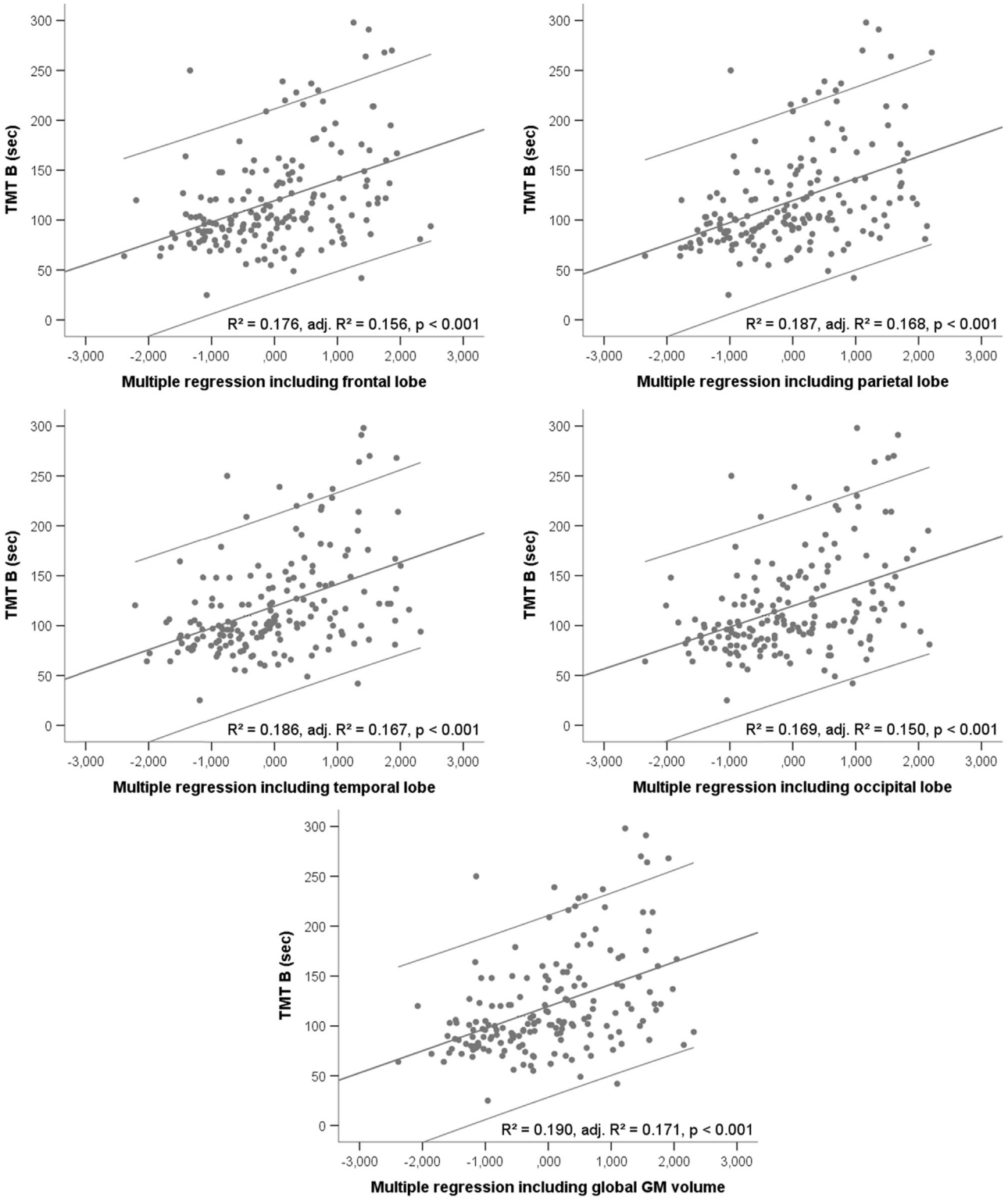

Fig. 1. Each scatterplot consists of the graph of the standardized predicted values derived from the regression equation composed of the individual GM volumes (excluding primary motor and sensory cortex) as well as the covariates age, BPF and sex (95% CI). Key: BPF, Brain Parenchymal Fraction; CI, Confidence Interval; GM, Grey Matter; sec, seconds; TMT B, Trail Making Test.

participants, however, these observations were not consistent and could not be demonstrated (see Fig. 3). For female participants, we found that the correlation of age and TMT B was weaker in the subgroup of smaller GM volume (R^2 = 0.001) compared to the subgroup of larger global GM volume (R^2 = 0.126).

Moderate negative correlations (all p values < 0.01, two-tailed) were observed for the TMT B with the IQ score (r = −0.397), and for the TMT B score with completed years of education (r = −0.354) whereas the IQ score was moderately positively correlated with completed years of education (r = 0.388). Additionally, we regressed the IQ score as well the educational attainment, reflected by the ISCED (International Standard Classification of Education) 97 Level, on global

Table 3
Associations of specific adjusted lobar volumes, age, the BPF and sex with executive functioning measured by the TMT B.

Independent Variable	Dependent variable	Estimate	Standard error	p-value
Adjusted frontal GM volume (frontal GM[a]/global GM[a,b])	**TMT B**	0.062	342.909	0.388
Age (years)		0.237	0.809	0.002
BPF (BPV/ICV)		-0.146	46.664	0.071
Sex (female)		-0.222	7.892	0.004
Adjusted parietal GM volume (parietal GM[b]/global GM[a,b])	**TMT B**	-0.029	399.303	0.689
Age (years)		0.234	0.811	0.003
BPF (BPV/ICV)		-0.155	47.019	0.059
Sex (female)		-0.230	7.845	0.003
Adjusted temporal GM volume (temporal GM/global GM[a,b])	**TMT B**	-0.026	423.045	0.717
Age (years)		0.231	0.808	0.003
BPF (BPV/ICV)		-0.150	46.675	0.064
Sex (female)		-0.227	7.885	0.003
Adjusted occipital GM volume (occipital GM/global GM[a,b])	**TMT B**	-0.019	410.687	0.789
Age (years)		0.232	0.808	0.003
BPF (BPV/ICV)		-0.147	47.449	0.075
Sex (female)		-0.229	7.857	0.003

The model consists of the adjusted specific grey matter volumes, age, the BPF and sex entered as independent variables and the TMT B score (sec) as dependent variable. Estimates are standardized regression coefficients of this model. The reference of the standardized regression coefficient of sex is female. Key: BPF, Brain Parenchymal Fraction; BPV, Brain Parenchymal Volume; GM, Grey Matter; ICV, Intracranial Volume; mm, millimeters; sec, seconds; TMT, Trail Making Test

[a] excluding primary motor cortex
[b] excluding sensory cortex

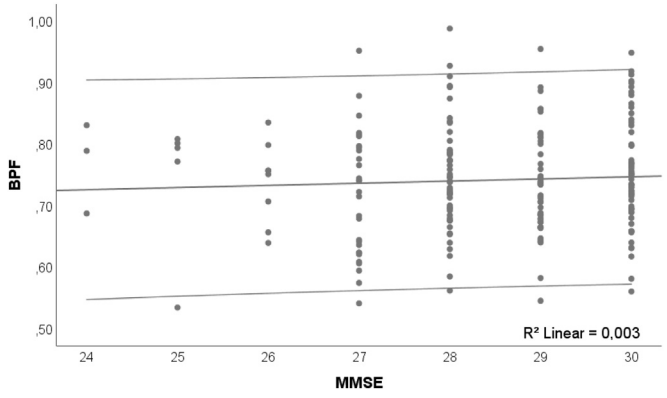

Fig. 2. The scatter plot consists of the brain parenchymal fraction (BPF) shown on the y-axis which is derived by dividing the total brain parenchymal volume (BPV) by the total intracranial volume (ICV). The MMSE score is shown on the x-axis (95% CI). **Key: CI, Confidence Interval; MMSE, Mini-Mental-State-Examination.**

GM volume as well as the covariates of age, the BPF and sex. Thereby, we observed that global GM volume could neither significantly predict the IQ score (beta = 0.179; p = 0.088) nor the ISCED 97 Level (beta = 0.093; p = 0.245).

4. Discussion

In this study, the associations of different lobar GM volumes and global GM volume with EF as well as the approach of using an atrophy-corrected global GM volume as a BR prediction marker were examined. We observed that global GM volume was most strongly associated with EF, i.e. patients with a larger GM volume demonstrated superior TMT B performance. The second strongest associations were observed for the parietal and temporal lobe followed by the frontal lobe, whereas the occipital lobe was the least correlated with EF. Since we corrected GM volume for brain atrophy as part of the multiple regression analyses, our measures of "corrected GM volume" can be considered an "archeological" estimate of the maximal brain size in youth (Royle et al., 2013). The neuropsychological and neuroimaging tests were conducted on the same day; thus, confounding factors such as day-to-day physiological variations of brain volumes (Duning et al., 2005) were minimized. We corrected the global GM volume for cerebral atrophy; accordingly, despite adopting a cross-sectional study design, the latter is applicable as a predictor of EF even in advanced aged subjects. Global GM volume also was a relevant predictor of TMT_{Diff} score, but we observed a stronger relationship for the temporal GM volume. Associations of the TMT_{DIFF} score with memory functioning are described in literature (Corrigan and Hinkeldey, 1987; Sánchez-Cubillo et al., 2009); thus, our observations are in line with several prior studies which showed that the temporal GM volume was most accurately related to working memory (Bailey et al., 2013; Bettcher et al., 2016). However, there is also literature indicating that the TMT B – TMT A score might rather be a relatively pure indicator of EF (Sánchez-Cubillo et al., 2009); further studies are needed to evaluate the significance and distinct interpretations for the TMT_{DIFF} score. Notably, our observations point in the same direction as previous studies showing a morphological advantage, e.g. larger ICV protects against dementia development (Guo et al., 2013; Negash et al., 2013; Groot et al., 2017). In any case, since it is suggested that CR and BR have independent and synergistic contributions to compensate for brain pathology (Stern, 2012) which may reciprocally influence each other (Persson et al., 2016) global GM volume at least appears to be a reasonable quantitative reserve marker in the elderly. In this way, both global GM volume and the associated EF can be used as reserve markers for the prediction of transition to MCI (Chen et al., 2017), transition of MCI to Alzheimer's disease (Albert et al., 2001) or to address the question of whether the clinical manifestation of existing Alzheimer pathology is concealed (Darby et al., 2017), which in turn may help to disentangle the heterogeneity of brain aging, including age-related changes to brain function (Burzynska et al., 2012).

In order to correct for possible age-related brain atrophy, we used the BPF as an independent variable in our regression analyses. Synek and Reuben (1976) first proposed the correlation of the ventricular to brain area (VBR) as an index based on a structure's area, whereas the introduction of the ratio BPV to ICV (BPF) is first referred to Rudick et al. (1999). By applying FreeSurfer, the reliability of measures is improved and the particular structure as well as the cerebral size is less subject to error compared to measurement results from earlier decades. Due to the improved reliability and reproducibility, we expected to introduce a lower error, consequently achieving a higher reliability of the BPF. In our study, the BPF did not, except for the parietal lobe, show a statistically significant effect on EF – although this was a non-significant trend. This is likely due to the sample composition in our study with clearly non-demented patients and only a slight variance of the MMSE score (see Fig. 2), as reflected by a median score of > 28.

As part of the moderation analyses, we showed a sex-specific buffer effect of global GM volume on the TMT B performance in the elderly (see Fig. 3). For male participants a positive influence of larger global GM volume, by means of a "buffering" effect, on the correlation between age and TMT B was observed. For female participants, however, contrasting observations were made. The subgroups were rather small (female = 73, male = 101), with a fairly large distribution of data values; therefore, interpretation of the prior moderation analyses are limited. However, it is conceivable that in a larger cohort, there might be a stronger, sex-independent effect of brain size, i.e. an age dependency of smaller GM volume being associated with worse EF. In

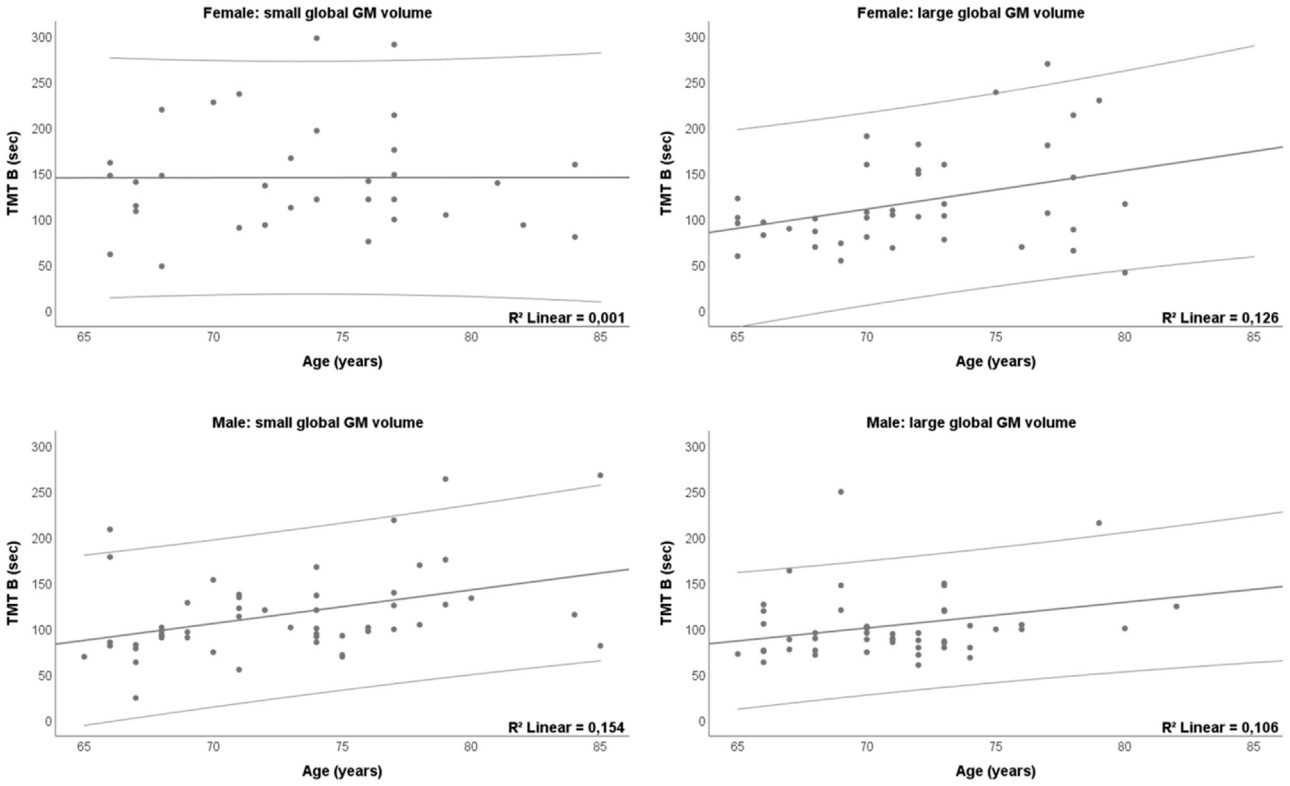

Fig. 3. To assess the effects of GM volume on the TMT B score, we assigned the subjects into four groups. This was done by a median split of the global GM volume (primary motor and sensory cortex are excluded) for the female and the male subjects separately. On the top of this figure, displayed for female participants (N = 73), the TMT B is regressed onto age and shown as dichotomized into small global GM volume (N = 33) on the left and into large global GM volume on the right side (N = 40). The lower part of this figure shows the regression of the TMT B onto age for male participants (N = 101). Displayed in the lower part, for male participants, is the global GM volume split into small (N = 51) on the left and large (N = 50) on the right side (95% CI). **Key: CI, Confidence Interval; GM, Grey Matter; sec, seconds; TMT B, Trail Making Test B.**

other words, the negative influence of age on EF might be moderated by global GM volume.

The observed associations of different brain volumes with EF are in line with reports from earlier studies. Elderkin-Thompson et al. (2008) manually masked the prefrontal cortex of MRIs of 23 healthy elderly individuals which were subsequently segmented automatically; different regions of the prefrontal GM volume were computed as ratios of intracranial volume. They found that specific prefrontal sub-regions are correlated with EF (Elderkin-Thompson et al., 2008). Using an explorative voxel-based morphometry approach, Zhang et al. (2011) reported associations of EF with four different brain lobes (frontal, temporal, parietal, and occipital) in 326 subjects. By applying deformation-based morphometry (DBM), Cardenas et al. (2011) showed that impaired EF is associated with smaller frontal lobe volumes (N = 71). The limitations of these three studies are mainly due to the applied image processing approaches that are accompanied by a compelling inter-observer variance. By applying the FreeSurfer software package, Dong et al. (2015) overcame these limitations and observed associations between GM volumes and cognitive performance in a large sample (N = 813) from the Northern Manhattan Study (NOMAS). Superior EF performance was primarily associated with greater frontal lobe volume (Dong et al., 2015). However, patients of different ethnicities with neurocognitive disorders such as dementia were not excluded, which impedes a direct comparison with our findings. In contrast, in the study of Bettcher et al. (2016), a sub-cohort of the NIH Aging and Cognition study (neurologically healthy older adults of undisclosed ethnicity), participants with neurocognitive disorders were not included and FreeSurfer was used for processing of the MR images with little inter-observer variance. In line with our findings, they found associations between EF performance and global as well as lobar structures, including frontal GM volumes. Accordingly, the study of Bettcher et al. (2016) and our study suggest that an isolated view on particular cortical volumes may not be sufficient to fully grasp association with EF in elderly non-demented subjects – in fact, our study results suggest that global GM volume is the best predictor. Most importantly, none of these studies specifically addressed BR; rather, the focus was on brain atrophy.

It is important to acknowledge that brain atrophy trajectories might be non-linear across different brain tissues, e.g. there is evidence that WM volume decline is significantly greater than GM volume decline in old age, particularly in the 9th decade (Royle et al., 2013). Since this is not entirely elucidated, in the future long-term data on changes in the grey/white matter ratio are needed to account for any divergence of trajectories; subsequently, the influence on the strategy to apply GM volume as a BR marker using BPF for brain atrophy correction will need to be carefully evaluated. From longitudinal measures acquired throughout the life span, it is known that regional brain volume does change in healthy adults (Raz et al., 2005). Neuroimaging in vivo data could demonstrate that there are global and spatially-localized relationships of normal ageing and brain morphology (Sowell et al., 2003; Fjell et al., 2013). Ubiquitous longitudinal cortical grey matter volume losses were observed in multiple studies (Scahill et al., 2003; Sowell et al., 2003), in particular in the prefrontal (Pfefferbaum et al., 1998; Resnick et al., 2003; Sowell et al., 2003) and parietal regions (Sowell et al., 2003). Fjell et al. (2013) found an accelerated decline for total brain volume at the end of the 20 s as well as from the age of 60 onwards. Pfefferbaum et al. (2013) described a cubic function for frontal lobe volume changes longitudinally, likewise indicating two points of accelerated decline - the first occurring in the late 20 s and the second after 60 years of age. One explanation might be that regions which

mature late contain more thin myelinated fibers and are consequently more vulnerable to age-related decline in terms of primary degenerative events in the early period of the 20s (Raz et al., 2000; Bartzokis, 2004). Furthermore, late critical ages accompanied by the demyelination of larger connections occurring in the late 60 s (Fjell et al., 2013). Hippocampal shrinkage was found to be substantial and accelerate with age (Scahill et al., 2003; Raz et al., 2005) following a slight increase in volume until the age of 50 (Pfefferbaum et al., 2013). Furthermore, the choice of post-processing method for brain volume quantification of longitudinal as well as cross-sectional data also impairs the opportunity for the direct comparability of data in general and in particular of the BPF (Vågberg et al., 2017), as well the ICV estimation (Nordenskjold et al., 2013). Also, the dehydration-rehydration status of each patient has a physiological effect on brain volume (Duning et al., 2005); thereby complicating the quantification of longitudinal change (Scahill et al., 2003). In the present study, the BPF index was applied to calculate the potential BR marker of atrophy-corrected grey matter volume. Since the literature indicates that the BPF varies throughout the individual's lifetime (Vågberg et al., 2017), further studies with multiple measurement time points investigating individual healthy subjects longitudinally, aiming to establish normative age-related values, are needed. As a further limitation to interpretation, it is prudent to highlight that TMT was the sole indicator of executive functions applied. Next to extensive neuroimaging assessments, additionally to the measured EF we also conducted many neuropsychological tests of other cognitive functions; thus, adding further EF domains could have led to higher dropout rates, and the tests might be ecologically less valid in an unfamiliar environment such as the laboratory (Luis et al., 2003). However, covering more extensive executive processing data is important to evaluate various EF domains and might therefore reduce bias. Future studies may want to include a more detailed characterization of executive functions (e.g. the Miyake's conceptual framework for executive functions (Miyake et al., 2000)) to validate the role of atrophy-corrected grey matter volume as potential reserve marker for EF in late life. For all of the conducted multiple regression analyses, rather small adjusted R-squared values were observed, ranging from 0.157 (occipital lobe) to 0.181 (parietal lobe and global GM volume). Thus, an essential part of residual variation between individuals in EF cannot be referred to cortical GM volume (corrected for key predictors) and the latter might have been operationalized in a rather simplified manner. This is in line with prior large-scale investigations observing that only 33% of the variance in cognition is explained by brain volumetrics (adjusted for ethnicity, age, education, and sex) (Gupta et al., 2015). Further investigations are needed to address the large gap in the knowledge regarding variables to explain the variation in cognition. To fulfill the need for an explanation of variations in cognitive performance, adding further neuroimaging and molecular variables (e.g. WM microstructure, neurotransmitter function or network connectivity) might also contribute to a more complete picture (Hedden and Growdon, 2015).

Nonetheless, in summary, our study suggests for the first time that GM brain volume, corrected for brain atrophy, predicts EF in the elderly. Thus, atrophy-corrected global GM volume appears to be a promising quantitative brain reserve marker. In addition, several prior studies reported an association of global and prefrontal cortical volume with executive function in the elderly population (Elderkin-Thompson et al., 2008; Cardenas et al., 2011; Zhang et al., 2011; Dong et al., 2015). Our findings strengthen the view that global GM volume is stronger associated with EF than lobar GM volumes.

Acknowledgements

The research leading to these results has received funding from European Union funded Seventh Framework Research Program [FP7/2007–2013], under grant agreement No. HEALTH-F2-2014-60246, BioCog (Biomarker Development for Postoperative Cognitive Impairment in the Elderly), www.biocog.eu. Additional (internal) funding was obtained from the Berlin Institute of Health (BIH).

Disclosure statement

This publication is part of the doctorate of Markus Laubach and Florian Lammers. Prof Winterer is the coordinator of the BioCog Consortium and chief executive of the company PharmaImage Biomarker Solutions GmbH. The company is one of the partners of the BioCog Consortium. The remaining authors declare no conflict of interest and all authors have no conflicting financial interests.

Appendix A. Supporting information

Supplementary data associated with this article can be found in the online version at doi:10.1016/j.neuropsychologia.2018.08.008.

References

Albert, M.S., Moss, M.B., Tanzi, R., Jones, K., 2001. Preclinical prediction of AD using neuropsychological tests. J. Int. Neuropsychol. Soc. 7, 631–639.
Arbuthnott, K., Frank, J., 2000. Trail making test, part B as a measure of executive control: validation using a set-switching paradigm. J. Clin. Exp. Neuropsychol. 22, 518–528.
Bailey, H.R., Zacks, J.M., Hambrick, D.Z., Zacks, R.T., Head, D., Kurby, C.A., Sargent, J.Q., 2013. Medial temporal lobe volume predicts elders' everyday memory. Psychol. Sci. 24, 1113–1122.
Bartrés-Faz, D., Arenaza-Urquijo, E.M., 2011. Structural and functional imaging correlates of cognitive and brain reserve hypotheses in healthy and pathological aging. Brain Topogr. 24, 340–357.
Bartzokis, G., 2004. Age-related myelin breakdown: a developmental model of cognitive decline and Alzheimer's disease. Neurobiol. Aging 25 (5–18), 49–62 (author reply).
Bettcher, B.M., Mungas, D., Patel, N., Elofson, J., Dutt, S., Wynn, M., Watson, C.L., Stephens, M., Walsh, C.M., Kramer, J.H., 2016. Neuroanatomical substrates of executive functions: beyond prefrontal structures. Neuropsychologia.
Buckner, R.L., Head, D., Parker, J., Fotenos, A.F., Marcus, D., Morris, J.C., Snyder, A.Z., 2004. A unified approach for morphometric and functional data analysis in young, old, and demented adults using automated atlas-based head size normalization: reliability and validation against manual measurement of total intracranial volume. NeuroImage 23, 724–738.
Burzynska, A.Z., Nagel, I.E., Preuschhof, C., Gluth, S., Bäckman, L., Li, S.-C., Lindenberger, U., Heekeren, H.R., 2012. Cortical thickness is linked to executive functioning in adulthood and aging. Hum. Brain Mapp. 33, 1607–1620.
Callahan, B.L., Ramirez, J., Berezuk, C., Duchesne, S., Black, S.E., 2015. Predicting Alzheimer's disease development: a comparison of cognitive criteria and associated neuroimaging biomarkers. Alzheimer's. Res. Ther. 7, 68.
Cardenas, V.A., Chao, L.L., Studholme, C., Yaffe, K., Miller, B.L., Madison, C., Buckley, S.T., Mungas, D., Schuff, N., Weiner, M.W., 2011. Brain atrophy associated with baseline and longitudinal measures of cognition. Neurobiol. Aging 32, 572–580.
Chen, Y., Denny, K.G., Harvey, D., Farias, S.T., Mungas, D., Decarli, C., Beckett, L., 2017. Progression from normal cognition to mild cognitive impairment in a diverse clinic-based and community-based elderly cohort. Alzheimer'S. Dement. J. Alzheimer's. Assoc. 13, 399–405.
Corrigan, J.D., Hinkeldey, N.S., 1987. Relationships between parts A and B of the trail making test. J. Clin. Psychol. 43, 402–409.
Dale, A.M., Fischl, B., Sereno, M.I., 1999. Cortical surface-based analysis. I. Segmentation and surface reconstruction. NeuroImage 9, 179–194.
Darby, R.R., Brickhouse, M., Wolk, D.A., Dickerson, B.C., 2017. Effects of cognitive reserve depend on executive and semantic demands of the task. J. Neurol., Neurosurg. Psychiatry 88, 794–802.
Desikan, R.S., Segonne, F., Fischl, B., Quinn, B.T., Dickerson, B.C., Blacker, D., Buckner, R.L., Dale, A.M., Maguire, R.P., Hyman, B.T., Albert, M.S., Killiany, R.J., 2006. An automated labeling system for subdividing the human cerebral cortex on MRI scans into gyral based regions of interest. NeuroImage 31, 968–980.
Dong, C., Nabizadeh, N., Caunca, M., Cheung, Y.K., Rundek, T., Elkind, M.S.V., Decarli, C., Sacco, R.L., Stern, Y., Wright, C.B., 2015. Cognitive correlates of white matter lesion load and brain atrophy: the northern Manhattan study. Neurology 85, 441–449.
Duning, T., Kloska, S., Steinsträter, O., Kugel, H., Heindel, W., Knecht, S., 2005. Dehydration confounds the assessment of brain atrophy. Neurology 64, 548–550.
Elderkin-Thompson, V., Ballmaier, M., Hellemann, G., Pham, D., Kumar, A., 2008. Executive function and MRI prefrontal volumes among healthy older adults. Neuropsychology 22, 626–637.
Feinkohl, I., Winterer, G., Spies, C.D., Pischon, T., 2017. Cognitive Reserve and the Risk of Postoperative Cognitive Dysfunction. Dtsch. Arzteblatt Int. 114, 110–117.
Fellows, R.P., Dahmen, J., Cook, D., Schmitter-Edgecombe, M., 2017. Multicomponent analysis of a digital trail making test. Clin. Neuropsychol. 31, 154–167.
Fischl, B., Dale, A.M., 2000. Measuring the thickness of the human cerebral cortex from magnetic resonance images. In: Proceedings of the National Academy of Sciences of the United States of America, 97, 11050–11055.

Fischl, B., Salat, D.H., Busa, E., Albert, M., Dieterich, M., Haselgrove, C., Van Der Kouwe, A., Killiany, R., Kennedy, D., Klaveness, S., Montillo, A., Makris, N., Rosen, B., Dale, A.M., 2002. Whole brain segmentation: automated labeling of neuroanatomical structures in the human brain. Neuron 33, 341–355.
Fischl, B., Van Der Kouwe, A., Destrieux, C., Halgren, E., Segonne, F., Salat, D.H., Busa, E., Seidman, L.J., Goldstein, J., Kennedy, D., Caviness, V., Makris, N., Rosen, B., Dale, A.M., 2004. Automatically parcellating the human cerebral cortex. Cereb. Cortex 14, 11–22.
Fjell, A.M., Westlye, L.T., Grydeland, H., Amlien, I., Espeseth, T., Reinvang, I., Raz, N., Holland, D., Dale, A.M., Walhovd, K.B., 2013. Critical ages in the life course of the adult brain: nonlinear subcortical aging. Neurobiol. Aging 34, 2239–2247.
Ge, Y., Grossman, R.I., Babb, J.S., Rabin, M.L., Mannon, L.J., Kolson, D.L., 2002. Age-related total gray matter and white matter changes in normal adult brain. Part I: volumetric MR imaging analysis. AJNR Am. J. Neuroradiol. 23, 1327–1333.
Groot, C., Van Loenhoud, A.C., Barkhof, F., Van Berckel, B.N.M., Koene, T., Teunissen, C.C., Scheltens, P., Van Der Flier, W.M., Ossenkoppele, R., 2017. Differential effects of cognitive reserve and brain reserve on cognition in Alzheimer disease. Neurology.
Guo, L.-H., Alexopoulos, P., Wagenpfeil, S., Kurz, A., Perneczky, R., 2013. Brain size and the compensation of Alzheimer's disease symptoms: a longitudinal cohort study. Alzheimer's. Dement.: J. Alzheimer's Assoc. 9, 580–586.
Gupta, M., King, K.S., Srinivasa, R., Weiner, M.F., Hulsey, K., Ayers, C.R., Whittemore, A., Mccoll, R.W., Rossetti, H.C., Peshock, R.M., 2015. Association of 3.0-T brain magnetic resonance imaging biomarkers with cognitive function in the Dallas heart study. JAMA Neurol. 72, 170–175.
Han, X., Jovicich, J., Salat, D., Van Der Kouwe, A., Quinn, B., Czanner, S., Busa, E., Pacheco, J., Albert, M., Killiany, R., Maguire, P., Rosas, D., Makris, N., Dale, A., Dickerson, B., Fischl, B., 2006. Reliability of MRI-derived measurements of human cerebral cortical thickness: the effects of field strength, scanner upgrade and manufacturer. NeuroImage 32, 180–194.
Hedden, T., Growdon, J.H., 2015. Challenges and opportunities in linking brain-based biomarkers to person-specific variation in cognition: pumping up the volume. JAMA Neurol. 72, 149–151.
Johnson, J.K., Lui, L.-Y., Yaffe, K., 2007. Executive function, more than global cognition, predicts functional decline and mortality in elderly women. J. Gerontol. Ser. A Biol. Sci. Med. Sci. 62, 1134–1141.
Jovicich, J., Czanner, S., Greve, D., Haley, E., Van Der Kouwe, A., Gollub, R., Kennedy, D., Schmitt, F., Brown, G., Macfall, J., Fischl, B., Dale, A., 2006. Reliability in multi-site structural MRI studies: effects of gradient non-linearity correction on phantom and human data. NeuroImage 30, 436–443.
Katzman, R., Terry, R., Deteresa, R., Brown, T., Davies, P., Fuld, P., Renbing, X., Peck, A., 1988. Clinical, pathological, and neurochemical changes in dementia: a subgroup with preserved mental status and numerous neocortical plaques. Ann. Neurol. 23, 138–144.
Kave, G., Shrira, A., Palgi, Y., Spalter, T., Ben-Ezra, M., Shmotkin, D., 2012. Formal education level versus self-rated literacy as predictors of cognitive aging. J. Gerontol. B Psychol. Sci. Soc. Sci. 67, 697–704.
Lehrl, S., 2005. Manual zum MWT-B: [Mehrfachwahl-Wortschatz-Intelligenztest], Balingen, Spitta-Verl.
Lehrl, S., Triebig, G., Fischer, B., 1995. Multiple choice vocabulary test MWT as a valid and short test to estimate premorbid intelligence. Acta Neurol. Scand. 91, 335–345.
Lotze, M., Montoya, P., Erb, M., Hulsmann, E., Flor, H., Klose, U., Birbaumer, N., Grodd, W., 1999. Activation of cortical and cerebellar motor areas during executed and imagined hand movements: an fMRI study. J. Cogn. Neurosci. 11, 491–501.
Luis, C.A., Loewenstein, D.A., Acevedo, A., Barker, W.W., Duara, R., 2003. Mild Cognitive Impairment. Dir. Future Res. 61, 438–444.
Misdraji, E.L., Gass, C.S., 2010. The trail making test and its neurobehavioral components. J. Clin. Exp. Neuropsychol. 32, 159–163.
Miyake, A., Friedman, N.P., Emerson, M.J., Witzki, A.H., Howerter, A., Wager, T.D., 2000. The unity and diversity of executive functions and their contributions to complex "Frontal Lobe" tasks: a latent variable analysis. Cogn. Psychol. 41, 49–100.
Mori, E., Hirono, N., Yamashita, H., Imamura, T., Ikejiri, Y., Ikeda, M., Kitagaki, H., Shimomura, T., Yoneda, Y., 1997. Premorbid brain size as a determinant of reserve capacity against intellectual decline in Alzheimer's disease. Am. J. Psychiatry 154, 18–24.
Negash, S., Xie, S., Davatzikos, C., Clark, C.M., Trojanowski, J.Q., Shaw, L.M., Wolk, D.A., Arnold, S.E., 2013. Cognitive and functional resilience despite molecular evidence of Alzheimer's disease pathology. Alzheimer's. Dement. J. Alzheimer's Assoc. 9. pp. e89–e95.
Nordenskjold, R., Malmberg, F., Larsson, E.M., Simmons, A., Brooks, S.J., Lind, L., Ahlstrom, H., Johansson, L., Kullberg, J., 2013. Intracranial volume estimated with commonly used methods could introduce bias in studies including brain volume measurements. Neuroimage 83, 355–360.
Persson, N., Ghisletta, P., Dahle, C.L., Bender, A.R., Yang, Y., Yuan, P., Daugherty, A.M., Raz, N., 2016. Regional brain shrinkage and change in cognitive performance over two years: the bidirectional influences of the brain and cognitive reserve factors. NeuroImage 126, 15–26.
Pfefferbaum, A., Rohlfing, T., Rosenbloom, M.J., Chu, W., Colrain, I.M., Sullivan, E.V., 2013. Variation in longitudinal trajectories of regional brain volumes of healthy men and women (ages 10 to 85 years) measured with atlas-based parcellation of MRI. Neuroimage 65, 176–193.
Pfefferbaum, A., Sullivan, E.V., Rosenbloom, M.J., Mathalon, D.H., Lim, K.O., 1998. A controlled study of cortical gray matter and ventricular changes in alcoholic men over a 5-year interval. Arch. Gen. Psychiatry 55, 905–912.
Phillips, L.H., Henry, J.D.A., Vicki, Jacobs, R., Anderson, P.J., 2008. Executive Functions and the Frontal Lobes: A Lifespan Perspective. Neuropsychology, Neurology, and Cognition. US: Taylor & Francis, Philadelphia, PA, pp. 57–79 (xxxiii, 541 pp.).
Pietschnig, J., Penke, L., Wicherts, J.M., Zeiler, M., Voracek, M., 2015. Meta-analysis of associations between human brain volume and intelligence differences: how strong are they and what do they mean? Neurosci. Biobehav. Rev. 57, 411–432.
Puente, A.N., Lindbergh, C.A., Miller, L.S., 2015. The relationship between cognitive reserve and functional ability is mediated by executive functioning in older adults. Clin. Neuropsychol. 29, 67–81.
Rabin, L.A., Barr, W.B., Burton, L.A., 2005. Assessment practices of clinical neuropsychologists in the United States and Canada: a survey of INS, NAN, and APA Division 40 members. Arch. Clin. Neuropsychol. 20, 33–65.
Raz, N., Lindenberger, U., Rodrigue, K.M., Kennedy, K.M., Head, D., Williamson, A., Dahle, C., Gerstorf, D., Acker, J.D., 2005. Regional brain changes in aging healthy adults: general trends, individual differences and modifiers. Cereb. Cortex 15, 1676–1689.
Raz, N., Williamson, A., Gunning-Dixon, F., Head, D., Acker, J.D., 2000. Neuroanatomical and cognitive correlates of adult age differences in acquisition of a perceptual-motor skill. Microsc. Res. Tech. 51, 85–93.
Reitan, R., 2004. The trail making test as an initial screening procedure for neuropsychological impairment in older children. Arch. Clin. Neuropsychol. 19, 281–288.
Resnick, S.M., Pham, D.L., Kraut, M.A., Zonderman, A.B., Davatzikos, C., 2003. Longitudinal magnetic resonance imaging studies of older adults: a shrinking brain. J. Neurosci. 23, 3295–3301.
Royall, D.R., Palmer, R., Chiodo, L.K., Polk, M.J., 2004. Declining executive control in normal aging predicts change in functional status: the freedom house study. J. Am. Geriatr. Soc. 52, 346–352.
Royle, N.A., Booth, T., Valdés Hernández, M.C., Penke, L., Murray, C., Gow, A.J., Maniega, S.M., Starr, J., Bastin, M.E., Deary, I.J., Wardlaw, J.M., 2013. Estimated maximal and current brain volume predict cognitive ability in old age. Neurobiol. Aging 34, 2726–2733.
Rozzini, L., Chilovi, B.V., Conti, M., Bertoletti, E., Delrio, I., Trabucchi, M., Padovani, A., 2007. Conversion of amnestic mild cognitive impairment to dementia of Alzheimer type is independent to memory deterioration. Int. J. Geriatr. Psychiatry 22, 1217–1222.
Rudick, R.A., Fisher, E., Lee, J.C., Simon, J., Jacobs, L., 1999. Use of the brain parenchymal fraction to measure whole brain atrophy in relapsing-remitting MS. Multiple sclerosis collaborative research group. Neurology 53, 1698–1704.
Salthouse, T.A., 2011. What cognitive abilities are involved in trail-making performance? Intelligence 39, 222–232.
Sánchez-Cubillo, I., Periáñez, J.A., Adrover-Roig, D., Rodríguez-Sánchez, J.M., Ríos-Lago, M., Tirapu, J., Barceló, F., 2009. Construct validity of the Trail Making Test: role of task-switching, working memory, inhibition/interference control, and visuomotor abilities. J. Int. Neuropsychol. Soc. JINS 15, 438–450.
Satz, P., Morgenstern, H., Miller, E.N., Selnes, O.A., Mcarthur, J.C., Cohen, B.A., Wesch, J., Becker, J.T., Jacobson, L., D'elia, L.F., et al., 1993. Low education as a possible risk factor for cognitive abnormalities in HIV-1: findings from the multicenter AIDS Cohort Study (MACS). J. Acquir Immune Defic. Syndr. 6, 503–511.
Scahill, R.I., Frost, C., Jenkins, R., Whitwell, J.L., Rossor, M.N., Fox, N.C., 2003. A longitudinal study of brain volume changes in normal aging using serial registered magnetic resonance imaging. Arch. Neurol. 60, 989–994.
Schmitter-Edgecombe, M., Parsey, C., Cook, D.J., 2011. Cognitive correlates of functional performance in older adults: comparison of self-report, direct observation, and performance-based measures. J. Int. Neuropsychol. Soc. JINS 17, 853–864.
Schofield, P.W., Logroscino, G., Andrews, H.F., Albert, S., Stern, Y., 1997. An association between head circumference and Alzheimer's disease in a population-based study of aging and dementia. Neurology 49, 30–37.
Segonne, F., Pacheco, J., Fischl, B., 2007. Geometrically accurate topology-correction of cortical surfaces using nonseparating loops. IEEE Trans. Med. Imaging 26, 518–529.
Sled, J.G., Zijdenbos, A.P., Evans, A.C., 1998. A nonparametric method for automatic correction of intensity nonuniformity in MRI data. IEEE Trans. Med. Imaging 17, 87–97.
Sowell, E.R., Peterson, B.S., Thompson, P.M., Welcome, S.E., Henkenius, A.L., Toga, A.W., 2003. Mapping cortical change across the human life span. Nat. Neurosci. 6, 309–315.
Spreen, O., Strauss, E., 1998. A Compendium of Neuropsychological Tests: Administration, Norms, and Commentary. Oxford Univ. Press, New York.
Stern, Y., 2002. What is cognitive reserve? Theory and research application of the reserve concept. J. Int. Neuropsychol. Soc. JINS 8, 448–460.
Stern, Y., 2012. Cognitive reserve in ageing and Alzheimer's disease. Lancet Neurol. 11, 1006–1012.
Strauss, E., Sherman, E.M.S., Spreen, O., 2006. A Compendium of Neuropsychological Tests: Administration, Norms, and Commentary. Oxford Univ. Press, Oxford.
Synek, V., Reuben, J.R., 1976. The ventricular-brain ratio using planimetric measurement of EMI scans. Br. J. Radiol. 49, 233–237.
Tombaugh, T.N., 2004. Trail making test A and B: normative data stratified by age and education. Arch. Clin. Neuropsychol. Off. J. Natl. Acad. Neuropsychol. 19, 203–214.
Vågberg, M., Granåsen, G., Svenningsson, A., 2017. Brain parenchymal fraction in healthy adults—a systematic review of the literature. PLoS One 12, e0170018.
Van Loenhoud, A.C., Wink, A.M., Groot, C., Verfaillie, S.C.J., Twisk, J., Barkhof, F., Van Berckel, B., Scheltens, P., Van Der Flier, W.M., Ossenkoppele, R., 2017. A neuroimaging approach to capture cognitive reserve: application to Alzheimer's disease. Hum. Brain Mapp. 38, 4703–4715.
Vibha, D., Tiemeier, H., Mirza, S.S., Adams, H.H.H., Niessen, W.J., Hofman, A., Prasad, K., Van Der Lugt, A., Vernooij, M.W., Ikram, M.A., 2017. Brain volumes and longitudinal cognitive change: a population-based study. Alzheimer Dis. Assoc. Disord.
Winterer, G., Androsova, G., Bender, O., Boraschi, D., Borchers, F., Dschietzig, T.B., Feinkohl, I., Fletcher, P., Gallinat, J., Hadzidiakos, D., Haynes, J.D., Heppner, F.,

Hetzer, S., Hendrikse, J., Ittermann, B., Kant, I.M.J., Kraft, A., Krannich, A., Krause, R., Kuhn, S., Lachmann, G., Van Montfort, S.J.T., Muller, A., Nurnberg, P., Ofosu, K., Pietsch, M., Pischon, T., Preller, J., Renzulli, E., Scheurer, K., Schneider, R., Slooter, A.J.C., Spies, C., Stamatakis, E., Volk, H.D., Weber, S., Wolf, A., Yurek, F., Zacharias, N., 2018. Personalized risk prediction of postoperative cognitive impairment - rationale for the EU-funded BioCog project. Eur. Psychiatry 50, 34–39.

Zhang, H., Sachdev, P.S., Wen, W., Kochan, N.A., Zhu, W., Crawford, J.D., Brodaty, H., Slavin, M.J., Reppermund, S., Kang, K., Trollor, J.N., 2011. Neuroanatomical correlates of cognitive performance in late life. Dement. Geriatr. Cogn. Disord. 32, 216–226.

Supplementary Materials

Supplementary Table 1

Associations of individual lobar and global GM volume, age, the BPF and sex with the score of the TMT B

Independent Variable	Dependent variable	Estimate	Standard error	p-value
Frontal GM volume (mm³)[a]	**TMT B**	-0.228	<0.001	0.006
Age (years)		0.190	0.806	0.014
BPF (BPV/ICV)		-0.148	45.657	0.062
Sex (female)		-0.121	8.671	0.152
Parietal GM volume (mm³)[b]	**TMT B**	-0.256	<0.001	0.002
Age (years)		0.199	0.793	0.009
BPF (BPV/ICV)		-0.156	45.407	0.048
Sex (female)		-0.102	8.717	0.228
Temporal GM volume (mm³)	**TMT B**	-0.263	0.001	0.002
Age (years)		0.190	0.797	0.013
BPF (BPV/ICV)		-0.146	45.368	0.065
Sex (female)		-0.095	8.805	0.270
Occipital GM volume (mm³)	**TMT B**	-0.201	0.001	0.012
Age (years)		0.209	0.799	0.007
BPF (BPV/ICV)		-0.124	46.220	0.121
Sex (female)		-0.139	8.551	0.096
Global GM volume (mm³)[a,b]	**TMT B**	-0.268	<0.001	0.002
Age (years)		0.187	0.797	0.015
BPF (BPV/ICV)		-0.145	45.329	0.065
Sex (female)		-0.090	8.845	0.298

[a] including primary motor cortex
[b] including sensory cortex

The model consists of the specific grey matter volumes, age, the BPF and sex entered as independent variables and the TMT B score (sec) as the dependent variable. Estimates are standardized regression coefficients of this model. The reference of the standardized regression coefficient of sex is female.

Key: BPF, Brain Parenchymal Fraction; BPV, Brain Parenchymal Volume; GM, Grey Matter; ICV, Intracranial Volume; mm, millimeters; sec, seconds; TMT, Trail Making Test

Supplementary Table 2

Associations of individual lobar and global GM volume, age, the BPF and sex with the TMT B – TMT A score (TMT_{DIFF} score)

Independent Variable	Dependent variable	Estimate	Standard error	p-value
Frontal GM volume (mm^3)[a]	**TMT B – TMT A**	-0.238	<0.001	0.004
Age (years)		0.155	0.691	0.046
BPF (BPV/ICV)		-0.183	39.227	0.022
Sex (female)		-0.092	7.451	0.281
Parietal GM volume (mm^3)[b]	**TMT B – TMT A**	-0.244	<0.001	0.004
Age (years)		0.167	0.685	0.030
BPF (BPV/ICV)		-0.189	39.208	0.018
Sex (female)		-0.084	7.528	0.330
Temporal GM volume (mm^3)	**TMT B – TMT A**	-0.284	0.001	0.001
Age (years)		0.152	0.683	0.048
BPF (BPV/ICV)		-0.177	38.875	0.026
Sex (female)		-0.059	7.545	0.491
Occipital GM volume (mm^3)	**TMT B – TMT A**	-0.145	0.001	0.075
Age (years)		0.181	0.694	0.021
BPF (BPV/ICV)		-0.163	40.151	0.046
Sex (female)		-0.140	7.429	0.099
Global GM volume (mm^3)[a,b]	**TMT B – TMT A**	-0.269	<0.001	0.002
Age (years)		0.154	0.687	0.046
BPF (BPV/ICV)		-0.178	39.040	0.025
Sex (female)		-0.064	7.643	0.426

[a] excluding primary motor cortex
[b] excluding sensory cortex

The model consists of the specific grey matter volumes, age, the BPF and sex entered as independent variables and the TMT B – TMT A scores (sec) as the dependent variable. Estimates are standardized regression coefficients of this model. The reference of the standardized regression coefficient of sex is female.

Key: BPF, Brain Parenchymal Fraction; BPV, Brain Parenchymal Volume; GM, Grey Matter; ICV, Intracranial Volume; mm, millimeters; sec, seconds; TMT, Trail Making Test

Supplementary Table 3

Associations of individual lobar and global GM volume, age, the GMF and sex with the score of the TMT B

Independent Variable	Dependent variable	Estimate	Standard error	p-value
Frontal GM volume (mm³)[a]	**TMT B**	-0.215	<0.001	0.010
Age (years)		0.214	0.786	0.005
GMF (GMV [a,b]/ICV)		-0.113	148.112	0.160
Sex (female)		-0.122	9.076	0.169
Parietal GM volume (mm³)[b]	**TMT B**	-0.248	<0.001	0.003
Age (years)		0.223	0.775	0.003
GMF (GMV [a,b]/ICV)		-0.116	146.782	0.147
Sex (female)		-0.100	9.109	0.260
Temporal GM volume (mm³)	**TMT B**	-0.254	0.001	0.003
Age (years)		0.209	0.781	0.005
GMF (GMV [a,b]/ICV)		-0.114	146.724	0.151
Sex (female)		-0.096	9.139	0.281
Occipital GM volume (mm³)	**TMT B**	-0.195	0.001	0.017
Age (years)		0.228	0.782	0.003
GMF (GMV [a,b]/ICV)		-0.088	152.304	0.288
Sex (female)		-0.135	9.005	0.125
Global GM volume (mm³)[a,b]	**TMT B**	-0.263	<0.001	0.002
Age (years)		0.211	0.779	0.005
GMF (GMV [a,b]/ICV)		-0.103	147.356	0.199
Sex (female)		-0.084	9.304	0.356

[a] excluding primary motor cortex
[b] excluding sensory cortex

The model consists of the specific grey matter volumes, age, the GMF and sex entered as independent variables and the TMT B score (sec) as the dependent variable. Estimates are standardized regression coefficients of this model. The reference of the standardized regression coefficient of sex is female.

Key: GM, Grey Matter; GMF, Grey Matter Fraction; GMV, Grey Matter Volume; ICV, Intracranial Volume; mm, millimeters; sec, seconds; TMT, Trail Making Test

5 Lebenslauf

Mein Lebenslauf wird aus datenschutzrechtlichen Gründen in der elektronischen Version meiner Arbeit nicht veröffentlicht.

Mein Lebenslauf wird aus datenschutzrechtlichen Gründen in der elektronischen Version meiner Arbeit nicht veröffentlicht.

Mein Lebenslauf wird aus datenschutzrechtlichen Gründen in der elektronischen Version meiner Arbeit nicht veröffentlicht.

6 Komplette Publikationsliste

Lammers, F., Mobascher, A., Musso, F., Shah, N.J., Warbrick, T., Zaborszky, L., Winterer, G., 2016. Effects of Ncl. Basalis Meynert volume on the Trail-Making-Test are restricted to the left hemisphere. Brain Behav 6, e00421. https://doi.org/10.1002/brb3.421

Journal-Details		
Name	Brain and Behavior	
Journal Metrics (siehe Appendix)	Zur Einreichung des Manuskriptes (2014)	Zur Eröffnung des Promotionsverfahrens (2017)
Impact Factor	2.243	2.219
Zugehöriger Rang in der Kategorie „Neurosciences“ (Gesamtzahl aller Journals)	164 (252)	184 (261)
Eigenfactor Score	0.001700	0.005000

Lammers, F., Borchers, F., Feinkohl, I., Hendrikse, J., Kant, I.M.J., Kozma, P., Pischon, T., Slooter, A.J.C., Spies, C., van Montfort, S.J.T., Zacharias, N., Zaborszky, L., Winterer, G., BioCog consortium, 2018. Basal forebrain cholinergic system volume is associated with general cognitive ability in the elderly. Neuropsychologia 119, 145–156. https://doi.org/10.1016/j.neuropsychologia.2018.08.005

Journal-Details	
Name	Neuropsychologia
Journal Metrics zur Einreichung des Manuskriptes und Eröffnung des Promotionsverfahrens (2017, siehe Appendix)	
Impact Factor	2.889
Zugehöriger Rang in der Kategorie „Neurosciences“ (Gesamtzahl aller Journals)	135 (261)
Eigenfactor Score	0.0.28000

Laubach, M., Lammers, F., Zacharias, N., Feinkohl, I., Pischon, T., Borchers, F., Slooter, A.J.C., Kühn, S., Spies, C., Winterer, G., BioCog Consortium, 2018. Size matters: Grey matter brain reserve predicts executive functioning in the elderly. Neuropsychologia 119, 172–181. https://doi.org/10.1016/j.neuropsychologia.2018.08.008

Journal-Details	
Name	Neuropsychologia
Journal Metrics zur Einreichung des Manuskriptes und Eröffnung des Promotionsverfahrens (2017, siehe Appendix)	
Impact Factor	2.889
Zugehöriger Rang in der Kategorie „Neurosciences“ (Gesamtzahl aller Journals)	135 (261)
Eigenfactor Score	0.0.28000

Zacharias, N., Lammers, F., Papadaki, E., Zaborszky, L., Winterer, G., 2017. Differences in Nucleus Basalis Magnocellularis Volume affects Resting State EEG α-Power. Posterpräsentation. Organization for Human Brain Mapping, OHBM Annual Meeting 2017 in Vancouver. https://www.humanbrainmapping.org/files/2017/OHBM_2017_Vancouver_Abstracts_final%20to%20OHBM.pdf

7 Danksagung

Ich danke Prof. Georg Winterer und Dr. Norman Zacharias für die Betreuung, Ausbildung, Anleitung und das zahlreiche Feedback (sowie sämtliche weitere Unterstützung, die in keine dieser Kategorien fällt) während der gesamten Arbeit. Nicht zu vergessen ist auch Dr. Konstanze Scheurer, die auch uns Doktoranden unzählige Male unterstützt hat, jede Unterschrift und jedes Empfehlungsschreiben besorgen konnte und für alle Anliegen ein offenes Ohr und meistens auch eine Lösung hatte.

Ich danke Prof. Claudia Spies und den Studienärzten an der Klinik für Anästhesiologie der Charité für die Möglichkeit, an der Klinik zu promovieren und die gute Zusammenarbeit. Insbesondere möchte ich all denen Studienärzten, Doktoranden, Praktikanten, etc. danken, die sich mit mir die Nächte am MRT um die Ohren geschlagen haben – ohne Anspruch auf Vollständigkeit gilt das vor allem für Dr. Friedrich Borchers, Dr. Gunnar Lachmann, Dr. Kwaku Ofosu, Dr. Daniel Hadzidiakos, Felix Müller, Markus Laubach, Marinus Fislage, Andrea Majoros, Lisa Alexander, Eleftheria „Betty“ Papadaki, Petra Kozma und noch so viele andere.

Ich danke dem BCAN und vor allem seinem Team aus Andrea Hassenpflug, Yvonne Kamm, Karl Bormann, Dr. Stefan Hetzer, Dr. Christian Labadie für die Unterstützung bei technischen Problemen (sowie auch häufig bei der Probandenbetreuung).

Ich danke Laszlo Zaborszky und den Teams der Phenotypes-Studie, von denen ich die meisten nie kennengelernt habe, die aber trotzdem tolle Mitarbeiter sind.

Zum Letzten, aber nicht zum Geringsten, danke ich meine Familie und Maria Lietz, deren Geduld immer ein bisschen länger reichte als meine.